ISSN 8755-6839

SCIENCE OF
TSUNAMI HAZARDS

The International Journal of The Tsunami Society

Volume 28 Number 3 Published Electronically 2009

INTERNATIONAL TSUNAMI SOCIETY

1741 Ala Moana Blvd. #70, Honolulu, HI 96815, USA.

WWW.TSUNAMISOCIETY.ORG

SCIENCE OF TSUNAMI HAZARDS is a CERTIFIED OPEN ACCESS Journal included in the prestigious international academic journal database DOAJ maintained by the University of Lund in Sweden with the support of the European Union. 'SCIENCE OF TSUNAMI HAZARDS is also preserved and archived at the National Library, The Hague, NETHERLANDS, at the Library of Congress, Washington D.C., USA, and in the Electronic Library of Los Alamos National Laboratory, New Mexico, USA.

OBJECTIVE: The Tsunami Society publishes its international journal SCIENCE OF TSUNAMI HAZARDS to increase and disseminate knowledge about tsunamis and their hazards.

Submit manuscripts of articles, notes or letters to the Editor. If an article is accepted for publication the author(s) must submit a scan ready manuscript, a Doc, TeX or a PDF file in the journal format. Issues of the journal are published electronically in PDF format. Recent journal issues are available at:
http://www.TsunamiSociety.org
http://www.sthjournal.org

Tsunami Society members will be advised by e-mail when a new issue is available. There are no page charges for one paper per calendar year for authors who are members of the Tsunami Society. Permission to use figures, tables and brief excerpts from this journal in scientific and educational works is hereby granted provided that the source is acknowledged.

Issues of the journal from 1982 thru 2005 are available in PDF format at http://epubs.lanl.gov/tsunami/
and on a CD-ROM from the Society to Tsunami Society members. ISSN 8755-6839
http://www.sthjournal.org

CAPTURING THE NEXT GENERATION OF CULTURAL MEMORIES – THE PROCESS OF VIDEO INTERVIEWING TSUNAMI SURVIVORS

W. Dudley[1], J. Goff[2], C. Chagué-Goff[2], and J. Johnston[3]

1. Department of Marine Science, University of Hawaii at Hilo, Hilo, HI 96720, USA

2. Australian Tsunami Research Centre, University of New South Wales, Sydney 2052, NSW, Australia

3. Disaster Preparedness Solutions, Inc., Kailua, HI 96734, USA

ABSTRACT

Traditional story telling is rare in many cultures these days and yet stories are an effective way of educating people of all ages. The technology of modern media is increasingly accessing all corners of the world and if used wisely can help capture and communicate messages of disaster preparedness. Planned video interviewing of tsunami survivors began around 1998 and an extensive archive has been assembled at the Pacific Tsunami Museum. Video interviewing is an effective way to collect data that are both educational and scientific. The technique however, is not simple and a protocol has been developed to achieve the best results. We explain the protocol in detail using examples where appropriate, and discuss a wide range of applications that have been developed using interview materials. Recent advances in analytical techniques mean that the previously difficult to access qualitative data of these interviews are now available for more robust scientific analysis. The database continues to grow each year. It seems likely that this publicly-available database will now be available for a whole suite of new applications that can be developed.

Keywords: Tsunami, video interview, community awareness, public education.

1. INTRODUCTION

"If history were taught in the form of stories, it would never be forgotten" (Rudyard Kipling Quotes 2009). The French explorer Jean-François de Galoup, Comte de la Pérouse, first entered Lituya Bay, Alaska on July 2, 1786. He soon encountered the local Tlingit tribe who recounted a legend which told the story of a monster that dwelt in the bay. This demon would periodically "destroy all who entered his domain by grasping the surface of the water and shaking it as if it were a sheet" (Emmons 1911). The truth behind the legend was demonstrated on July 9, 1958, when a powerful, local, landslide-generated tsunami swept through the bay. The life-saving power of such legends was demonstrated during the 2004 Indian Ocean Tsunami (2004 IOT), when stories handed down from generation to generation saved lives in the Simeulue Islands, Indonesia (McAdoo et al. 2006) and Surin Islands, Thailand (Arunotai 2008). The value of these stories was once again shown during the 2007 Solomon Islands tsunami when the indigenous population suffered fewer deaths than immigrant Gilbertese who had no traditional stories about tsunamis as part of their cultural memory (McAdoo et al. 2008).

Traditional story telling is becoming a lost art, as this form of knowledge sharing is increasingly limited to adults and the elderly, and rarely passed on to the young generations (Arunotai 2008). Meyers and Watson (2008) note that "modern communication methods are less focussed on information pertaining to the local area and disseminate information in a much broader manner. Lessons are taken from the world beyond instead of from the past or the specific local context". They go on to add that "new means to inform communities about the threats of disaster in their localities must be found. These means must carry relevant information and must also replicate the effectiveness of the oral story-telling tradition in dissemination and immediate relevance to local communities."

The technology of modern media will ultimately infiltrate every corner of the planet, hastening the loss of traditional story telling, but modern technology can also be used wisely to help capture and communicate the life saving messages of disaster preparedness (Dudley 2008a). This paper lays out approaches and techniques for capturing the stories of tsunami survivors on high quality video for use in hazard education and as a valuable source of both physical and social science information about hazards and the human response to these events. Though not replacing traditional story telling, capturing these powerful stories of survival on video presents the information in a format that is relevant to younger generations. Furthermore, the video recording of these stories permanently archives an important part of community cultural memory.

2. WHY VIDEO?

Until recently there have been few first-hand post-event accounts of tsunami disasters collected in a timely manner. Following the 2004 IOT commendable efforts were made to gather information from eye witnesses through questionnaires distributed to survivors (e.g. Tinti et al. 2005; Kelman et al. 2008). These are a valuable aid for integrating the physical data acquired through field surveys however, they lack the emotive power of stories. Written collections of tsunami stories have been used as part of education programs in school curricula in Hawaii and by the U.S. Geological Survey (Atwater et al. 1999). In 2004, the offices of emergency management of Washington State and British Columbia jointly produced a compelling 14-minute video recounting a native American legend about tsunamis and earthquakes, which is narrated by an elder of the Hoh Tribe (WA-EMD, 2004). Yet, none of these have the power of the first-hand experiences told by tsunami survivors.

The collection of oral histories has long been a valuable part of many disciplines including anthropology, history, psychology and sociology (King et al. 2007). These have mostly been carried out with audio recording equipment, the prevailing view being that video was too intrusive and that it made the subject too nervous (Nishimoto W. pers. comm. 1999). However, this was prior to the widespread use of consumer video equipment, when video recording was confined to professional news media. The news media regularly cover natural disasters. They rushed to the areas impacted by the 2004 IOT and recorded scenes of death and destruction. However, their coverage was largely confined to their own national news media and nearly all interviews were brief in order to fit short format news time slots. Furthermore, the material collected by professional media is typically not available or difficult to obtain for scholarly or educational use.

Even if professional video crews were available to carry out detailed survivor interviews, there are several advantages to not using a media crew. In addition to the appreciable cost of a professional video crew, our experience has been that communities respond better to scientists and their local student assistants, whose objective is not to make a television news story or commercial documentary, but to create materials for education that can be used at the local level (Dudley and Lee 1998). The typical community experience with professional media is that they come, they shoot, they leave, and the community never hears from them again. Furthermore, professional media are more concerned with the quality of their production than with community sensibilities (Bryan, T. pers. comm. May 2007).

If used appropriately, the process of video interviewing can show sensitivity to individual being videotaped and to the community. Furthermore, the finished products can contain important physical and social science information, and provide a valuable education tool for both the local community and international use (Dudley 2007).

2.1 Video Interview Techniques

For over a decade the Pacific Tsunami Museum has sponsored the collection of video oral histories of tsunami survivors. At present the museum's archives contain over 400 survivor interviews representing first-hand accounts of some ten different tsunamis in the Pacific and India Ocean from 1923 to 2006 (Dudley 2008b). Accounts prior to 1998 were recorded many years after the events and memories may have changed over time, or even been replaced with details learned during the intervening years (the archival material provide a useful database to study this metamorphosis of memory). In one instance, we interviewed five siblings who all experienced the same tsunami in the same location and their recollections were quite different from one another. All five had vivid recollections, one talked about the sounds, another about the smell, still another about how it felt physically to be in the water. If you did not know they were together you never would have guessed they were in the same location. However, together they wove a tapestry of what it was like to be on the second floor of a wooden building and see a tsunami come through the window, destroy the building and have the roof fall in on top of them.

Accounts collected from survivors of the 2004 IOT and the 2006 Java tsunami were recorded as soon as was feasible allowing sufficient time for recovery from immediate post-event trauma (Bryant 2006). The current protocol is based upon a combination of scientific and pragmatic lessons learned during the time that we have been carrying out tsunami survivor interviews. The progression from set questionnaires, to written accounts, to a combination of audio tapes and their transcription, and finally to a combination of video recordings and their transcription, is indicative of this learning process. From our experience, scientifically and pragmatically, video recordings and their transcription provide the richest data source.

These videos are of excellent quality, having been recorded on sophisticated digital video equipment. This has been made possible by recent advances in video technology and the advent of "prosumer" equipment. This is less expensive than top-of-the-line professional equipment, but is capable of recording video of a higher quality than inexpensive, consumer-grade cameras. The current model in use is a Sony HDR FX1 high-definition (1080i) digital video camera with a BeachTek DXA-FX audio adaptor to allow for XLR stereo microphone inputs. Good equipment however, is only one aspect of achieving high quality interviews. During a decade of video-interviewing we have developed a protocol which has proved successful under a wide range of different and challenging circumstances in a variety of nations around the world.

3. PROTOCOL

A team of four people is used. A Project Director (PD) serves as producer, camera operator, sound and light technician. A Field Coordinator (FC) serves as production assistant and who is chosen on the basis of previous experience in the region. The On-Site Facilitator (OSF) is typically a local resident, with expertise and/or sincere interest in tsunami preparedness, knowledge of the tsunami event(s) in question, fluency in local languages and the ability to translate interviews into English (if required). A Logistical Coordinator (LC) liaises between interviewees and team members. Normally the OSF serves as interviewer (after on-site coaching), although the role can also be carried out by either the FC or LC.

For organisational purposes, the process of collecting video interviews is divided into three phases: pre-interview, interview, post-interview.

3.1 Pre-interview Phase

The OSF contacts potential interviewees, explains the reason why the data are being collected and the interview process. Among the factors the OSF considers in the selection of potential interviewees are:

- The individual's personal experience during the tsunami event.
- The ability to effectively communicate this experience.
- The lesson(s) that can be learned from the experience.

When possible, interviewees should also reflect a range of ages, sexes, and community positions. If the OSF believes the interviewee meets the necessary criteria, an appointment for the video interview will be set up and a location chosen. Typically the location is one that makes the interviewee feel comfortable, but where feasible it also needs to fulfil certain criteria to ensure the overall quality of the video output. The site should not be a high noise area and, where possible, should be away from all motor traffic noise. The OSF uses their judgment and local knowledge to select the initial interview site.

It is often desirable to schedule time to meet with, and potentially arrange to interview, local leaders or other community members. This serves two purposes. It helps establish community cooperation for the project and also makes it more likely that there will be effective use of the outputs in sustainable local community disaster education programmes.

Several important steps are followed before the first on-site interview. A test interview is carried out by the entire crew and reviewed for all aspects of the process to include interview technique, camera work, lighting and sound. At this time the OSF is provided with a list of recommended interview questions which include queries designed to gather important physical and social science data, as well as deliver a powerful tsunami experience. They are coached in the interviewing techniques required and practice asking the questions to ensure that they are grammatically and culturally appropriate. This is particularly important when dealing with material translated from English. If necessary, culturally appropriate behaviour is discussed with the OSF once the mix of interviewees is known. The LC ensures that all appropriate documentation is in order to record key personal information for each interviewee (Fig. 1a). Each individual (or authorised guardian for minors) signs a release form which allows use of the recording for educational purposes (Fig. 2). The contents and reasons for completing the Biographical Data Sheet (Fig. 1a) and Oral/Video Tape Release Form (Fig. 2) are explained to the interviewee prior to completion. Where possible, the forms should be translated into the local language so that the interviewee understands fully what they are signing. The nature and extent of the questions to be asked are also discussed at this time either by the LC or OSF (Sample questionnaire: Fig. 3).

Prior to the interview, all forms (biographical, release) and the tape (and case) for each interviewee are assigned a unique Interview Code number consisting of a location abbreviation, the date of interview, and the interview number in the series for the particular assignment. Photos of the site and interviewee (full face) are taken either prior to, during, or after the interview, whichever is felt to be least intrusive. These actions help to minimise the likelihood of incorrect archiving in the future.

Tsunami survivor interviews are unlike most in that there are no second takes. For many survivors this is not the telling of a story but the reliving of an intense emotional experience, the most traumatic experience of their lives. Interviewees must be allowed to recall and describe events without coaching. They must also be allowed to tell their story without interrupting their train of thought and should never be interrogated with closed-questions. Interviewees should also never be "led". This can give the interviewee a sense of what the interviewer might be "looking for" leading them to give the responses that they perceive are desired. When the initial narrative is complete however, the interviewee may be gently prodded for additional information, overlooked details, and other useful information.

3.2 Interview Phase

Interviews are scheduled for a minimum of two hours. This includes travel to and from the site, equipment set-up and repacking, pre-interview and interview activities. Experience has shown that, depending upon travel times between sites, a maximum of six interviews can be accomplished in a full day. If an interviewee is willing and capable, additional footage may be shot at sites meaningful to the story, otherwise background footage (B-roll) is shot separately.

Upon arrival at the interview site it is important for the PD and FC to determine if it meets the criteria for sound, light and movement. If not, then an alternative site must be chosen in consultation with the OSF. A powerful interview will be ruined by the sounds of passing motorcycles, trucks, motorboats, barking dogs, or background conversations. Once a suitable site has been found with reasonable sound quality, it must be checked for appropriate lighting. It is important to take as much advantage of the "golden hours" as possible, those hours of the day when the sun is low in the sky producing gentle, warm light effects. It is impossible however, to carry out all interviews at dusk, so in order to avoid the harsh light of mid-day a partially shaded area should be selected. In these circumstances, the subject is placed in the shade with their face illuminated by reflected light without making them squint. This cannot always be successfully achieved. In one instance, an early morning interview was arranged with a resort manager but he was called away to the reception. He returned an hour later by which time the sun was so bright that the background was over-saturated with light, resulting in a video with too much contrast. Greenery, such as a backyard garden or jungle back drop, makes a good background because it absorbs and diffuses light, allowing most skin colours to show adequate contrast. It is important though to choose an area where nothing can move behind the subject. People or animals wandering around in the background are distracting to the viewer. One way to mitigate these effects is to use a low "F stop" on the camera to help blur the background while keeping the subject in clear focus.

Spending time on site selection is vital, but ensuring that the interviewee is well set-up is equally important. The subject should always be comfortably seated so that they do not fidget, and on a seat that does not squeak. It is important to let the subject attach the microphone themselves, only providing assistance when asked, so as to do nothing offensive in the host culture. Nothing should actually touch the microphone however, such as a scarf or jewellery and this often requires assistance to ensure the interviewee understands. A lavaliere microphone attached at shirt collar level works best. Under windy conditions the interviewee is shielded from direct wind blowing over the microphone. A microphone windscreen is also used to further dampen wind noise. In spite of all possible care, one must always expect the unexpected. In one instance, the sound location was perfect, lighting was excellent at dusk, and the interviewee was comfortable. Suddenly the village loudspeakers began broadcasting the evening call to prayer at full volume and the interview was abandoned. It pays to check on regularly scheduled events which may require adjusting the scheduled interview time.

3.3 Immediate Post-interview Phase

Following each interview our practice has been to have the OSF immediately provide a short written summary of the story in English. This applies equally to English and non-English interviews. This is given to the LC and placed with the basic personal data collected about each survivor (Fig. 1b). It is important to allow time for this process immediately after the interview. While this can sometimes be difficult when several interviews are scheduled in one session, it is crucial to double-check the information on Biographical Data Sheet and the interview summary (e.g. do we have the name of all the children mentioned in the interview on the biographical data sheet? Was the child mentioned a daughter or son?). The immediate post-interview phase also offers the opportunity to arrange for the copying of any documentation of the tsunami provided by the interviewee (e.g. photos), and to accept and process any donated memorabilia.

At the end of the day, the team meets to review the day's interviews. Any necessary revisions or additions to the descriptive data that accompany the interview tapes are made immediately while the details are still fresh. An electronic summary interview document is set-up for each assignment. This is updated daily with each reference number assigned to the appropriate interviewee photograph, and brief biographical details.

Some interviews are naturally more powerful than others and some contain new or critical information. Our practice has been to create a backup copy of these particular interview tapes during the evening following the interview. It would be best for all originals to be backed-up immediately, but because copying occurs in real-time this is time consuming and as such is not feasible during an expedition. To partially address this issue it is best to have the capability to simultaneously record directly to a hard drive. This will produce a digital videotape and a hard drive copy of interviews, thereby eliminating the chore of making backup videotape copies during an expedition. If travelling by plane during or at the end of an expedition, the original videotapes should never placed in the airline's checked baggage.

Immediately following an expedition, all interview tapes are backed up and the back-ups stored in separate, secure, climate-controlled locations. The process is lengthy because as mentioned it is carried out in real-time, but we also simultaneously burn a DVD copy of each interview. These DVDs are complete, unedited copies of the interview and contain the time code recorded on the original videotape.

3.4 Transcription and Translation of Interviews

Where translation is necessary the DVDs are sent to the OSF who carries out or supervises the transcription and translation of the interviews. The video time code must be entered at frequent intervals alongside the translated transcription of the interview in order to permit editing of the video. Typically we ask that the time code be entered at two to five minute intervals depending upon the context and before and after every important "sound bite" (i.e. a statement of special value). These transcriptions can then be easily converted into a video storyboard.

A typical interview lasts between 20 and 40 minutes, although we have had interviews of up to two hours (requiring two 60-minute videotapes). Selected interviews may be edited to a three to four minute final product, which includes the most important lessons learned. This is a suitable length without exceeding the typical listener's attention span. Our practice has been to offer DVD copies of the interviews to the interviewee whenever feasible, typically in full form. Due to the different video standards used internationally (NTSC, PAL, SECAM), providing copies of interviews for commercial video players can be both an unexpectedly problematic and expensive component of any project. The provision of videotape copies however, if often a necessary expense.

Interviews are recorded in a searchable archive database keyed to specific tsunami events.

4. APPLICATION OF INTERVIEW MATERIALS

The use to which tsunami survivor interviews have been put has far exceeded our expectations when we first began collecting them on video in 1998. The interviews carried out for the Pacific Tsunami Museum have been routinely copied to videotape and made available for viewing by visitors to the museum (The Pacific Tsunami Museum 2009). Several books and peer-reviewed papers have already been written as a result of the open access to the materials (Dudley 1999a;

1999b; Dudley and Stone 2000; Johnston 2003a; Goff et al. 2006). An interview with a tsunami survivor in Hawaii was combined with stories about the 1960 tsunami in Chile and Japan to produce a published circular by the U.S. Geological Survey (Atwater et al. 1999) which has been widely distributed and republished several times. These products help increase public awareness of the tsunami hazard.

From a scientific perspective the interviews have produced valuable new information about tsunamis. For example, prior to an interview with former Navy Petty Officer, Lee Edtl, no information existed about the impact of the 1946 tsunami at French Frigate Shoals, a group of small islands in the leeward chain of the Hawaiian Islands. Mr. Edtl provided data concerning wave height and timing, as well as discussing his fear of being washed off the low-lying island (Edtl 2001).

Research on disaster communication was carried out using a number of interviews with survivors of the 1946 and 1960 tsunami in Hawaii (Johnston 2003b). Among the facts that emerged was the distrust by local police of “high technology”. They required an officer to stand on the local pier, watch the water level, and radio in to the station confirming the arrival of tsunami waves. On the Island of Hawaii in 1960, the Kau Police Department dispatched a fisherman with a walkie-talkie and a flashlight to the southernmost point of the island to watch for the tsunami. He was to call the officer stationed uphill when he saw the first wave. The officer in turn was to radio the information to the Hilo Police Department even though waves actually reached the easternmost point of the island, close to Hilo, first (Johnston 2003b).

Survivor interviews have become a key element in many of the major exhibits at the Pacific Tsunami Museum. Exhibits focussing on particular events use survivor stories chosen for their emotional power and the vital lessons they offer. Interviews are also selected based on their appeal to particular demographics, with an attempt made to represent children and elders, as well as young and middle-aged men and women. Furthermore, we believe that hearing from a wide range of people within a community is instructive hence interviews with government officials, teachers, fisher people, resort staff, school children, religious figures, artisans, and labourers are all presented in the hope of “connecting” with the visitors to the museum. Interviews that were originally in a language other than English have been dubbed using a voice similar in age and tenor to that of the interviewee. A synopsis of each survivor interview is presented in a display adjacent to the touch-screen computer kiosk. The visitor may then select an interview of particular interest by pushing on an icon, usually a photo of the survivor, on the monitor (Muffler 2009). Similar accessibility and displays will be an integral part of a new travelling tsunami museum that is being planned for the Hawaiian Islands. The museum will be installed in a standard shipping container and house educational displays, touch-screen computer kiosk with animations of tsunami wave generation and propagation, and video footage of tsunami wave inundation. A second touch-screen computer kiosk will have different modules for each separate island featuring interviews with tsunami survivors from that island. This will provide added relevance for local residents, and included within these interviews will be those with respected elders discussing indigenous knowledge of the tsunami hazard.

The popularity of survivor interviews as museum exhibits has ultimately led to the establishment in 2007 of community tsunami museums in Kamphuan, Thailand (USAID 2008) and Alappad, Kerala, India (Anon. 2008). In these small museums, computer kiosks offer the choice of hearing the interviews dubbed into English or in the original language, thereby serving both the local population and the majority of visitors. Museums using tsunami survivor interviews as key exhibits are also planned for Sri Lanka and Indonesia.

Video interviews have also been incorporated into a number of different outreach education activities:

- A selection of interviews, representing areas most impacted by the 2004 IOT, have been placed on DVDs and made available to school teachers as a supplement to their curriculum materials on natural hazards.
- The availability of high-quality video footage featuring tsunami survivors has led to the production of public service announcements (PSAs) which have been broadcasted throughout the Hawaiian Islands. Six PSAs are currently being shown on different channels dedicated to programming for children, (cartoon networks), adolescents (music video networks) and adults (vintage movie, financial, and all news networks), hence covering different age groups and demographics.
- Local affiliates of major national television networks have produced news stories about natural hazards based around survivor interviews. Recording broadcast quality audio and video is essential, and giving the network stations use of the materials at no cost, has resulted in free public education reaching many thousands.

It is perhaps not surprising that many of the initiatives discussed above are US-based, because the archive is maintained and stored in Hawaii. All archived data are however, available for educational activities and research scholars. The Pacific Tsunami Museum is a non-profit organisation and as such requires only a data management fee to ensure the ongoing support of their archivists. It seems likely that the value of the existing, and growing, dataset will become increasingly recognised over time and be used in more international venues. For example, a recent study carried out in Sri Lanka considered audio-visual means to be the most effective tool for disaster education (Kurita et al. 2006). In the past the ability to effectively interrogate and interpret such complex qualitative datasets has been limited. There are however, new software packages that can be used for analysing complex qualitative datasets and it is hoped that this will enable a more effective use of the information contained in the interview archive (e.g. Crowley et al. 2002).

5. CONCLUSIONS

From the perspective of the survivor, one of us (JJ- survivor of the 1946 tsunami) felt that in the pre-2004 IOT world it was important to collect and save the stories because she did not want them lost as the survivors of the 1946 and 1960 tsunamis died. She felt that the stories should be saved for historical purposes and for them to be used for public education in tsunami mitigation programmes.

Video interviewing of tsunami survivors is an effective and efficient way to gather data and learn from tsunami survivors. Videotapes also make compelling educational tools because they contain visual emotive elements not found in other media. Set questionnaires fail to adequately cover the broad range of data that can be acquired through video, but can be more easily gathered. Since 1998 (audio interviewing began in 1996) the collection of video interviews has added to a growing archive of material that has only recently been seen to add immense value to education initiatives and scientific research. If they are to continue to be valuable and add value, then it is vitally important that a consistent and pragmatic protocol be adopted so that we can effectively harness the technology of modern media.

Acknowledgements

We would like to thank Warren Nishimoto, Mick Kalber, and Tim Bryan for helpful comments about audio and video interviewing techniques.

REFERENCES

Anon., 2008. Tsunami documented. *Kerala Calling*, **28**, 3, 46.

Arunotai, N., 2008. Saved by an old legend and keen observation: The Case of Moken Sea Nomads in Thailand, In: Indigenous Knowledge for Disaster Reduction: Good Practices and Lessons Learned from Experiences in the Asia-Pacific Region, Shaw, R., Uy, N., and Baumwoll, J. (Eds.), United Nations International Strategy for Disaster Reduction, Bangkok, 73-78.

Atwater, B. F., Cisternas V., M., Bourgeois, J., Dudley, W. C., Hendley II, J. W., and Stauffer, 1999. Surviving a Tsunami — Lessons from Chile, Hawaii, and Japan, U.S. Geological Survey, Circular 1187, Dept. of Interior, U. S. Government Printing Off.

Bryant, R.A., 2006. Recovery after the tsunami: Timeline for rehabilitation. *J. Clin. Psychiat.*, **67**, Supp. 2, 50-55.

Crowley, C., Harré, R., and Tagg, C., 2002. Qualitative research and computing: methodological issues and practices in using QSR NVivo and NUD*IST. *Int. J. Social Res. Methodol.*, **5**, 193-197.

Dudley, W. C., 1999a. The Pacific Tsunami Museum: A memorial to those lost to tsunamis, and an educational center to prevent further casualties. *Sci. Tsunami Haz.*, **17**, 1, 127-134.

Dudley, W. C., 1999b. Local Tsunamis in Hawaii, Pacific Tsunami Museum Publications, Hilo, 56 pp.

Dudley, W. C., 2007. Learning from the victims. Proceedings of the 1st International Tsunami Training Institute, University of Washington, Seattle.

Dudley, W. C., 2008a. Remembering the tsunami. Proc. Report Post-Tsunami Sustainable Livelihoods and Integrated Ecosystem Management workshop, Asian Institute of Technology, Bangkok. 28.

Dudley, W. C., 2008b: Pacific Tsunami Museum and International Community Preparedness Activities. In: Report North Pacific Tsunami Awareness Conference, Hendricks, T. (Ed.), Honolulu, 20-21.

Dudley, W. C. and Lee, M., 1998. Tsunami!, 2nd edition, University of Hawaii Press, Honolulu, 375 pp.

Dudley, W. C. and Stone, S. C., 2000. The Tsunamis of 1946 and 1960, Donning Press, Virginia Beach, 64 pp.

Edtl, L., 2001. The Tsunami of April 1, 1946 at French Frigate Shoals, event report submitted to the Pacific Tsunami Museum archive.

Emmons, G. T., 1911. Native account of the meeting between La Perouse and the Tlingit, *Am. Anthropol.*, **13**, 294-298.

Goff, J. R., Dudley, W. C., deMaintenon, M. Cain, G., and Coney, J. P., 2006. The largest local tsunami in 20th century Hawaii. *Mar. Geol.*, **226**, 65-79.

Johnston, J. B., 2003a. Tsunamis in Maui County: Oral Histories, Center for Oral History, University of Hawaii Press, Honolulu, 501 pp.

Johnston, J. B., 2003b. Personal accounts from survivors of the Hilo tsunamis of 1946 and 1960: Toward a disaster communication model, ProQuest Company, Ann Arbor, 142 pp.

Kelman, I., Spence, R., Palmer, J., Petal, M., and Saito, K.,2008. Tourists and disasters: lessons from the 26 December 2004 tsunami. *J. Coast. Conservation*, **12**, 105-113.

King, D., Goff, J. R., and Skipper, A., 2007. Māori environmental knowledge and natural hazards in New Zealand. *J. Royal Soc. N. Z.*, **37**, 59-73.

Kurita, T., Nakamura, A., Kodama, M., and Colombage, S. R. N., 2006. Tsunami public awareness and the disaster management system of Sri Lanka. *Disaster Prev. Managt*, **15**, 1, 92-110.

McAdoo, B. G., Baumwell, J., and Moore, A., 2008. Indigenous knowledge saved lives during 2007 Solomon Islands tsunami, In: Indigenous Knowledge for Disaster Reduction: Good Practices and Lessons Learned from Experiences in the Asia-Pacific Region, Shaw, R., Uy, N., and Baumwoll, J. (Eds.), United Nations International Strategy for Disaster Reduction, Bangkok, 64-67.

McAdoo, B. G., Dengler, L., Prasetya, G., and Titov, V., 2006. Smong: How an oral history saved thousands on Indonesia's Simeulue Island during the December 2004 and March 2005 tsunamis. *Earthq. Spectra*, **22**, S3, S661-S669.

Meyers, K. and Watson, P., 2008. Legend, ritual and architecture on the Ring of Fire. In: Indigenous Knowledge for Disaster Reduction: Good Practices and Lessons Learned from Experiences in the Asia-Pacific Region, Shaw, R., Uy, N., and Baumwoll, J. (Eds.), United Nations International Strategy for Disaster Reduction, Bangkok, 17-22.

Muffler, B., 2009. Successful Exhibit Opening, Museum News, Pacific Tsunami Museum, 13, 1.

Rudyard Kipling Quotes, 2009. Rudyard Kipling.net – Biography, pictures, videos, & quotes http://www.rudyardkipling.net/more.html. Accessed 22 March 2009.

The Pacific Tsunami Museum, 2009. http://www.tsunami.org/ Accessed 22 March 2009.

Tinti, S., Maramai, S. A., Tonini, R., Graziani, L., Topazio, S., and Boschi, E., 2005. Sai dello Tsunami: Tell us your tsunami: a way to collect eye-witnesses accounts of the 26th December 2004 Sumatra tsunami. Poster EGU05-A-11104, EGU 2005, Vienna.

USAID (United States Agency for International Development), 2008. Kamphuan Memorial Tsunami Museum opens. USAID Tsunami Reconstruction Update, June 2007, 6.

WA-EMD (Washington State/Local Tsunami Workgroup, Washington State Military Department Emergency Management Division and the Provincial Emergency Program of British Columbia), 2004. Run to High Ground. WA-EMD and Global Net Productions, Video/DVD, Las Vegas, New Mexico.

FIGURES

Fig. 1. a) Summary Biographical Data Sheet used by the Pacific Tsunami Museum (it should be noted that legal requirements may cause variations in the format). When working in predominantly non-English speaking countries this form is translated into the appropriate language. The OSF and LC liaise to produce the summary of the interview. A unique Interview Code is assigned to each interviewee record; b) Tsunami Recollection Summary used by the Pacific Tsunami Museum – this is filed together with the Biographical Data Sheet.

INTERVIEW CODE (Fig. 1a)

Pacific Tsunami Museum
P.O. Box 806 • Hilo, Hawai'i 96721
(808) 935-0926 • (808) 935-0842
tsunami@tsunami.org

BIOGRAPHICAL DATA SHEET

Contacted by:		Date:
Name:	M/F	Phone:
Address:		
Ethnicity:		Language(s) spoken:
Birthdate:	Birthplace:	Citizenship:
Marital status:	Spouse's name:	
	Children	
Child's name (son/daughter)		Birthdate/age
Education:		
Occupation/Job:		
Other relevant information		

(a)

INTERVIEW CODE (Fig. 1b)

Pacific Tsunami Museum
P.O. Box 806 • Hilo, Hawai'i 96721
(808) 935-0926 • (808) 935-0842
tsunami@tsunami.org

TSUNAMI RECOLLECTION SUMMARY

Tsunami Recollections summarized by OSF
Tsunami Year/Location:
Brief summary of experience noting details of other family members and friends (names, age, sex, relationship) where not mentioned in the Biographical Data Sheet

(b)

Fig. 2. (below). Summary Oral/Video Tape Release Form used by the Pacific Tsunami Museum (it should be noted that legal requirements may cause variations in the format). A unique Interview Code is assigned to each interviewee record. Separate archival numbers are logged in the searchable database (For Museum Reference only). When working in predominantly non-English speaking countries this form is translated into the appropriate language, so that interviewees understand what they are signing, although the English form is to be signed.

INTERVIEW CODE (Fig. 2)

Pacific Tsunami Museum
P.O. Box 806 • Hilo, Hawai'i 96721
(808) 935-0926 • (808) 935-0842
tsunami@tsunami.org

ORAL/VIDEO TAPE RELEASE FORM

I, ____(**interviewee**), hereby give, grant, assign, forever to the Pacific Tsunami Museum, as a donation, all my rights, title and interest in and to the recorded conversations made by me and

____(**interviewer**), as further described below, and any written summaries or transcripts or copies thereof and any documentation, materials and things accompanying the recordings, for use and disposition by the Pacific Tsunami Museum or its successors and assign in any lawful way including publication, except as specified below, if any:

The **audio/video** tape-recorded material is further described as follows:

Number of tapes**:** _________ Date(s) **recorded:** _____________ Place**:**____________

Length of interview**:** ____________ Camera crew**:**_______________________

Tsunami Year(s)/Location(s): ____

Topics:____

____

Signed: _________________________________ **Date:** ___________
(interviewee)

Interviewee Address:____

____

Signed: _________________________________ **Date:** ___________
(interviewer)

THE FOREGOING MATERIAL IS ACCEPTED FOR THE PACIFIC TSUNAMI MUSEUM

by________________________________,________________on_______________
(name) (title) (date)

For Museum Reference only Accession No. _________________ Object ID No. _________________

Fig. 3. A representative set of questions for tsunami interviews. It is important to note that for the bulk of the interview the interviewee is allowed to talk freely without interruption.

Pacific Tsunami Museum

P.O. Box 806
Hilo, HI 96721
808-935-0926 • 808-935-0842
tsunami@tsunami.org

INTERVIEW QUESTIONNAIRE

A. PRE-EVENT QUESTIONS

1. What is your full name? When and where were you born?

2. Did you grow up in the area the tsunami struck?

3. Could you describe the area you were in before the tsunami (e.g. house, building, street, people around you)? Tell us what it looked like.

B. EVENT QUESTION – *LET THEM TALK*

4. Please describe your experience starting the morning of that day?

AND THEN, IF NOT SAID DURING INTERVIEW

5. What can you tell us about the actual tsunami? For example, how many waves were there? How high was it/were they? How far inland did it/they go? Did you hear any sound associated with any of the waves?

C. POST-EVENT QUESTIONS

6. How did the tsunami affect the area and the people in the area?

7. Where do you live now? If you moved because of the tsunami, please tell us why.

8. What would be your advice to people who hear a tsunami warning, feel a large earthquake, and/or see the sea recede?

GOVERNING EQUATIONS FOR MULTI-LAYERED TSUNAMI WAVES

Monzur Alam Imteaz
Senior Lecturer, Faculty of Engineering & Industrial Sciences, Swinburne University of Technology, Hawthorn, Melbourne, VIC3122, AUSTRALIA.
Email: mimteaz@swin.edu.au

Fumihiko Imamura
Professor, Disaster Control Research Centre, Tohoku University, Sendai, JAPAN.

Jamal Naser
Senior Lecturer, Faculty of Engineering & Industrial Sciences, Swinburne University of Technology, Hawthorn, Melbourne, VIC3122, AUSTRALIA.

ABSTRACT

In order to develop generalized governing equations for multi-layered long wave system, a three layer system was considered. It was anticipated that equations for top layer and bottom layer will be independent on number of intermediate layer(s) and equation for intermediate layer will be generalized depending on number of intermediate layers. However, from derived equations, it is found that only top layer equations are independent of number of intermediate layers; equations for all other layers are dependent on number, extent and density of intermediate layer(s). Momentum and continuity equations for the top layer are exactly same as in the case of earlier developed governing equations for two layered system. Continuity equation for the bottom layer is also exactly same as in the case of two-layered system. Momentum equation for the bottom layer is dependent on extent and density of top layer as well as all intermediate layers. Continuity equation for intermediate layer is affected by levels of immediate bottom layer. Momentum equation for the intermediate layer is affected by extent and density of upper layer(s). Six governing equations, two for each layer are derived from Euler equations of motion and continuity, assuming long wave approximation, negligible friction and interfacial mixing. This paper depicts details derivations of the governing equations.

1. INTRODUCTION

Multi-layered flow is related with many environmental phenomena. Thermally driven exchange flows through doorways to oceanic currents, salt water intrusion in estuaries, spillage of the oil on the sea surface, spreading of dense contaminated water, sediment laden discharges into lakes, generation of lee waves behind a mountain range and tidal flows over sills of the ocean are examples of multi-layered flow. In hydraulics, this type of flow is often termed as gravity current. An extensive review on hydrodynamics of various gravity currents was provided by Simpson, J.E. (1982).

Tsunamis are generated due to disturbances of free surfaces caused by not only seismic fault motion, but also landslide and volcanic eruptions (Imamura and Imteaz, 1995). Tsunami waves are also affected by density differences along the depth of ocean. There are some studies on two-layered long waves or flows in the case of underwater landslide generated tsunamis (Hampton, 1972; Parker, 1982; Harbitz, 1991; Jiang & Leblond, 1992). Imamura & Imteaz (1995) developed a linear numerical model on two-layered long wave flow, which was successfully validated by a rigorous analytical solution. Later the linear model was extended to a non-linear model and effects of non-linearity were investigated (Imteaz & Imamura, 2001).

Madsen et al. (2002) developed a model of multi-layered flow based on Boussinesq-type equations, which are suitable for shallow depth flow. Lynett and Liu (2004) developed another model of multi-layered flow using piecewise integration of Laplace equation for each individual layer and expanded the model for deep water. This paper provides detailed derivation of multi-layered flow equations based on Navier-Stokes equation (Fig. 1).

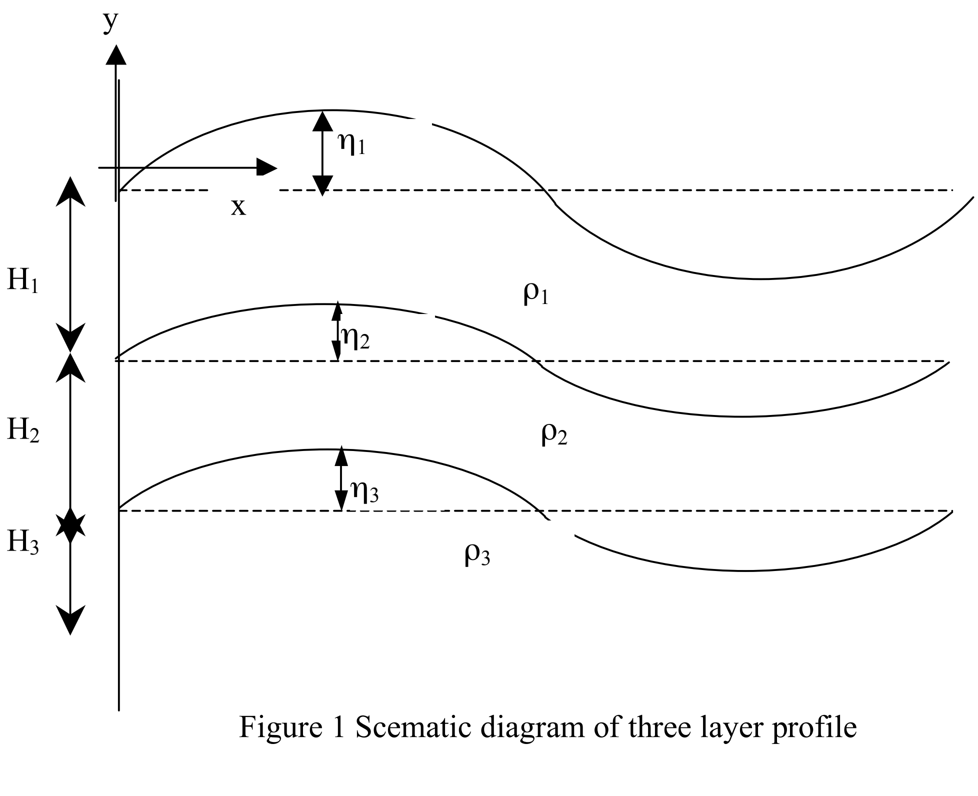

Figure 1 Scematic diagram of three layer profile

2. THEORETICAL CONSIDERATION

Considering two-dimensional case and a three-layered system, continuity equations are as follows:

For upper layer,

$$\frac{\partial u_1}{\partial x} + \frac{\partial v_1}{\partial y} = 0 \tag{1}$$

For intermediate layer,

$$\frac{\partial u_2}{\partial x} + \frac{\partial v_2}{\partial y} = 0 \tag{2}$$

For bottom layer,

$$\frac{\partial u_3}{\partial x} + \frac{\partial v_3}{\partial y} = 0 \tag{3}$$

Momentum equations in X-direction are as follows:

For upper layer,

$$\frac{\partial u_1}{\partial t} + u_1 \frac{\partial u_1}{\partial x} + v_1 \frac{\partial u_1}{\partial y} = -\frac{1}{\rho_1} \frac{\partial P_1}{\partial x} \tag{4}$$

For intermediate layer,

$$\frac{\partial u_2}{\partial t} + u_2 \frac{\partial u_2}{\partial x} + v_2 \frac{\partial u_2}{\partial y} = -\frac{1}{\rho_2} \frac{\partial P_2}{\partial x} \tag{5}$$

For bottom layer,

$$\frac{\partial u_3}{\partial t} + u_3 \frac{\partial u_3}{\partial x} + v_3 \frac{\partial u_3}{\partial y} = -\frac{1}{\rho_3} \frac{\partial P_3}{\partial x} \tag{6}$$

Where,
u = Uniform velocity over the depth along x-direction
v = Uniform velocity over the depth along y-direction
g = Acceleration due to gravity
P = Hydrostatic pressure of fluid
ρ = Density of fluid
't' represents for time
Subscripts '1', '2' and '3' denotes for upper layer, intermediate layer and bottom layer respectively.

3. BOUNDARY CONDITIONS

Considering a function along any flow streamline, which is constant with time and differentiating it with time, the following boundary conditions have been derived.

At top surface (i.e. at $y = \eta_1$),

$$\frac{\partial \eta_1}{\partial t} + u_1 \frac{\partial \eta_1}{\partial x} = v_1 \tag{7}$$

At interface between top layer and intermediate layer (i.e. at $y = \eta_2 - h_1$),

$$\frac{\partial \eta_2}{\partial t} + u_1 \frac{\partial \eta_2}{\partial x} = v_1 + u_1 \frac{\partial h_1}{\partial x} \tag{8}$$

$$\frac{\partial \eta_2}{\partial t} + u_2 \frac{\partial \eta_2}{\partial x} = v_2 + u_2 \frac{\partial h_2}{\partial x} \tag{9}$$

At interface between bottom layer and intermediate layer (i.e. at $y = \eta_3 - h_1 - h_2$),

$$\frac{\partial \eta_3}{\partial t} + u_2 \frac{\partial \eta_3}{\partial x} = v_2 + u_2 \frac{\partial h_2}{\partial x} + u_2 \frac{\partial h_1}{\partial x} \tag{10}$$

$$\frac{\partial \eta_3}{\partial t} + u_3 \frac{\partial \eta_3}{\partial x} = v_3 + u_3 \frac{\partial h_2}{\partial x} + u_3 \frac{\partial h_1}{\partial x} \tag{11}$$

At bottom (i.e. at $y = -h_3 - h_1 - h_2$),

$$u_3 \left(\frac{\partial h_1}{\partial x} + \frac{\partial h_2}{\partial x} + \frac{\partial h_3}{\partial x}\right) = -v_3 \tag{12}$$

Where,
η_1 = Water surface elevation above still water level of layer '1'
η_2 = Water surface elevation above still water level of layer '2'
η_3 = Water surface elevation above still water level of layer '3'
h_1 = Still water depth of layer '1'
h_2 = Still water depth of layer '2'
h_3 = Still water depth of layer '3'

4. GOVERNING EQUATIONS

After integrating continuity equations along the depth, applying some substitution and boundary conditions, following governing equations can be derived considering hydrostatic pressure distribution.

For upper layer- Continuity equation,

$$\frac{\partial M_1}{\partial x} + \frac{\partial(\eta_1 - \eta_2)}{\partial t} = 0 \tag{13}$$

Momentum equation,

$$\frac{\partial M_1}{\partial t} + \frac{\partial(M_1^2 / D_1)}{\partial x} + g D_1 \frac{\partial \eta_1}{\partial x} = 0 \tag{14}$$

For intermediate layer- Continuity equation,

$$\frac{\partial M_2}{\partial x} + \frac{\partial(\eta_2 - \eta_3)}{\partial t} = 0 \tag{15}$$

Momentum equation,

$$\frac{\partial M_2}{\partial t} + \frac{\partial(M_2^2 / D_2)}{\partial x} + g D_2 \left\{ \frac{\alpha_1}{\alpha_2} \left(\frac{\partial \eta_1}{\partial x} + \frac{\partial h_1}{\partial x} - \frac{\partial \eta_2}{\partial x} \right) + \frac{\partial \eta_2}{\partial x} - \frac{\partial h_1}{\partial x} \right\} = 0 \tag{16}$$

For lower layer-
Continuity equation,

$$\frac{\partial M_3}{\partial x} + \frac{\partial \eta_3}{\partial t} = 0 \tag{17}$$

Momentum equation,

$$\frac{\partial M_3}{\partial t} + \frac{\partial(M_3^2 / D_3)}{\partial x} + g D_3 \left\{ \alpha_1 \left(\frac{\partial \eta_1}{\partial x} + \frac{\partial h_1}{\partial x} - \frac{\partial \eta_2}{\partial x} \right) + \frac{\partial \eta_3}{\partial x} - \frac{\partial h_1}{\partial x} - \frac{\partial h_2}{\partial x} + \alpha_2 \left(\frac{\partial \eta_2}{\partial x} + \frac{\partial h_2}{\partial x} - \frac{\partial \eta_3}{\partial x} \right) \right\} = 0 \tag{18}$$

Where,
η_1 = Water surface elevation above still water level of layer '1'
η_2 = Water surface elevation above still water level of layer '2'
η_3 = Water surface elevation above still water level of layer '3'
$D_1 = \eta_1 + h_1 - \eta_2$, $D_2 = h_2 + \eta_2 - \eta_3$, $D_3 = h_3 + \eta_3$, $\alpha_1 = \rho_1/\rho_3$, $\alpha_2 = \rho_2/\rho_3$
h_1 = Still water depth of layer '1'
h_2 = Still water depth of layer '2'
h_3 = Still water depth of layer '3'

$$M_1 = \int_{-h_1+\eta_2}^{\eta_1} u_1 \, dy, \quad M_2 = \int_{-h_1-h_2+\eta_3}^{-h_1+\eta_2} u_2 \, dy, \quad M_3 = \int_{-h_1-h_2-h_3}^{-h_1-h_2+\eta_3} u_3 \, dy$$

Above derived equations can be further simplified neglecting non-linear terms, assuming small amplitude waves (i.e. $\eta << h$ and $D \approx h$) and no variations of 'h' along x direction (i.e. $\partial h/\partial x=0$).
Final simplified equations are as follows:

For upper layer - Continuity equation,

$$\frac{\partial M_1}{\partial x} + \frac{\partial(\eta_1 - \eta_2)}{\partial t} = 0 \tag{19}$$

Momentum equation,

$$\frac{\partial M_1}{\partial t} + g\, h_1 \frac{\partial \eta_1}{\partial x} = 0 \tag{20}$$

For intermediate layer - Continuity equation,

$$\frac{\partial M_2}{\partial x} + \frac{\partial(\eta_2 - \eta_3)}{\partial t} = 0 \tag{21}$$

Momentum equation,

$$\frac{\partial M_2}{\partial t} + g\, h_2 \left\{ \frac{\alpha_1}{\alpha_2} \left(\frac{\partial \eta_1}{\partial x} - \frac{\partial \eta_2}{\partial x} \right) + \frac{\partial \eta_2}{\partial x} \right\} = 0 \tag{22}$$

For lower layer - Continuity equation,

$$\frac{\partial M_3}{\partial x} + \frac{\partial \eta_3}{\partial t} = 0 \tag{23}$$

Momentum equation,

$$\frac{\partial M_3}{\partial t} + g\, h_3 \left\{ \alpha_1 \left(\frac{\partial \eta_1}{\partial x} - \frac{\partial \eta_2}{\partial x} \right) + \frac{\partial \eta_3}{\partial x} + \alpha_2 \left(\frac{\partial \eta_2}{\partial x} - \frac{\partial \eta_3}{\partial x} \right) \right\} = 0 \tag{24}$$

From the derived equations, it is found that momentum equation for upper layer is not affected by the properties of adjacent layer (layer underneath). However, continuity equation of upper layer is affected by surface elevation of intermediate layer. Continuity equation for intermediate layer is affected by the surface elevation of bottom layer. Momentum equation for intermediate layer is affected by density and spatial change of surface elevation of upper layer. Continuity equation for bottom layer is not affected by either uppermost layer or intermediate layer. However, momentum equation of bottom layer is affected by densities and spatial changes in surface elevations of all the layers above it. Properties of all these equations are outlined in Table 1.

TABLE 1 Affect of a particular layer for a particular equation from adjacent layer(s)

Layer	Equation	Effect from adjacent layer
Upper layer	Continuity	• Water surface elevation of intermediate layer
	Momentum	• Not affected
Intermediate layer	Continuity	• Water surface elevation of bottom layer
	Momentum	• Spatial change of water surface elevation of upper layer • Density of upper layer
Bottom layer	Continuity	• Not affected
	Momentum	• Spatial change of water surface elevation of upper layer • Spatial change of water surface elevation of intermediate layer • Density of upper layer • Density of intermediate layer

Differentiating continuity equations with 't' and momentum equations with 'x' and then subtracting each from other, three different equations (one for each layer) can be deduced as follows:

For upper layer-

$$\frac{\partial^2 \eta_1}{\partial t^2} - \frac{\partial^2 \eta_2}{\partial t^2} - gh_1 \frac{\partial^2 \eta_1}{\partial x^2} = 0 \tag{25}$$

For intermediate layer-

$$\frac{\partial^2 \eta_2}{\partial t^2} - \frac{\partial^2 \eta_3}{\partial t^2} - gh_2 \left[\frac{\alpha_1}{\alpha_2} \left(\frac{\partial^2 \eta_1}{\partial x^2} - \frac{\partial^2 \eta_2}{\partial x^2} \right) + \frac{\partial^2 \eta_2}{\partial x^2} \right] = 0 \tag{26}$$

For lower layer-

$$\frac{\partial^2 \eta_3}{\partial t^2} - gh_3 \left[\alpha_1 \left(\frac{\partial^2 \eta_1}{\partial x^2} - \frac{\partial^2 \eta_2}{\partial x^2} \right) + \frac{\partial^2 \eta_3}{\partial x^2} + \alpha_2 \left(\frac{\partial^2 \eta_2}{\partial x^2} - \frac{\partial^2 \eta_3}{\partial x^2} \right) \right] = 0 \tag{27}$$

Substituting Equation (26) to Equation (25) and rearranging,

$$\frac{\partial^2 \eta_1}{\partial t^2} - gh_1 (1 + \alpha_3 \beta_1) \frac{\partial^2 \eta_1}{\partial x^2} - gh_2 (1 - \alpha_3) \frac{\partial^2 \eta_2}{\partial x^2} - \frac{\partial^2 \eta_3}{\partial t^2} = 0 \tag{28}$$

Substituting Equation (27) to Equation (26) and rearranging,

$$\frac{\partial^2 \eta_2}{\partial t^2} - gh_2\left[(1-\alpha_3)+\beta_2(\alpha_2-\alpha_1)\right]\frac{\partial^2 \eta_2}{\partial x^2} - gh_3\left(\alpha_1\frac{\partial^2 \eta_1}{\partial x^2}+\frac{\partial^2 \eta_3}{\partial x^2}-\alpha_2\frac{\partial^2 \eta_3}{\partial x^2}\right)=0 \quad (29)$$

In Equations 28 & 29, $\alpha_3=\rho_1/\rho_2$, $\beta_1=h_2/h_1$ and $\beta_2=h_3/h_2$. From Equations 27, 28 & 29 wave celerity for each layer can be defined as:

$$C_1=\sqrt{gh_1(1+\alpha_3\beta_1)}$$
$$C_2=\sqrt{gh_2(1+\beta_2(\alpha_2-\alpha_1))}$$
$$C_3=\sqrt{gh_3(1-\alpha_2)}$$

5. CHARACTERISTICS OF MULTI-LAYER EQUATIONS

It is found that the developed governing equations are complicated having influence from upper and/or lower layer flow. However, wave celerities for three different layers are derived as shown above. Wave celerity of a particular layer can be compared with the wave celerity of other layer considering reasonable values of the associated parameters.

Figure 2 shows the relationship of normalized celerity of upper layer with β_1 for different α_3 values. Upper layer celerity increases with the increase of both the β_1 and α_3 values having a power relationship.

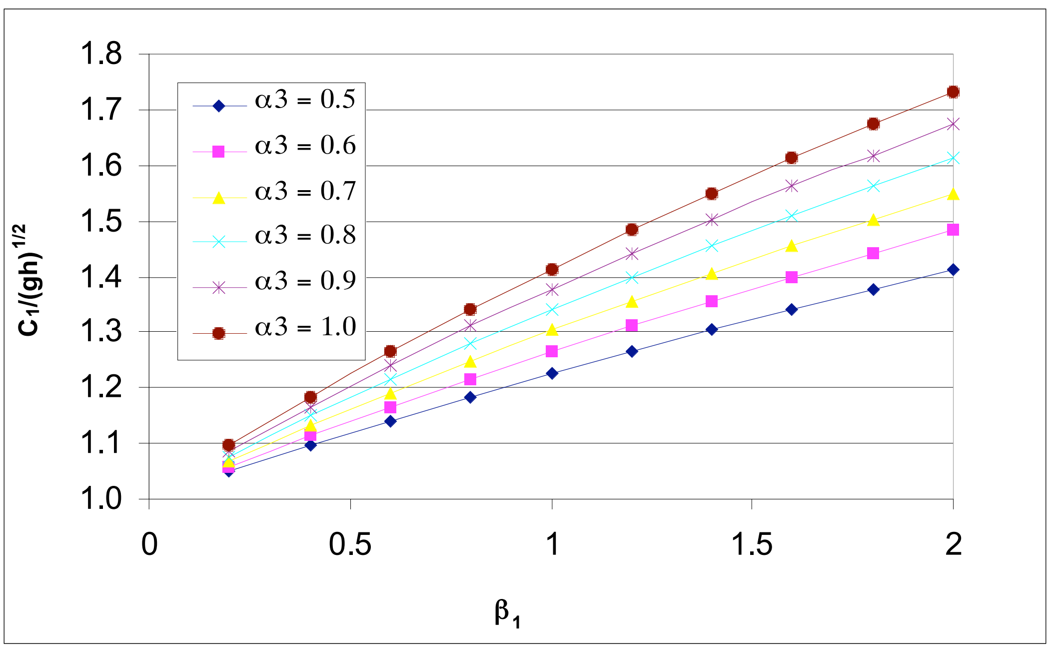

Figure 2 Relationship of normalized celerity of upper layer with β_1

Figure 3 shows the relationship of normalized celerity of intermediate layer with β_2 for different $(\alpha_2 - \alpha_1)$ values. Intermediate layer celerity increases with the increase of both the β_2 and $(\alpha_2 - \alpha_1)$ values having a power relationship. However, normalized celerity of lower layer depends only on the ratio of density of intermediate layer to the density of lower layer (i.e. $\alpha_2 = \rho_2/\rho_3$).

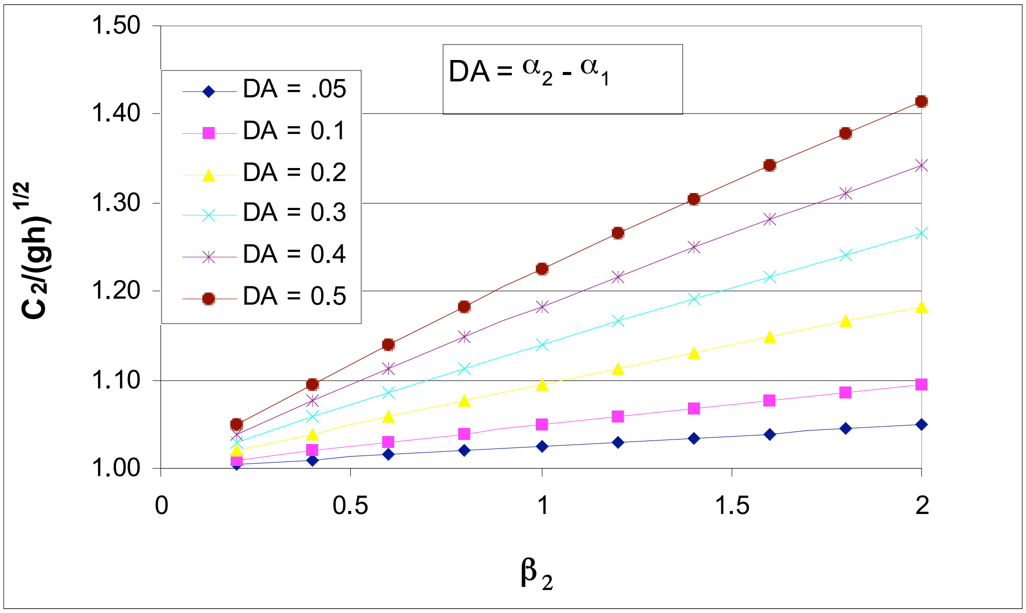

Figure 3 Relationship of normalized celerity of intermediate layer with β_2

Celerity decreases rapidly with the increase of α_2 values as shown in Figure 4.

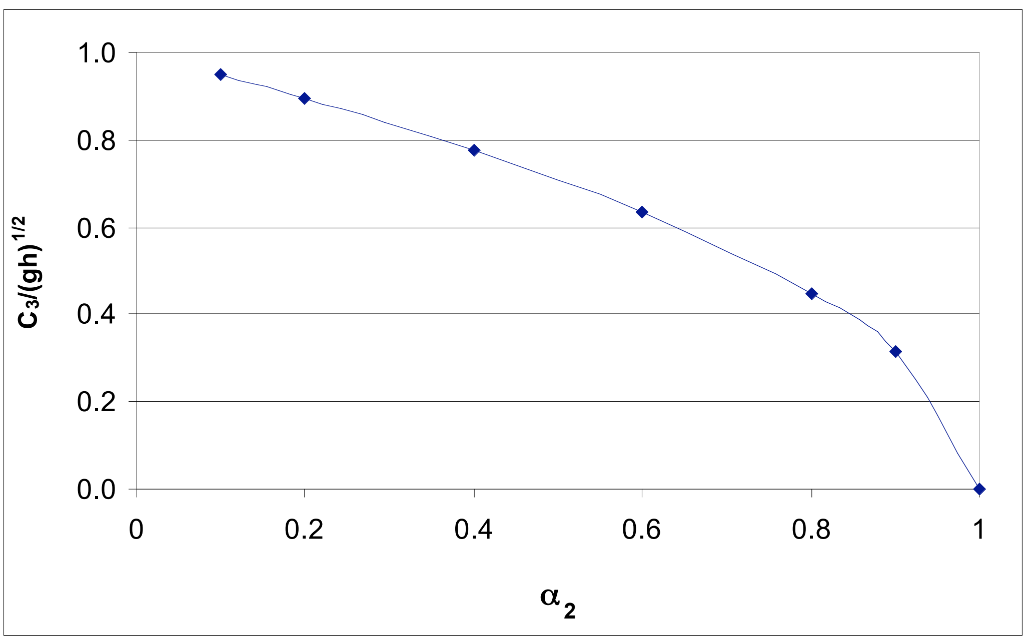

Figure 4 Relationship of normalized celerity of lower layer with α_2

Figure 5a shows the relationship of C_1/C_2 with $(\alpha_2 - \alpha_1)$ for different values of α_3 and Figure 5b shows the relationship of C_1/C_2 with α_3 for different $(\alpha_2 - \alpha_1)$ values. It is shown that C_1/C_2 decreases significantly with the increase of $(\alpha_2 - \alpha_1)$. However, C_1/C_2 increases with the increase of α_3.

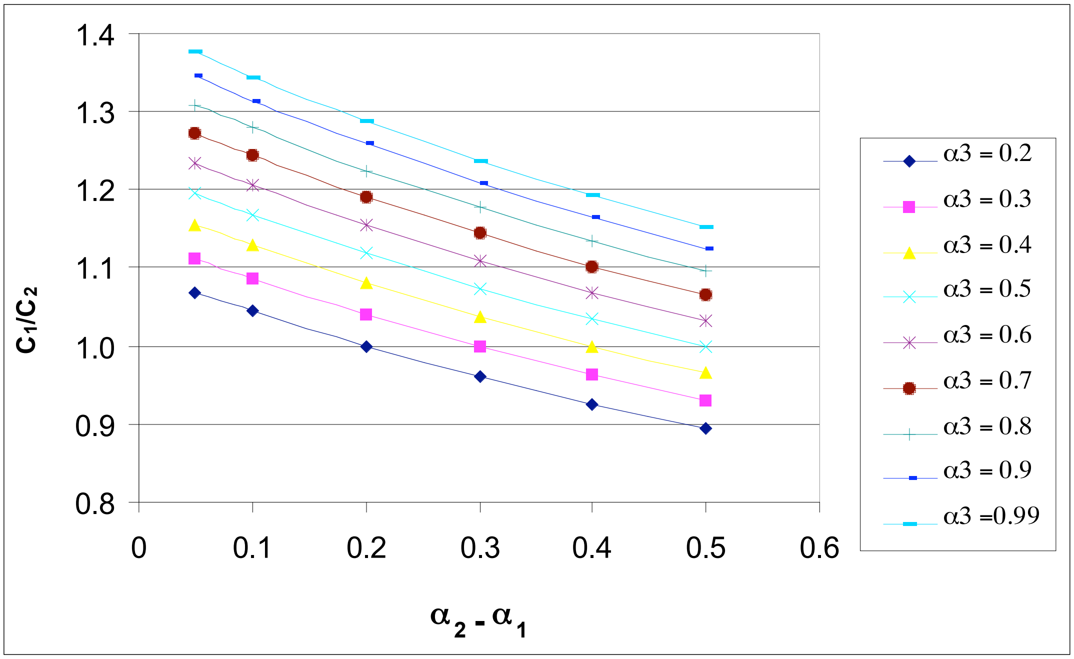

Figure 5a Relationship of C_1/C_2 with $(\alpha_2 - \alpha_1)$

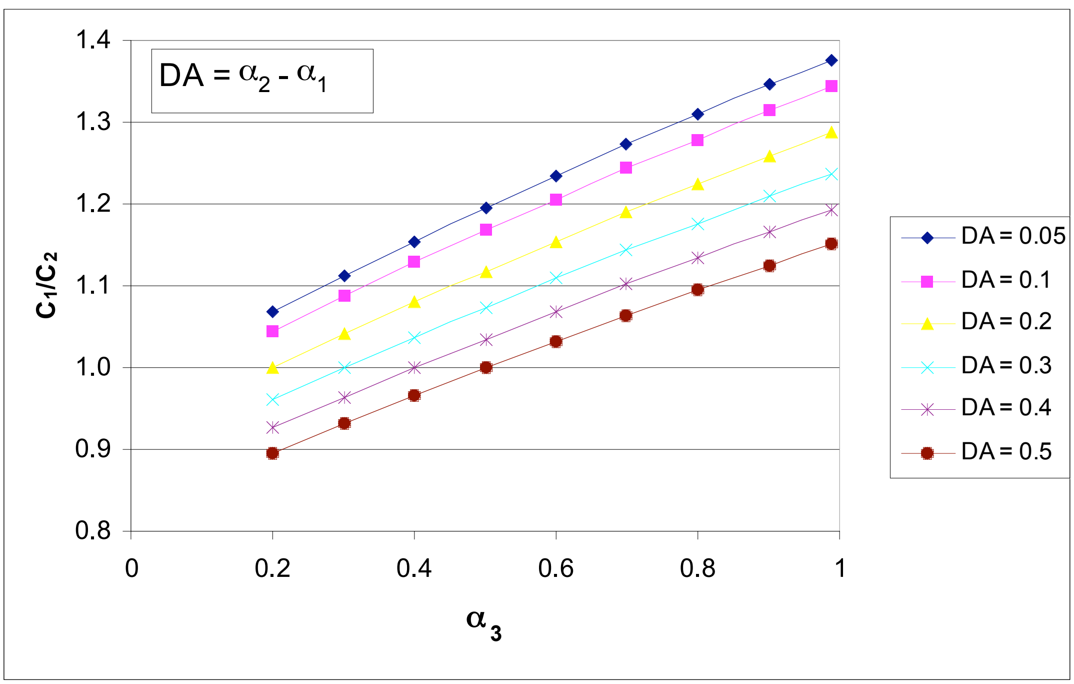

Figure 5b Relationship of C_1/C_2 with α_3

Figure 6a shows the relationship of C_2/C_3 with $(\alpha_2 - \alpha_1)$ for different values of α_2 and Figure 6b shows the relationship of C_2/C_3 with α_2 for different $(\alpha_2 - \alpha_1)$ values. It is shown that C_2/C_3 increases almost linearly with the increase of $(\alpha_2 - \alpha_1)$. However, for a particular value of $(\alpha_2 - \alpha_1)$, C_2/C_3 increases almost exponentially with the increase of α_2.

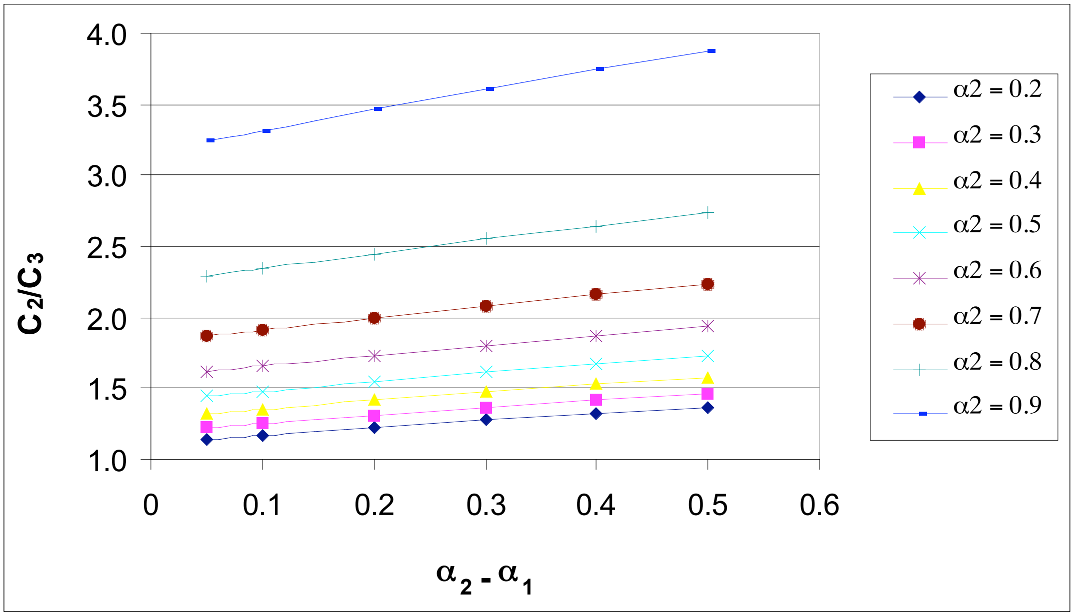

Figure 6a Relationship of C_2/C_3 with $(\alpha_2 - \alpha_1)$

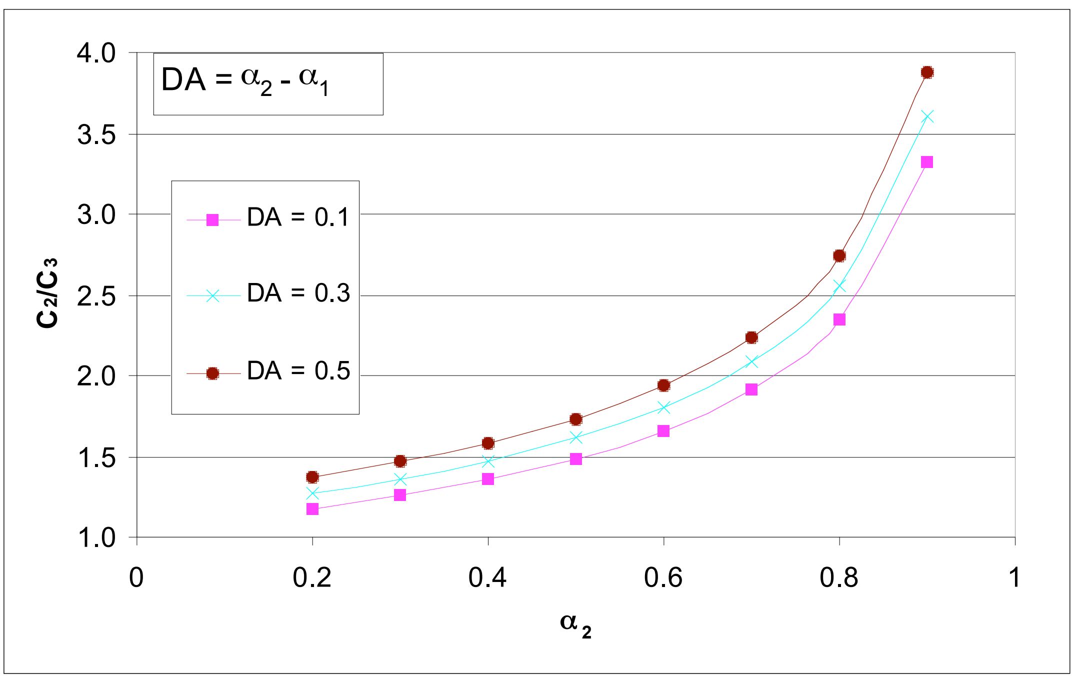

Figure 6b Relationship of C_2/C_3 with α_2

Figure 7a shows the relationship of C_1/C_3 with α_3 for different values of α_2 and Figure 7b shows the relationship of C_1/C_3 with α_2 for different α_3. It is shown that C_1/C_3 increases almost linearly with the increase of α_3. However, for a particular value of α_3, C_1/C_3 increases almost exponentially with the increase of α_2.

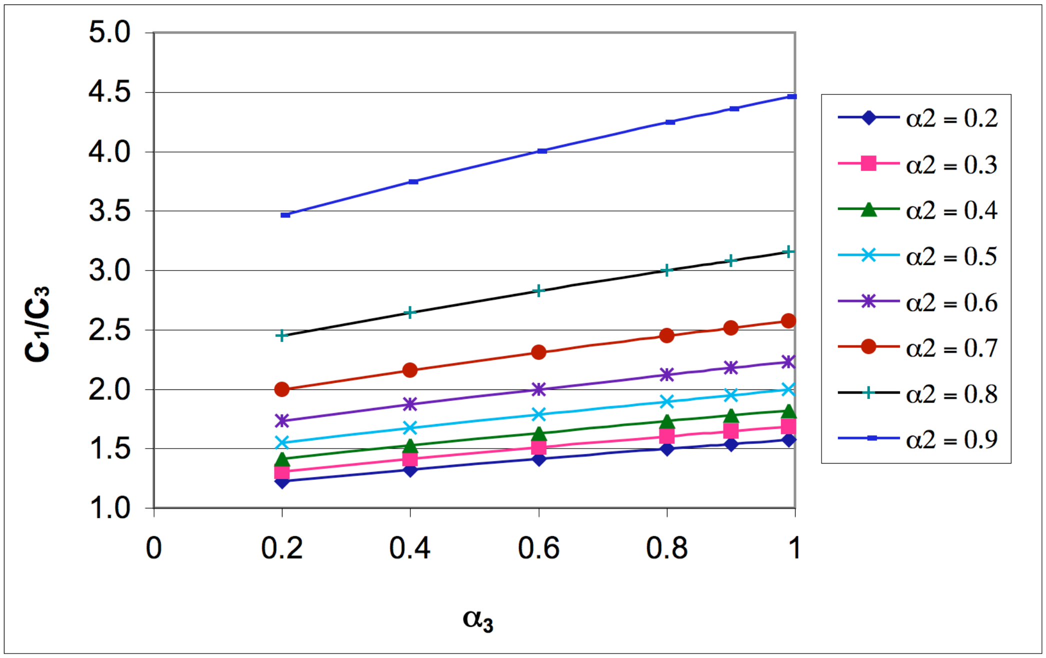

Figure 7a Relationship of C_1/C_3 with α_3

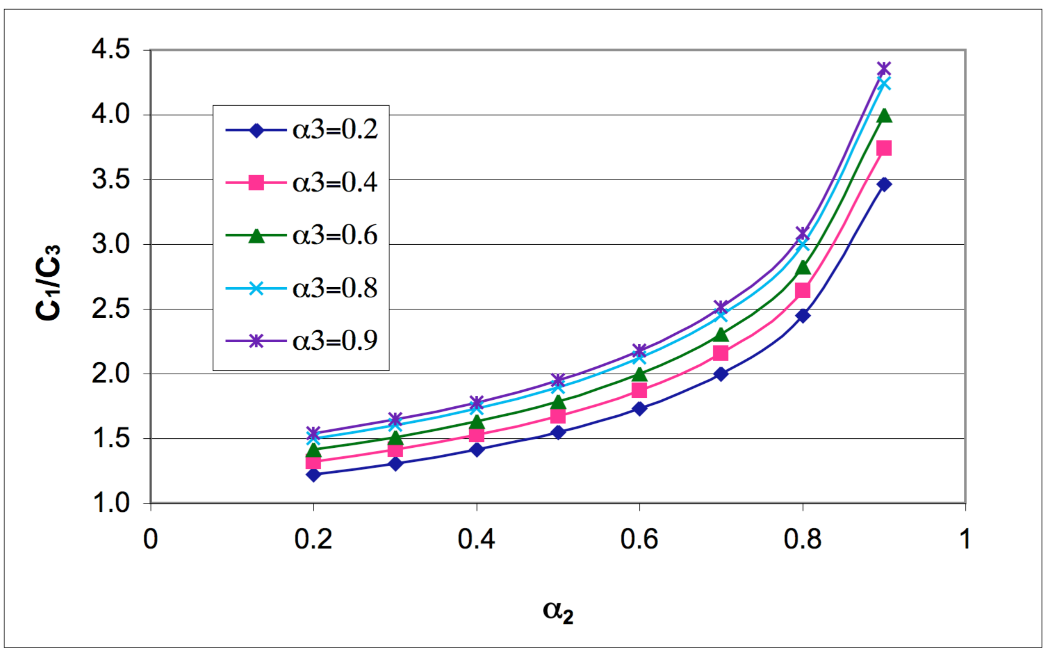

Figure 7b shows the relationship of C_1/C_3 with α_2

Figure 8a shows the relationship of C_2/C_3 with α_2 for different values of β and Figure 8b shows the relationship of C_2/C_3 with $(\alpha_2 - \alpha_1)$ for different values of α_2. It is shown that C_2/C_3 increases almost exponentially with the increase of α_2. However, for a particular value of α_2, C_2/C_3 increases almost linearly with the increase of $(\alpha_2 - \alpha_1)$.

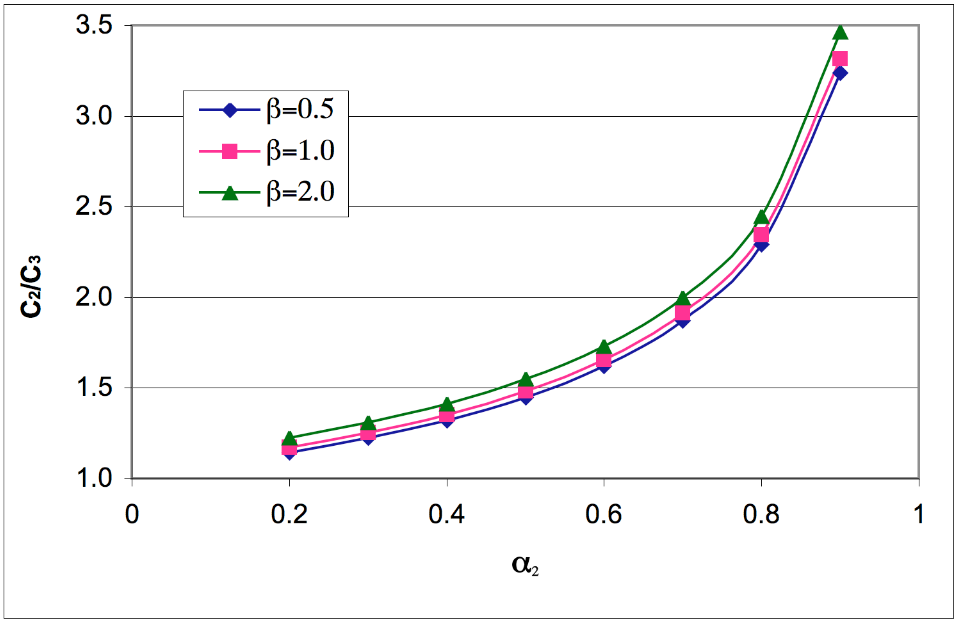

Figure 8a shows the relationship of C_2/C_3 with α_2

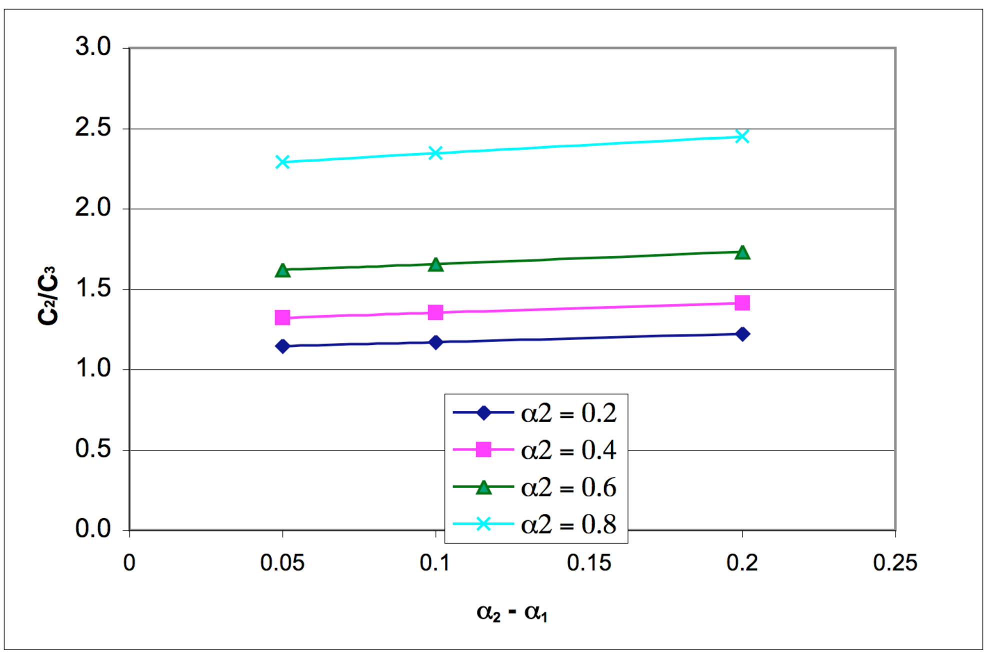

Figure 8b shows the relationship of C_2/C_3 with $(\alpha_2 - \alpha_1)$

6. CONCLUSION

Governing equations for three layered tsunami waves were developed transforming Navier-Stoke equations using proper boundary conditions and long wave approximation. Developed equations for three layers can be easily transformed to equations of any number of layers, considering the effect(s) of adjacent layer(s). Eventually three separate equations (one for each layer) were derived. From these derived equations wave celerity for each layer wave was extracted and presented. Characteristics of wave celerity for each layer were discussed in relation to relative density and/or relative layer depth. In regards to effect of adjacent layer on a particular layer, it is found that the upper layer wave equation is only affected by water surface elevation of intermediate layer. However, intermediate layer equation is affected by water surface elevation of bottom layer, spatial change of elevation of upper layer and density of upper layer. Bottom layer equation is affected by spatial changes and densities of all the layers above this layer. A generalized system of governing equations, which will be able to calculate wave properties for any number of layers, can be developed from these equations. A numerical finite difference model of developed equations will be developed and simulated. For numerical simulations, as Staggered Leap-Frog scheme produced very good results for a two-layer long wave system, it expected that same numerical scheme would be able to produce good results for a multi-layered system as well.

REFERENCES

Hampton, M. H. (1972) The Role of Subaqueous Debris Flow in Generating Turbidity Currents, J. *Sedimentary Petrology,* Vol. 42, No. 4, pp.775-793.

Harbitz, C. (1991) Numerical Simulations of Slide Generated Water Waves, *Sci. of Tsunami Hazards,* Vol. 9, No. 1, pp. 15-23.

Imamura, F. & Imteaz, M. A. (1995) Long Waves in Two-Layers: Governing Equations and Numerical Model, *Sci. of Tsunami Hazards,* Vol. 13, No. 1, pp. 3-24.

Imteaz, M. A. & Imamura, F. (2001) A Non-linear Numerical Model for Stratified Tsunami Waves and its Application, *Sci. of Tsunami Hazards,* Vol. 19, pp. 150-159.

Jiang, L. & Leblond, P. H. (1992) The Coupling of Submarine Slide and the Surface Waves which it Generates, J. Geophys. Res., Vol. 97, No. C8, pp.12713-12744.

Lynett, P. & Liu, P.L.-F. (2004) Linear Analysis of the Multi-layer Model, Journal of Coastal Engineering, Vol. 51, pp. 439-454.

Madsen, P.A., Bingham, H.B. & Liu, H. (2002) A New Boussinesq Method for Fully Nonlinear Waves from Shallow to Deep Water, J. Fluid Mech., Vol. 462, pp. 1-30.

Parker, G. (1982) Conditions for Ignition of Catastrophically Erosive Turbidity Currents, *Marine Geology,* Vol. 46, pp. 307-327.

Simpson, J.E. (1982) Gravity Currents in the Laboratory, Atmosphere and Ocean, Ann. Rev. Fluid Mech., Vol. 14, pp. 213-234.

NOTATIONS

□ = Density of fluid
M = Discharge per unit width of flow
□ = Water surface elevation above still water level
D = Total depth of layer
□ = Ratio of density of upper layer fluid to lower layer fluid
x = Distance along downstream direction
y = Distance perpendicular to x-direction
u = Uniform velocity over the depth along x-direction
v = Uniform velocity along y-direction
g = Acceleration due to gravity
P = Hydrostatic pressure of fluid
□ = Ratio of depths of lower layer to upper layer
C = Wave celerity

ANALYSIS AND DESIGN OF REINFORCED EARTH WALL FOR SHORE PROTECTION SYSTEM AGAINST TSUNAMI

Amit Srivastava
Department of Civil Engineering Indian Institute of Science
Bangalore – 560 012, India

G. L. Sivakumar Babu
Department of Civil Engineering, Indian Institute of Science
Bangalore – 560 012, India

Tel:+91-80-22933124; FAX: +91-80-23600404
E-mail: gls@civil.iisc.ernet.in

ABSTRACT

The evaluation and design of coastal shore protection works for tsunamis assumed considerable importance following the impact of the 26th December 2004 tsunami in India and other countries of Asia. The lack of proper guidelines made matters worse and resulted in the great damage that occurred. Subsequent surveys indicated that scour resulting from high water velocities was one of the prime reasons in the damage of simple structures. In some cases, it became apparent that sea walls were helpful in minimizing the degree of damage. The objective of the present study is to illustrate how proper design analysis for expected wave heights as well as the use of flexible systems such as geocells, are likely to provide better shoreline protection. Protective systems can be designed that can withstand wave forces that correspond to a variety of incidence probabilities. The present study illustrates such an analytical design approach that is necessary for a shoreline protection system and provides references to relevant wave height data for the east coast of India.

1. INTRODUCTION

The structures such as bulkheads, seawalls or revetments are generally provided along the beach or the shoreline, for the protection of upland area from the wave action of the sea water. Unlike wind generated waves, tsunamis are generated due to underwater displacement of tectonic plates, volcanic eruption or landslide and travel unnoticed across the open sea with amplitude of only few centimeters and a velocity as high as 800 km/hr. However, as they approach sea shore, they gradually build up and in areas where the topography of the seabed is especially suited they reach heights in meters with a speed of 10 to 80 km/hr. The terminal effects of tsunami are observed in terms of damage to coastal areas including structural damages, high water mark in the region, scour, and deposition of both sediments and floating debris. Due to lack of awareness and the proper implementation of protective measures, the recent tsunami on 26th December 2004 caused enormous damage to the economic and social life of the people in India and other countries of Indian Ocean (BAPPENAS 2005). It has also prompted various researchers and practitioners in the world to provide suitable protective measures and design guidelines for the protection of seashore area from such events in future. The provision of massive concrete sea wall with vertical, concave or stepped seaward faces are given in some of the design manuals (USACE) for protecting the upland area from intense wave actions. Such structures, being perfect wave reflectors, create possibilities for scouring of the beach in front of them. In the present study, the authors propose the use of reinforced earth retaining structure that can meet all the design requirements in terms of its stability and strength and it will be able to protect the upland area.

2. TSUNAMI - STRUCTURE INTERACTION

As tsunami propagates shoreward, large turbulent bores rush inland and cause significant damages to the coastal area. In general, the problems related to tsunami waves is studied in terms of its development, shape and propagation characteristics, run up at the shore (Whitman, 1958; Keller et al., 1960; Shen et al., 1963; Hoyt et al., 1989; Yeh et al., 1989; Titot et al., 1995) and its interaction with the structures that are constructed near the shore or that are built as barrier (Cumberbatch, 1960; Kamel, 1970; Ramsden and Raichlen, 1990; Ramsden, 1996). In the present study, only the last part i.e., the tsunami-structure interaction is presented in terms of estimation of hydrodynamic force on the structure built as a tsunami barrier and also the stability analysis of such structures from those forces.

3. CHARACTERISTICS OF TSUNAMI (Wave Velocity, Wave Length and Wave Period)

The estimation of wave characteristics of the tsunami waves such as design wave height, wave period, wave length and wave velocity are the important input parameters. In the classical tsunami theory, a rigid floor overlain by an incompressible, homogeneous and non-viscous ocean subjected to constant gravity field is considered. The phase velocity (C) and the group velocity (C_g) of surface gravity wave on a flat ocean of uniform depth are given by Eq. 1 and Eq. 2 respectively (USACE).

$$C = \sqrt{\frac{gh \tanh(kh))}{kh}} \qquad (1)$$

$$C_g = C\left[\frac{1}{2} + \frac{kh}{\sinh(2kh)}\right] \quad (2)$$

h is the ocean depth below sea water level (SWL); g = acceleration due to gravity (9.81 m/sec^2) and k is defined as the wave number which is related to the wave length as below:

$$k = \frac{2\pi}{\lambda} \quad (3)$$

The wave number also satisfies the relation shown in Eq. 4.

$$\omega^2 = g\,k\tanh(kh) \quad (4)$$

The water waves are either treated as long wave (shallow water waves) or short wave (deep water waves). In the long wave approximation (λ>>h, 1/k>>h), as kh→0 tanh(kh) ≈ kh; the phase velocity and group velocity are dependent on the depth of sea floor (h) only and can be obtained using the Eq. 5.

$$C = C_g \approx \sqrt{gh} \quad (5)$$

In the short wave approximation (kh→∞), the waves generated are dispersive in nature. The dispersive waves are those waves whose velocity of propagation depends on the wave frequency (ω). For estimating the phase velocity and group velocity, the following Eq. 6 is used.

$$C = 2C_g = \sqrt{g\lambda/2\pi} \quad (6)$$

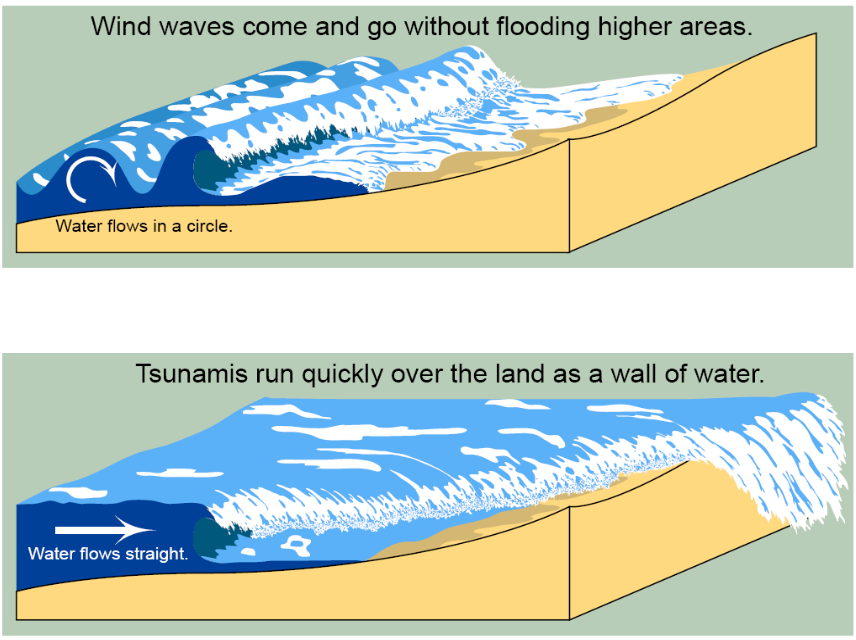

Figure 1. Difference between winds generated wave and tsunami

Unlike wind generated waves, tsunami waves [Fig (1)] behave like shallow water waves for the longer wave period and it behaves like deep water waves at their shortest periods.
Although a tsunami may be generated in the deep ocean; it becomes dangerous when it reaches the sea shore area as a shallow water wave having very long period (upto or more than 1 hr) and wave length (in kilometers). For the known values of wave period (T) and depth of sea floor below the SWL (h), the estimation of wave length (λ) can be made using the following Eq. 7 (USACE).

$$\lambda = \frac{gT^2}{2\pi}\sqrt{\tanh\left(\frac{4\pi^2 h}{T^2 g}\right)} \qquad (7)$$

The above equation explicitly gives λ in terms of wave period T and sufficiently accurate with the maximum error is 10% when $h/\lambda \approx 1/2$(USACE). The estimation of design wave height and wave period need the statistical analysis of the past records. The significant wave height (H_s) is defined as the average height of the highest one-third of the waves in a wave train. In the similar way, H_{10} and H_1 can be defined as the average of the 10 % and 1% of the highest waves in a wave train respectively. Assuming a Rayleigh distribution for the wave heights in a wave train, the values of H_{10} and H_1 will be approximately 1.27 H_s and 1.67 H_s. In the design, the choice of wave height depends on the type of structure to be built. The wave heights H_1, H_1 to H_{10} and H_s or H_{10} is preferred for rigid, semi rigid and flexible structure respectively (USACE).
The different wave periods are defined as the period of the peak energy density of the spectrum (T_p), average wave period (T_z) and significant wave period (T_s). In the design, an appropriate choice of design wave height (H) and wave period (T) depends on the designer's choice or the recommendations given by the codes or the design manuals.

4. DESIGN OF VERTICAL BARRIER

The estimation of maximum breaking wave height at the structure and the amount of expected run up helps in deciding the hydrodynamic force coming on the structure and the provision of maximum crest level to prevent an overtopping. The proposed site specific vertical reinforced soil wall [Fig (2)] is designed and its external and internal stability is checked under static and dynamic condition against the forces coming from the backfill material.

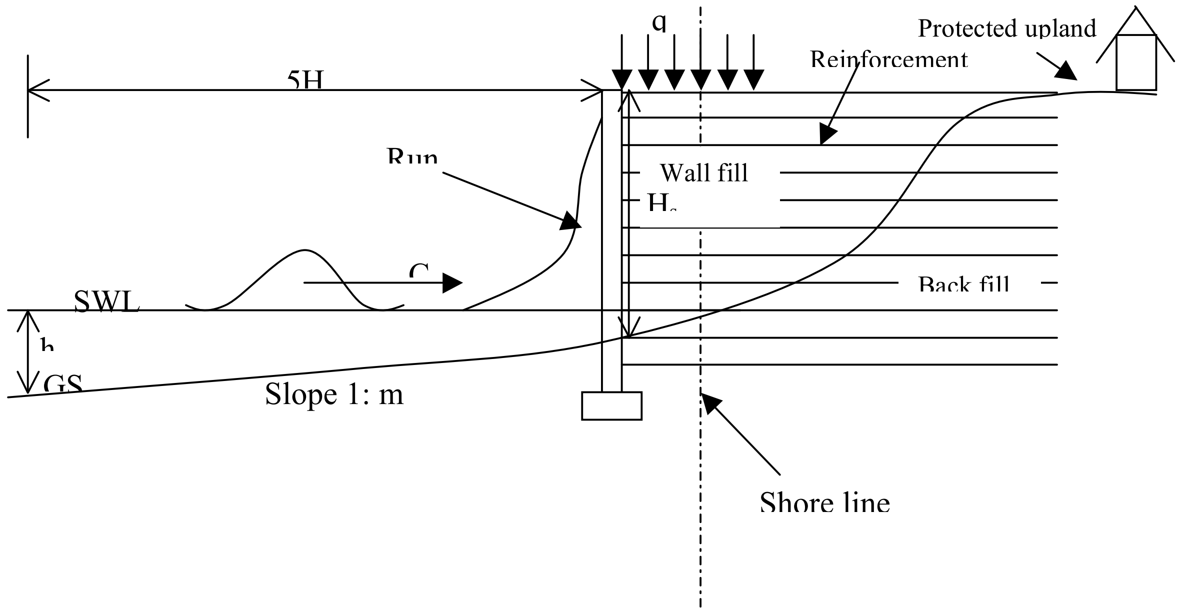

Figure 2. Schematic diagram showing wave propagation, run up and reinforced earth wall as a barrier

It will help in deciding the base width of the structure (B). After estimating the value of hydrodynamic forces on the structure due to impact of tsunami waves from the front, it is compared with the passive resistance of the back fill soil using friction circle method. The depth of scour at the toe is also a major factor in the stability of such structures and design for proper preventive measures are given.

The Height (H_s) of the structure

The total height of the structure [Fig (2)] above the still sea water level is the sum of design wave height (H) plus extra allowance given for the wave run up, anticipated settlement of the structure and additional freeboard to avoid overtopping. The following Eq. 8 can be used to calculate the wave run up on the wall (USACE).

$$\frac{Rg}{C^2} = 1.467(H/h)^{-0.0504} \qquad (8)$$

C is the celerity of the water wave, H is the wave height and h is the still water depth at a distance of 5H from the structure.

5. STABILITY ANALYSIS

Following the stability analysis, the base width (B) of the wall can be estimated

5.1 Static condition

In the stability analysis of the reinforced soil wall, the external and internal stability is ensured by giving proper dimensions to the structure and reinforcement. The basic external failure mechanism is sliding, overturning and bearing failure and the basic internal mechanism are tension failure and wedge/pull out failure. Considering the height of the wall as H_s and the set of values for cohesion, angle of internal friction, angle of wall friction and unit weight for the wall fill (subscript 1) and for the back fill (subscript 2) as (c_1, ϕ_1, δ_1, γ_1 c_1, ϕ_2, δ_2, γ_2). Take γ_{b1} and γ_{b2} as the submerged unit weight of the wall fill and backfill. As most of the areas of east coast of India are located in the seismic zone III (IS: 1893-2000), the dynamic stability of the structure should be ensured taking the horizontal and vertical seismic coefficients as α_0 and α_v. Further a surcharge of intensity q (Live load) is assumed to act on the wall and back fill portion.

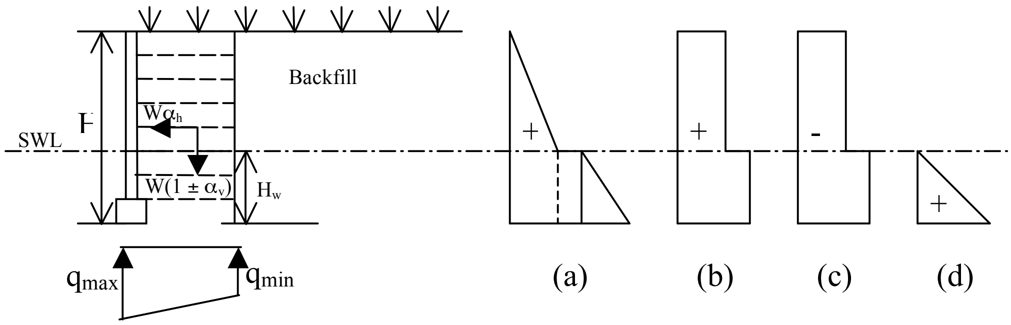

Figure 3. Section of reinforced earth wall (a) Earth pressure due to backfill soil (b) Earth pressure due to surcharge on the backfill (c) Earth pressure due to cohesion of the backfill soil (d) water pressure

From the Fig (3), the coefficients of active earth pressures above water table (K_a) and below water table (K'_a) can be calculated as below.

$$K_a = \frac{\cos^2 \phi_2}{\cos \delta} \frac{1}{\left[1 + \left\{\frac{\sin(\phi_2 + \delta_2)\sin(\phi_2)}{\cos \delta_2}\right\}^{1/2}\right]^2} \tag{9}$$

The value of K'_a is obtained from the Eq. 9 by replacing δ_2 with $\delta_2/2$. The following equations give the estimate for $P_{a\gamma}$, P_{aq}, P_{ac} and P_{aw}.

$$P_{a\gamma} = \frac{1}{2}\gamma_2 K_a (H - H_w)^2 + \gamma_2 K'_a H_w (H - H_w) + \frac{1}{2}\gamma_{b2} K'_a H_w^2 \tag{10}$$

$$P_{aq} = qK_a (H - H_w) + qK'_a H_w \tag{11}$$

$$P_{ac} = 2c\sqrt{K_a}(H - H_w) + qK'_a H_w \tag{12}$$

$$P_{aw} = \frac{1}{2}\gamma_w H_w^2 \tag{13}$$

As the water table is on the both side of the wall, the effect of P_{aw} is neglected. Total static earth pressure P_T is the sum of $P_{a\gamma}$, P_{aq} and P_{ac}.
The moment of static earth pressure about the base can be obtained as below.

$$M_{a\gamma} = \frac{1}{2}\gamma_2 K_a (H - H_w)^2 . \left(H_w + \frac{H - H_w}{3}\right) + \gamma_2 K'_a H_w (H - H_w)\frac{H_w}{2} + \frac{1}{2}\gamma_{b2} K'_a H_w^2 \frac{H_w}{3} \tag{14}$$

$$M_{aq} = qK_a (H - H_w)\left(H_w + \frac{H - H_w}{2}\right) + qK'_a H_w \frac{H_w}{2} \tag{15}$$

$$M_{ac} = c\sqrt{K_a}(H + 2H_w)(H - H_w) + c\sqrt{K_a} H_w^2 \tag{16}$$

$$M_{aw} = \frac{1}{6}\gamma_w H_w^3 \tag{17}$$

Neglecting the effect of M_{aw}, the total moment about base (M_T) will be $M_{a\gamma}$+M_{aq}-M_{ac}.

5.2 Dynamic condition

As per IS: 1893-4-2000**,** the dynamic increment due to seismic load is computed as below. The coefficient of active earth pressure for the soil above the water table (K_{ad}) is obtained as below.

$$K_{ad} = \frac{(1 \pm \alpha_v)\cos^2(\phi_2 - \psi)}{\cos\psi \cos(\delta_2 + \psi)} \frac{1}{\left[1 + \left\{\frac{\sin(\phi_2 + \delta_2)\sin(\phi_2 - \psi)}{\cos(\delta_2 + \psi)}\right\}^{1/2}\right]^2} \tag{18}$$

Where $\psi = \tan^{-1} \frac{\alpha_h}{1 \pm \alpha_v}$

The coefficient of active earth pressure for the dynamic case for soil below the water table is obtained replacing δ and ψ with δ/2 and $\tan^{-1} \frac{\gamma_{s2}}{\gamma_{s2} - 1} \frac{\alpha_h}{1 \pm \alpha_v}$ respectively.

The lateral dynamic increment in active case is obtained using the Eq. 19.

$$P_{a\gamma i} = \frac{1}{2}\gamma_2 (K_{ad} - K_a)\frac{(H - H_w)^2}{H}(H + 2H_w) + \frac{1}{2}\left[K'_{ad} - K'_a\right]\frac{H_w^2}{H}\left[3\gamma_2 (H - H_w) + \gamma_{b2} H_w\right] \tag{19}$$

The additional dynamic increment due to surcharge q is calculated using Eq. 20.

$$P_{aqi} = 3q\left[(K_{ad} - K_a)\frac{H^2 - H_w^2}{2H} + (K'_{ad} - K'_a)\frac{H_w^2}{2H}\right] \tag{20}$$

The value of moment of dynamic increment about the base of the wall and dynamic increment due to surcharge q is obtained from Eq. 21 and Eq. 22.

$$M_{a\gamma i} = \frac{\gamma_2 (K_{ad} - K_a)(H - H_w)^2}{4H}\left(H^2 + 2HH_w + 3H_w^2\right) + \frac{(K'_{ad} - K'_a)H_w^3}{4H}\left[4\gamma_2 (H - H_w) + \gamma_{b2} H_w\right] \tag{21}$$

$$M_{aqi} = \frac{q(K_{ad} - K_a)(H - H_w)}{H}\left(H^2 + H_w^2 + HH_w\right) + \frac{q(K'_{ad} - K'_a)H_w^3}{H} \tag{22}$$

The weight of the wall (W_w)

$$W_w = L\{\gamma_1 (H - H_w) + \gamma_{s1} H_w\} \tag{23}$$

Effective weight of the wall W'_w

$$W'_w = L\{\gamma_1 (H - H_w) + \gamma_{s1} H_w - \gamma_w H_w\} \tag{24}$$

The moment of weight of the wall about toe (M_w).

$$M_w = W_w \left(L/2 \right) \tag{25}$$

Surcharge force on the wall (Q) per unit width

$$Q = q.L \tag{26}$$

The horizontal and vertical seismic force on the weight of the wall will be $\alpha_h W$ and $\pm\alpha_v W$. The moment of seismic force acting on the weight of the wall (M_{sw}) is given below.

$$M_{sw} = \frac{L}{2}\left[\gamma_1 \left(H^2 - H_w^2\right) - \gamma_{s1} H_w^2\right]\alpha_h \pm W_w \alpha_v \frac{L}{2} \tag{27}$$

The moment of the seismic forces on the surcharge acting on the wall (M_{sq}).

$$M_{sq} = Q\alpha_h H \pm Q\alpha_v \frac{L}{2} \tag{28}$$

Now after calculating all the forces for static and dynamic conditions, the external stability of the structure is checked as described in the next section.

6. Check for the external stability of the structure

6.1 Factor of safety against sliding

The horizontal component of force acting on the vertical wall is resisted by the resisting shearing force acting at the base on the structure. To make the wall safe against sliding, the resisting force should always be more than the driving horizontal force. In general, the factor of safety against sliding can be calculated using the following Eq. 29.

$$FS_{(sliding)} = \frac{\sum F_R}{\sum F_D} \tag{29}$$

Where $\sum F_R$ = sum of the horizontal resisting forces and $\sum F_D$ = sum of the horizontal driving forces

In static condition

$$FS_s = \frac{\mu\left(W_w + Q\right)}{P_T} > 2.0 \tag{30}$$

In dynamic case

$$FS_s = \frac{\mu\left(W_w^{'} + Q\right)\left(1 \pm \alpha_v\right)}{P_T + P_{a\gamma i} + P_{aqi} + \left(W_w + Q\right)\alpha_h} > 1.5 \tag{31}$$

6.2 Factor of safety against overturning

The vertical retaining wall is also subjected to the overturning moment about its toe due to the action of the horizontal force at some height from the base of the wall. The factor of safe against overturning will be the ratio of the resisting moment (M_R) and the overturning moment (M_0) and can be evaluated easily.

In static condition:

$$F_{os} = \frac{\left(W_w^{'} + Q\right)\frac{L}{2}}{M_T} > 2.0 \tag{32}$$

In dynamic condition:

$$F_{od} = \frac{\left(W_w^{'} + Q\right)\left(1 \pm \alpha_v\right)\frac{L}{2}}{M_T + M_{a\gamma i} + M_{a\gamma i} + \alpha_h QH} > 1.5 \tag{33}$$

6.3 Factor of safety against bearing capacity

The vertical pressure is transmitted to the soil due to self weight of the structure and the moment caused by the horizontal force H. As shown in Fig (3), the base pressure varies linearly and it is maximum at toe and minimum at heel. The magnitude of the base pressure at the toe and heel can be determined using the following equations.

In Static case

$$q_{\max} = \frac{\left(W_w^{'} + Q\right)}{L} + M_T \frac{6}{L^2} < q_a \tag{34}$$

$$q_{\min} = \frac{W_w^{'} + Q}{L} - M_T \frac{6}{L^2} > 0.0 \tag{35}$$

In dynamic case

Net moment about the centre of base of wall

$$M_{nT} = M_T + M_{a\gamma i} + M_{aqi} + Q\alpha_h H \tag{36}$$

$$q_{\max} = \frac{(W_w' + Q)(1 \pm \alpha_v)}{L} + M_{nT}\frac{6}{L^2} > 1.25 q_a \quad (37)$$

$$q_{\min} = \frac{(W_w' + Q)(1 \pm \alpha_v)}{L} - M_{nT}\frac{6}{L^2} < 0.0 \quad (38)$$

q_a is the allowable bearing pressure of the base of the wall.

7. INTERNAL STABILITY

7.1 Tension failure

The tension force (T_i) per meter width in the grid at depth h_i is given as below.

$$T_i = K_{aw}\,\sigma_{vi}\,S_z \quad (39)$$

Where σ_{vi} is the maximum vertical pressure intensity.

Static case

For $h_i \le (H-H_w)$, Moment of pressure about center of horizontal section passing at depth h_i is given as.

$$M_1 = \frac{1}{6}\gamma_2 K_a h_i^3 + \frac{q h_i^2 K_a}{2} - \frac{6\sqrt{K_a}\,h_i^2}{2} \quad (40)$$

$$\sigma_{vi} = (\gamma_i h_i + q) + M_1\frac{6}{L^2} \quad (41)$$

For $h_i > (H-H_w)$, obtain the value of $M_{a\gamma}$, M_{aq} and M_{aw} by replacing H by h_i and H_w by ($h_{wi} = h_i - (H-H_w)$). The value of M2 is calculated as below neglecting the effect of M_{aw}.

$$M_2 = M_{a\gamma} + M_{aq} - M_{ac} \quad (42)$$

$$\sigma_{vi} = (\gamma_1 h_i + q) + M_2\frac{6}{L^2} \quad (43)$$

For satisfactory performance $T_i < R_T$
Where RT is the permissible design strength of reinforcement.

Dynamic case

For hi ≤ (H-H_w), obtain the value of M_3 and M_4 by replacing H and H_w by h_i and 0 in the expression M $_{a\gamma i}$ and M_{aqi}. The value of M_{nTi} will be as below.

$$M_{nTi} = M_1 + M_3 + M_4 + \alpha_h h_i \left(\frac{\gamma_1 L h_i}{2} + Q \right) \quad (44)$$

$$\sigma_{vi} = (\gamma_1 h_i + q)(1 \pm \alpha_v) + M_{nTi} \frac{6}{L^2} \quad (45)$$

For hi > (H-H_w), the value of M_5 and M_6 are calculated by replacing H by h_i and H_w by (h_{wi}=h_i-(H-H_w)) in the expression of $M_{a\gamma i}$ and M_{aqi}.

$$M_{nTi} = M_2 + M_5 + M_6 + \alpha_h L \left(\gamma_1 (H - H_w) \left\{ h_i - \frac{H - H_w}{2} \right\} + \gamma_{s1} \frac{(h_i - H + H_w)^2}{2} \right) + Q\alpha_h H \quad (46)$$

$$\sigma_{vi} = \left[\gamma_1 (H - H_w) + \gamma_{s1} (h_i - H + H_w)(1 \pm \alpha_v) + M_{nTi} \frac{6}{L^2} \right] \quad (47)$$

For satisfactory action
$T_i \geq 1.25\, R_T$

7.2 Wedge or Pull out failure

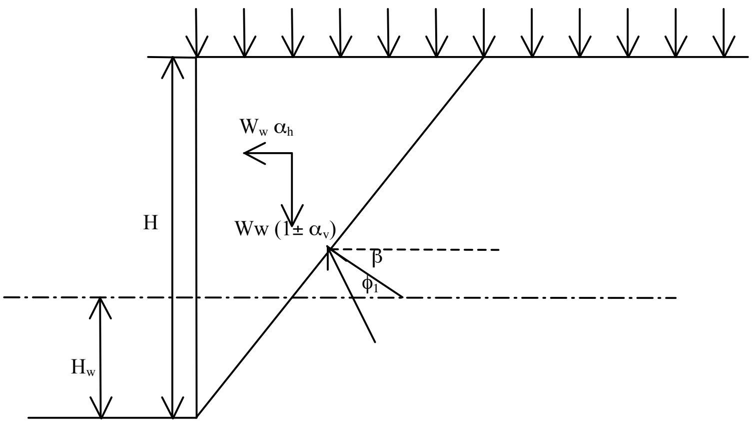

Figure 4. Forces considered in wedge/pullout failure in seismic condition

In Static case

The forces to be considered in the analysis [Fig (4)] are self weight of the fill in the wedge (W_w), uniformly distributed surcharge (q), resultant force (R) on the potential failure plain and total tension (T) in the reinforcements intercepted by the potential failure plain.

$$W_w = \left[\frac{1}{2}\gamma_s H_w^2 + \gamma_1 (H - H_w)\left[H_w + \frac{H - H_w}{2}\right]\right] \quad (48)$$

Considering the equilibrium of the wedge, the value of T can be obtained as

$$T = a_1 \frac{\tan\beta}{\tan(\phi_1 + \beta)} \quad (49)$$

Where $a_1 = qH + \frac{1}{2}\left[\gamma_s H_w^2 + \gamma_1 (H^2 - H_w^2)\right]$

To obtain the maximum value of T (T_{max}), the above equation is differentiated with respect to β and equated to zero.

$$T_{max} = a_2 \frac{\tan(45 - \phi_1 / 2)}{\tan(45 + \phi_1 / 2)} \quad (50)$$

The maximum tension per reinforcement = T_{max}/n which should be less than the allowable value.

In dynamic case

In seismic condition, the maximum value of tension (T_{max}) can be computed as below.

$$T_{max} = \frac{a_2 \tan\beta_c}{\tan(\phi_1 + \beta_c)} + a_3 \tan\beta_c \quad (51)$$

Where $\tan\beta_c = \frac{-2a_4 \pm \sqrt{4a_4^2 - 4(a_2^2 - a_5^2)}}{2(a_3 - a_5)}$

And $a_2 = \alpha_h a_1$, $a_3 = a_1(1\pm\alpha_v)$, $a_4 = a_3\cos2\phi_1 - a_3 + a_3\sin2\phi_1$ and $a_5 = a_3\sin2\phi_1 - a_2\cos2\phi_1$

The maximum tension per reinforcement = T_{max}/n that should be less than the allowable value. The anchorage length of reinforcement (L_{ip}) at depth h_1 can be obtained using the following equation.

Static case:

$$L_{ip} = \frac{T_i F_{ss}}{2\alpha \tan\phi_1 (\gamma_1 h_1 + q)} \quad (52)$$

Where h_i is the depth of first layer of reinforcement from top of the wall. F_{ss} = factor of safety, 2.0. $T_i = T_{max}/n$, α = coefficient of interaction.

Dynamic case:

$$L_{ip} = \frac{T_i F_{sd}}{2\alpha \tan\phi_1 (\gamma_1 h_1 + q)} \quad (53)$$

Where F_{sd} = factor of safety, 1.5.
The required length of the reinforcement = L_{ip} + (H-h_1) tanβ.

8. ESTIMATION OF WAVE FORCE

In the literature, analytical, experimental and numerical solutions (using finite difference codes) are available for estimating the hydrodynamic force on the wall due to tsunami waves (Cross 1967, Ramsden and Raichlen 1990, Ramsden 1996, Hamzah 2000). Ramsden (1996) gave empirical relationships (as shown below) for finding the hydrodynamic Force (F) and moment (M) on the vertical wall type barrier.

$$\frac{F}{F_1} = 1.325 + 0.347\left(\frac{H}{h}\right) + \frac{1}{58.5}\left(\frac{H}{h}\right)^2 + \frac{1}{7160}\left(\frac{H}{h}\right)^3 \quad (54)$$

The above equation is applicable for the range of values $0.62 \leq H/h \leq 30$ and can be used to estimate the maximum force due to bore impact. F_1 is the linear force scale (assuming hydrostatic distribution for the wave run up equal to two times the wave height) which is used to normalize F. The value of F_1 can be calculated as below.

$$F_1 = \frac{1}{2}\gamma\, b(2H + h_w)^2 \quad (55)$$

h_w is the water depth at the wall, γ is the unit weight of the water and b is the width of the wall.

$$\frac{M}{M_t} = 1.923 + 0.454\left(\frac{H}{h}\right) + \frac{1}{8.21}\left(\frac{H}{h}\right)^2 + \frac{1}{808}\left(\frac{H}{h}\right)^3 \quad (56)$$

The moment M_t is calculated using the Eq. 57 after assuming hydrostatic pressure distribution for the same assumption as R = 2H.

$$M_t = \frac{1}{6}\gamma\, b(2H + h_w)^3 \quad (57)$$

9. DESIGN CALCULATIONS

For the east coast of India which is situated in the seismic zone III (IS: 1893-2000), the values of horizontal (α_h) as well as vertical (α_v) seismic coefficient is taken as 0.08 and 0.04. The unit weight of the foundation soil and reinforced soil structure are taken as 20 and 22 kN/m^3. The soil strength parameters cohesion (c) and angle of internal friction (ϕ) are taken as 0 and 25° respectively.

9.1 Depth of foundation

The depth of foundation (D_f) can be obtained from the Rankine formula.

$$D_f = \frac{p}{\gamma}\left[\frac{1-\sin\phi}{1+\sin\phi}\right]^2 \tag{58}$$

Table (1) shows the calculation of the forces and moment due to striking of tsunami wave of height 3.5 m. To ensure the external and internal stability of the wall from the backfill soil, the base width of the wall is calculated as shown in Table (2). From these calculations the height and base width of the wall is obtained as 9.15 m and 15.0 m. The soil reinforcement is provided at a spacing of 0.5 m c/c. The internal stability of the wall for tension failure is checked under static and dynamic condition as shown in table (3) and table (4) respectively. From the pull out failure criterion, the maximum tensions in the reinforcement under static and dynamic loading conditions are obtained as 20.5 and 24.52 kN respectively. To check the resistance of the backfill soil from the hydrodynamic forces from the front, the friction circle method [Fig (5)], is used to find the passive resistance of the backfill soil. It was obtained as 1354.21 kN which is approx. 2.0 times more than the hydrodynamic force. Hence the above calculations show that the wall will be safe for all the forces coming on it and the design is adequate.

Table 1. Calculation of forces and moment at the wall due to tsunami waves

Estimation of Forces on the wall due to tsunami waves		
Depth of sea water at the wall (h_w)	**1.50**	m
Wave height (H)	**3.50**	m
Time period (T)	**1000.00**	sec
Celerity (C)	3.84	m/sec (13.8 km/hr)
Wave length (λ)	3836.01	wave length of tsunami = 3.8 km
Run up on the wall (R)	2.12	m
Free board	2.00	m
Total height of the structure (H_s)	9.12	**height of structure 9.15 m**
unit weight of water (γ_w)	9.79	kN/m^3
Unit weight of the reinforced soil (γ_s)	22.00	kN/m^3
slope (1: m)	20.00	
Estimation of hydrostatic force (F)		
Estimation of hydrostatic force (F_1)	**353.56**	kN
H/h	1.47	
F/F_1	1.87	
Hydrodynamic force on the structure F	**662.54**	kN
Estimation of Moment (M) on the wall		
Estimation of Moment M_t	**1001.74**	KN-m
M/M_t (using equation 11)	2.86	
Moment M	**2865.52**	KN-m

Table 2. The static and dynamic analysis of the reinforced soil wall

Stability Analysis of the reinforced soil wall
Soil properties for wall fill (c_1=0, ϕ_1=30, γ_1=18 kN/m3, δ_1=20, γ_{s1} = 22 kN/m3 and γ_{b1}=12 kN/m3)
Soil properties for wall fill (c_2=0, ϕ_2=27, γ_2=17 kN/m3, δ_2=18, γ_{s2} = 20 kN/m3 and γ_{b2}=10 kN/m3)
Surchagre load on the wall = 10 kN/m2
External stability Analysis
The coefficient of active earth pressure (Ka) in static case above the water table = 0.326
The coefficient of active earth pressure (K'a) in static case below the water table = 0.349
The total static earth pressure (PT) = 438.73 kN/ m width of wall
The total Moment of static pressure about the base (MT) = 3905.86 kN-m
Dynamic Increment
The horizontal (αh) and vertical seismic coefficient (αv)= 0.08 and 0.04 respectively
The coefficient of active earth pressure for the soil above the water level in dynamic case = 0.404
The value of lateral dynamic increment in active case (Pa γi)= 96.96 kN/m width of the wall
The value of additional dynamic increment due to uniform surcharge (Paqi) = 13.94 kN/ m width of the wall
The moment of dynamic increment about the base of the wall (Ma γi) in active case = 628.62 kN-m
The moment of dynamic increment about the base of the wall (Maqi) in active case due to surcharge q=115.05 kN-m
Assuming the base width of the wall = L
The weight of the wall (Ww) = 235.8 L
The effective weight of the wall (W'w) = 190.8 L
The moment of weight of wall about toe (Mw) = 117.9 L^2
The surcharge force on the wall (Q) = 10 L
The moment of surcharge force about toe (Mq) = 5 L^2
Seismic force on the weight of the wall
In horizontal direction = 18.86 L
In vertical direction = 9.43 L
The moment of seismic forces acting on the weight of the wall (Msw) = 292.06 L ± 4.716 L^2
Seismic forces acting on the wall due to surcharge load
Horizontal seismic force = 0.8 L
Vertical seismic force = 0.4 L
The moment of seismic forces due to the surcharge acting on the wall about toe (Msq) = 9.68L ± 0.2 L^2
The Factor of safety against sliding = 2.0
Static condition: The length L is obtained as 13.44 m
Dynamic condition: The length L is obtained as 14.87 m
Factor of safety against overturning = 2.0
Static condition: The length L is obtained as 9.15 m
Dynamic condition: The length L is obtained as 11.8 m
From the above analysis, the base width of the wall (L) is provided as 15 m
Check for tilting/bearing failure
Static condition: qmax = 241.00 kpa and qmin = 160.45 kPa
Dynamic condition: qmax = 357.03 kPa and qmin = 340.96 kPa

Table 3. Checking the internal stability of the reinforced wall in tension failure (Static condition)

Tension Failure (Static condition)								
h_i	M_1	σ_{vi}	Ti	$M_{a\gamma}$	M_{aq}	M_2	σ_{vi}	T_i
0.50	9.88	19.09	2.86					
1.00	39.96	28.38	4.33					
1.50	90.96	37.87	5.87					
2.00	163.55	47.57	7.49					
2.50	258.44	57.48	9.20					
3.00	376.31	67.61	10.99					
3.50	517.86	77.97	12.87					
4.00	683.78	88.56	14.83					
4.50	874.76	99.40	16.90					
5.00	1091.50	110.48	19.06					
5.50	1334.69	121.81	21.32					
6.00	1605.02	133.41	23.68					
6.50	1903.19	145.27	26.15					
7.00	2229.89	157.41	28.73					
7.50	2585.81	169.82	31.42					
8.00				473.81	17.99	491.80	158.72	29.76
8.50				571.85	31.76	603.61	168.79	32.07
9.00				684.72	46.41	731.13	179.02	34.46
9.50				813.30	61.92	875.22	189.40	36.93
10.00				958.45	78.31	1036.77	199.95	39.49
10.50				1121.06	95.58	1216.64	210.68	42.14
11.00				1301.99	113.71	1415.70	221.59	44.87
11.50				1502.11	132.72	1634.83	232.69	47.70
12.00				1722.30	152.60	1874.90	244.00	50.63

Table 4. Checking the internal stability of the reinforced wall in tension failure (Dynamic condition)

	Tension Failure (seismic condition)														
h_i	M3	M4	M_{Tni}	σ_{vi+}	σ_{vi-}	T_{i+}	T_{i-}	hi-(H-Hw)	M_5	M_6	M_{Tni}	σ_{vi+}	σ_{vi-}	T_{i+}	T_{i-}
0.50	0.08	0.20	24.65	20.76	17.72	3.11	2.66								
1.00	1.33	0.78	80.07	31.01	26.53	4.73	4.05								
1.50	6.71	1.76	169.93	41.59	35.67	6.45	5.53								
2.00	21.22	3.12	299.89	52.56	45.20	8.28	7.12								
2.50	51.80	4.88	477.61	63.99	55.19	10.24	8.83								
3.00	107.41	7.02	712.73	75.96	65.72	12.34	10.68								
3.50	198.98	9.56	1016.89	88.60	76.92	14.62	12.69								
4.00	339.46	12.48	1403.71	102.04	88.92	17.09	14.89								
4.50	543.74	15.80	1888.80	116.41	101.85	19.79	17.31								
5.00	828.75	19.50	2489.75	131.90	115.90	22.75	19.99								
5.50	1213.37	23.60	3226.16	148.69	131.25	26.02	22.97								
6.00	1718.50	28.08	4119.60	166.99	148.11	29.64	26.29								
6.50	2366.99	32.96	5193.64	187.02	166.70	33.66	30.01								
7.00	3183.73	38.22	6473.84	209.03	187.27	38.15	34.18								
7.50	4195.55	43.88	7987.73	233.28	210.08	43.16	38.87								
8.00								0.40	171.97	49.92	714.68	152.81	152.11	28.65	28.52
8.50								0.90	229.68	56.35	890.64	165.94	164.36	31.53	31.23
9.00								1.40	342.13	63.15	1137.41	179.75	177.29	34.60	34.13
9.50								1.90	540.86	70.33	1487.41	194.55	191.21	37.94	37.29
10.00								2.40	859.79	77.88	1975.43	210.68	206.45	41.61	40.77
10.50								2.90	1335.17	85.79	2638.59	228.48	223.38	45.70	44.68
11.00								3.40	2005.60	94.06	3516.35	248.35	242.36	50.29	49.08
11.50								3.90	2911.97	102.69	4650.49	270.68	263.81	55.49	54.08
12.00								4.40	4097.49	111.68	6085.08	295.89	288.14	61.40	59.79

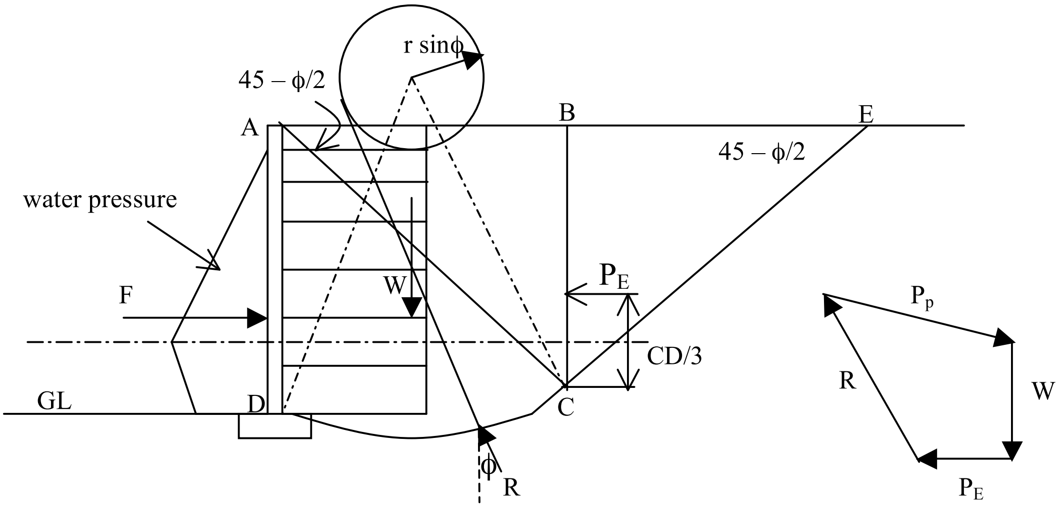

Fig. 5. Friction circle method employed to obtain the passive resistance of the backfill

9.2 Toe Protection

The toe of the structure should be protected from the scouring and undercutting due to passage of waves in order to make the structure stable. The extent of the toe scour depends on several factors like wave breaking (when occur at the toe), wave reflection and grain size distribution of the material. In the case of vertical sea wall structures, the toe material gives additional stability against overturning by providing passive resistance and therefore should be designed and maintained properly. It is suggested that the design of toe apron should be based on both geotechnical and hydraulic factors. From geotechnical point of view, the minimum width of the apron can be obtained using Rankine theory (USACE) and it should be more than the product of the height of the apron and Rankine passive earth pressure coefficient. From the hydraulic consideration, the width of the toe apron should be at least equal to the incident wave height. Fig (6) shows the arrangement for the toe protection. The total weight of the toe stone can be calculated using the following Eq. 59 (USACE).

$$W = \frac{\gamma_t H^3}{N_s^3 (S_t - 1)^3} \qquad (59)$$

Where Ns is the minimum design stability number obtained from the curve provided in Fig (6). γ_t and S_t are the unit weight and specific gravity of the stone material. H is the design wave height taken between H_1 and H_{10}.

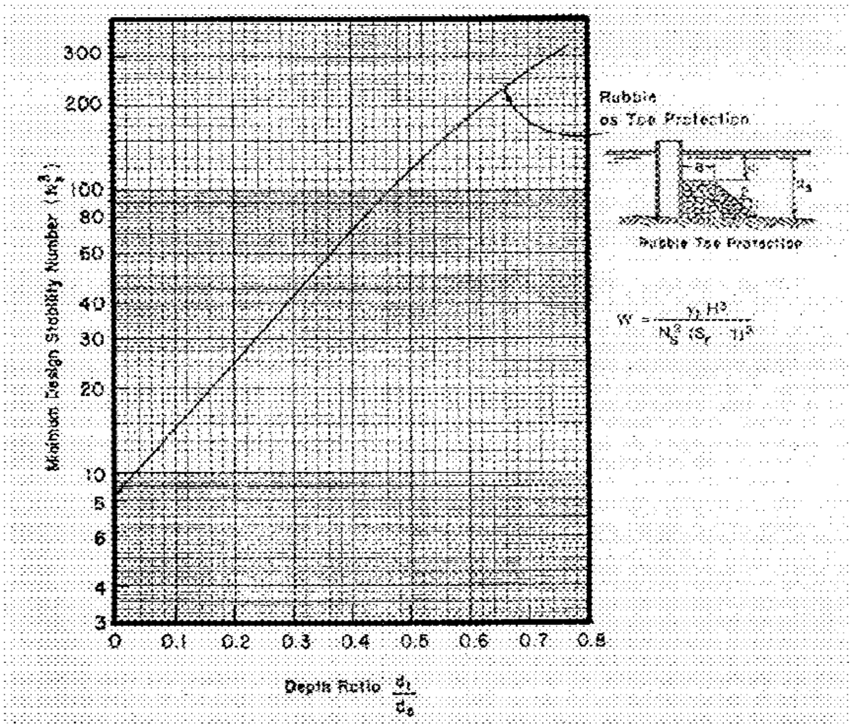

Figure 6. Value of Ns, toe protection design for vertical walls (from Brebner and Donnelly 1962)

10. CONCLUDING REMARK

In the present study, a vertical reinforced retaining wall is proposed for protecting the sea shore area in the event like tsunami. The procedures are given to find the hydrodynamic force expected to act on the structure and to check the external stability of the structure from different modes of failure. The advantage of using reinforced earth retaining wall can be said in terms of the economy and the flexibility of the structure. Being flexible, it has the capability of absorbing some part of kinetic energy of the water waves coming on it but the quantification of the same could be an active area of research in this field.

11. REFERENCES

BAPPENAS (2005). Indonesia: Preliminary damage and loss assessment, the December 26 2004 natural disaster. A technical report prepared by BAPPENAS and the international donor community. The article is available at the following web site: http://www.crid.or.cr/digitalizacion/pdf/eng/doc16324/doc16324.htm

Cross, R.H. (1967). Tsunami surge forces. Journal of waterways and harbor division ASCE. 93(4), 201-231.

Cumberbatch, E. (1960). The impact of a water wedge on a wall. Journal of fluid mechanics. 7(3), 353-373.

Hamzah, M.A., Mase, H., and Takayama, T. (2000). Simulation and experiment of hydrodynamic pressure on a tsunami barrier. Coastal Engineering, 1501-1507.

Hoyt, J.W. And Sellin, R.H. (1989). Hydraulic jumps as a mixing layers. Journal of hydraulic engineering division, ASCE. 115(12), 1607-1614.

Kamel, A.M. (1970). Laboratory study for design of tsunami barrier. J. Waterway. Horbor and Coastal Engrg. Division. 96(WW4), 767-779.

Keller, H.B., Levine, D.A. and Whitham, G.B. (1960). Motion of a bore over a sloping beach. Journal of fluid mechanics. 7(2), 302-316.

Ramsden, J.D. (1996). Forces on a vertical wall due to long waves, bores, and dry-bed surges. Journal of waterway, port, coastal, and ocean engineering, ASCE. 122(3), 134-141

Ramsden, J.D. and Raichlen, F. (1990). Forces on vertical wall caused by incident bores. Journal of waterway, port, coastal, and ocean engineering, ASCE. 116(5), 592-613

Shen, M.C. and Meyer, R.E. (1963). Climb of a bore on a beach Part 3: Run-up. Journal of fluid mechanics,16(1), 113-125.

Titov, V.V. and Synolakis, C.E. (1995). Modeling of breaking and nonbreaking long-wave evolution and runup using VTCS-2. Journal of waterway, port, coastal, and ocean engineering, ASCE, 121(6), 308-316.

USACE (2002). Coastal Engineering Manual. Part I-V.

Whitham, G.B. (1958). On the propagation of shock waves through regions of non-uniform area of flow. Journal of fluid mechanics, 4(4), 337-360.

Yeh, H.H., Ghazali, A. And Marton, I. (1989). Experimental study of bore run up”. Journal of fluid mechanics. 206, 563-578.

MULTIPLE LAYER IDENTIFICATION AND TRANSPORTATION PATTERN ANALYSIS FOR ONSHORE TSUNAMI DEPOSIT AS THE EXTENDING TSUNAMI DATA – A CASE STUDY FROM THE THAI ANDAMAN COAST

CHANCHAI SRISUTAM, JEAN-FRANK WAGNER

Department of Geology, University of Trier, D-54286 Trier, Germany
E-mail: chanchai50@yahoo.com, wagnerf@uni-trier.de

ABSTRACT

On 26th December 2004, a strong Indian Ocean earthquake of moment magnitude 9 generated a deadly tsunami that hit the west coast of southern Thailand and many coastal nations of the Indian Ocean. Two tsunami-affected areas on the Thai Andaman coast (Ao Kheuy beach and Khuk Khak beach) were investigated. Multiple sediment layers in the tsunami deposits are identified and are analyzed. The sediment transportation patterns are also determined. Tsunami deposits consist of graded sand layers overlying the pre-existing soil. The particle size profile of the tsunami sediment and the plot of grain-size standard deviation with depth are used to identify major layers in tsunami deposit. There are three major sediment layers in the tsunami deposit in the study areas. They reflect three depositional sequences created by three tsunami run-ups. The mean grain-size of tsunami deposit and the results of sediment trend analysis show that the tsunami deposit is generally fining upwards and landwards. Each major sediment layer is created by sediments settled from suspension in a set of run-up and backwash. The percentage by weight of sediment settled from suspension during the backwash is small when it is compared to the percentage by weight of sediment settled from suspension during the run-up. The 1st depositional sequence has higher quantity of coarse grain particles than the following depositional sequences. At a mild slope shore face, sediments are transported and deposited on land far from their origins. The number of major sediment layers in tsunami deposit can be used as the extending data for reconstructing individual tsunami run-up by using numerical and/or simple models.

Keywords: Tsunami deposit; depositional sequence; sediment layer identification; sediment transportation; extending tsunami data

INTRODUCTION

A sedimentary signature for onshore tsunami deposits has been defined (e.g. Nelson et al., 1996; Dawson and Shi, 2000; Whelan and Kelletat, 2003) but the particular hydrodynamic behavior of the long-period surge associated with tsunamigenic flooding is still under debate. In many tsunami studies, scientists have used data on tsunami run-up (e.g. number of tsunami run-ups, run-up height) to calibrate numerical models for undersea fault-generated and submarine landslide-generated tsunami (Dawson et al., 1991). Almost all cases, the number of tsunami run-ups have been based on eyewitness reports of the tsunami flood. This paper presents and describes methods to evaluate the number of tsunami run-ups and the tsunami sediment transportation pattern from the onshore tsunami deposit found after the December 26th, 2004 tsunami event (Indian Ocean tsunami) at Ao Kheuy beach and Khuk Khak beach, Phangnga province, Thailand.

STUDY AREAS

The study areas are Ao Kheuy beach and Khuk Khak beach located in Phangnga province, west coast of southern Thailand (Fig. 1). The reference coordinates are (432009E, 1029826N) for Ao Kheuy beach and (416269E, 961298N) for Khuk Khak beach. The geomorphic feature of study areas is described as open coastal zone. The pre-existing soils are coastal deposit and agricultural soil.

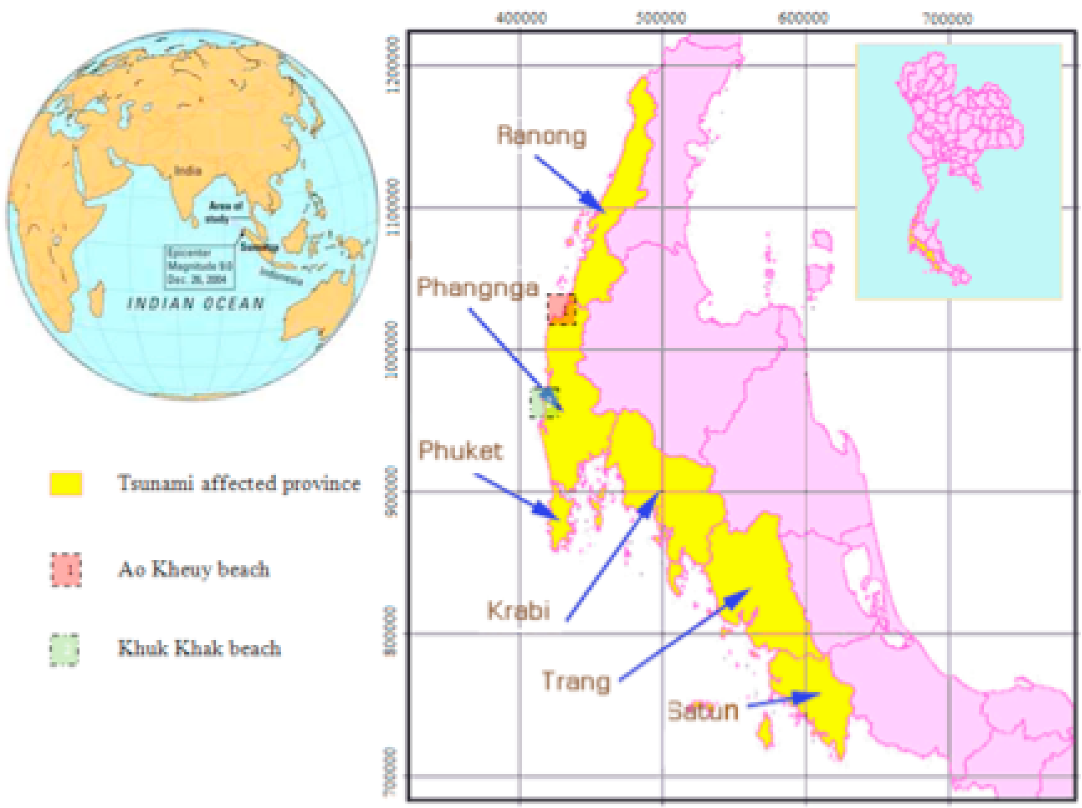

Figure 1. Study areas: 1) Ao Kheuy beach, 2) Khuk Khak beach.

METHODOLOGY

Initially, number of tsunami run-ups and run-up heights were obtained from eyewitness reports and local people's observations. Topographical profile investigations, tsunami deposit thickness measurements and sediment sample collections were made in study areas in August to October 2007. Tsunami deposit samples were collected at a distance between 50 to 300 m inland from coastline. Topographical profiles are established by the combination of the automatic level measurement and Thai topographical map. Collecting samples are analyzed for grain-size distribution by the wet-sieve method. Mean grain-size, standard deviation, skewness, and kurtosis are calculated on the basis of the percentile statistics of Folk and Ward (1957). The major sediment layers in the tsunami deposit are evaluated from the particle size profile for the tsunami sediment layer (grain-size distribution curve contiguous 1 cm-thick samples) and the plot of standard deviation with depth. The sediment transportation patterns are analyzed by a sediment trend analysis (STA) followed McLaren et al. (2007).

RESULTS

Topography of study areas

Ao Kheuy beach is an agricultural area with coconut and palm trees. The shore face slope is about 1:100 (Fig. 2). The backshore and upland zone consist of berm, dune and channel. The tsunami run-up inundation is about 250 m inland from the coastline. From local people's observations, there were 3 waves, which came inland, and the run-up height was about 4-6 meters.

Khuk Khak beach is an agricultural area with coconut trees. The shore face slope is about 1:600 (Fig. 3). The backshore and upland zone consist of berm, dune and road. The tsunami run-up inundation reached about 2 km inland from the coastline. From local people's observations, tsunami run-up height was about 8-10 meters.

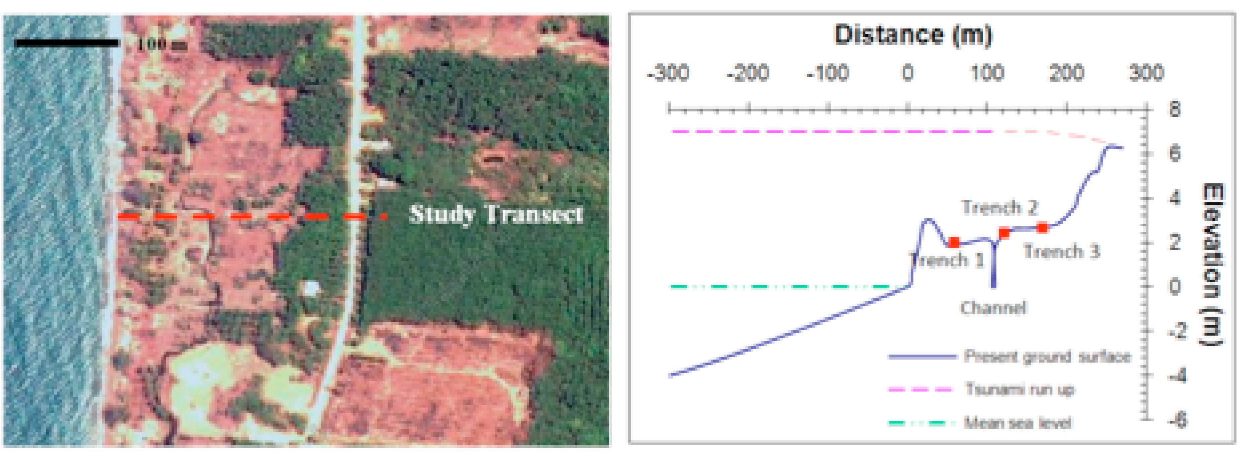

Figure 2. Satellite photo and profile of Ao Kheuy beach to show coastal characteristics and locations of onshore tsunami deposit sample collections.

Figure 3. Satellite photo and profile of Khuk Khak beach to show coastal characteristics and locations of onshore tsunami deposit sample collections.

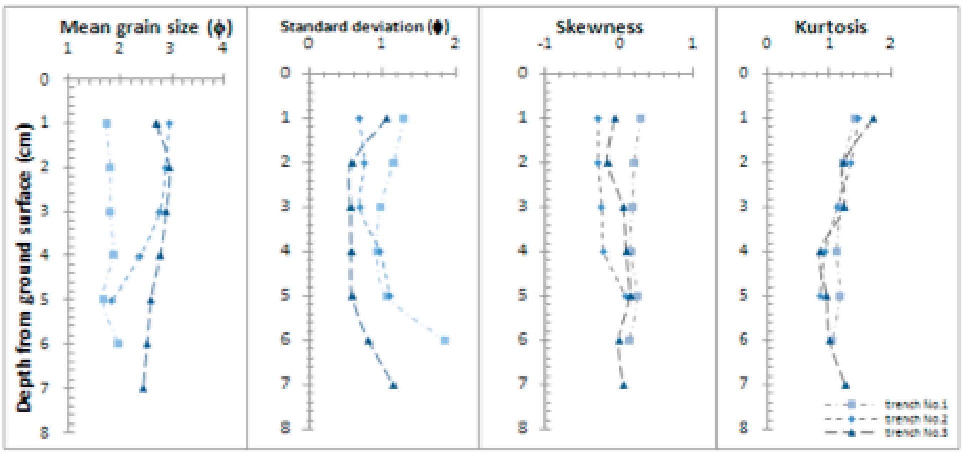

a) Ao Kheuy beach

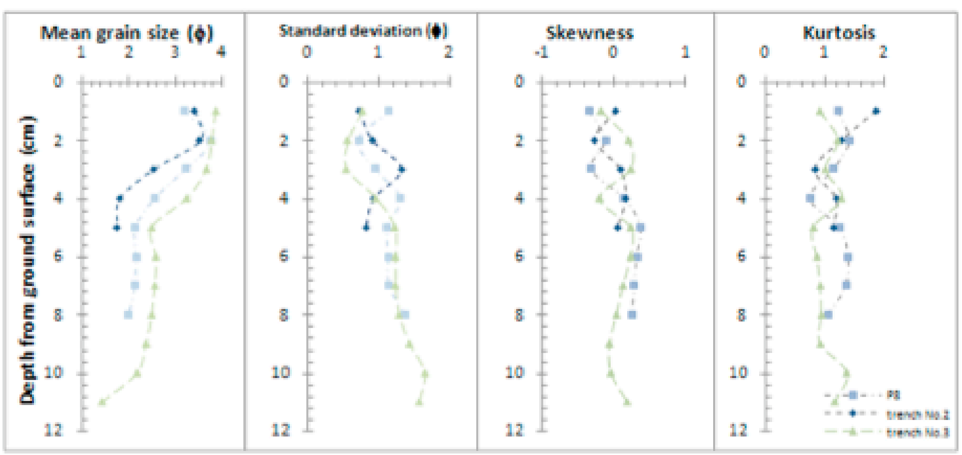

b) Khuk Khak beach

Figure 4. Vertical variations of mean grain-size, standard deviation, skewness and kurtosis for tsunami deposits at a) Ao Kheuy beach and b) Khak Khak beach.

Grain-size analysis

The tsunami deposit grains present within each location largely occur within the size rage between gravel and clay with shell materials. The mean grain-size of the tsunami deposit varies between medium sand to very fine sand ($1<\phi_{mean}<4$). Entirely, tsunami deposit is characterized by a fining landward deposit (Fig. 4). There are variations in the composition of the particle size distributions as illustrated by the plot of standard deviation with depth that range from well sorted to poorly sorted sediments. The particle size distributions appear to have similar kurtosis values to the tsunami sediments presented by Singarasubramanian et al. (2006) which are lower than that described by Shi et al. (1995) and Dawson et al. (1996).

INTERPRETATIONS

Identification for major sediment layers in the tsunami deposit

The tsunami deposit is a sand layer overlying pre-existing soil (rooted soil) with coarse particles near the base and fine particles toward the top (Fig. 5). In a few places, the tsunami deposit contains small rip-up clasts eroded from the pre-existing soil.

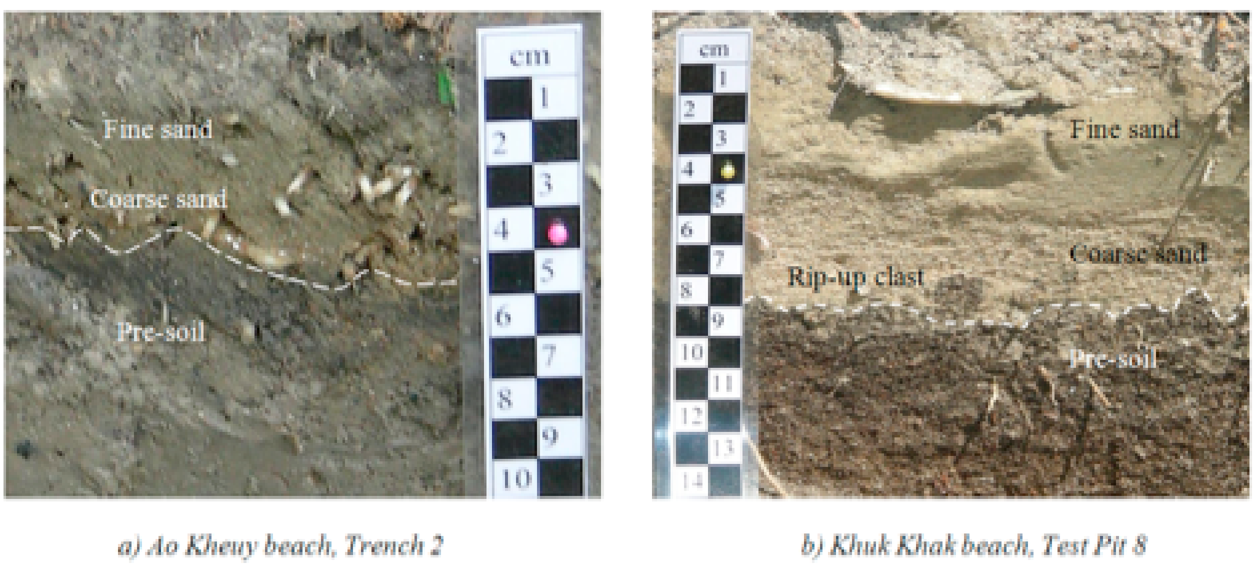

Figure 5. Tsunami deposits overlying pre-existing soil; a) tsunami deposit overlying agricultural soil at Ao Kheuy beach, b) tsunami deposit overlying coastal deposit at Khuk Khak beach.

The tsunami sediment layer exhibits an erosional base and normal graded sand. The grain-size analysis as determined by the wet-sieve method for contiguous 1 cm-thick samples shows the sediment size profile as figure 6 and figure 7. In the study areas, fining-upwards sequence with variable thickness deposit is presented. Deposits have a bi-modal grain-size distribution at the lower

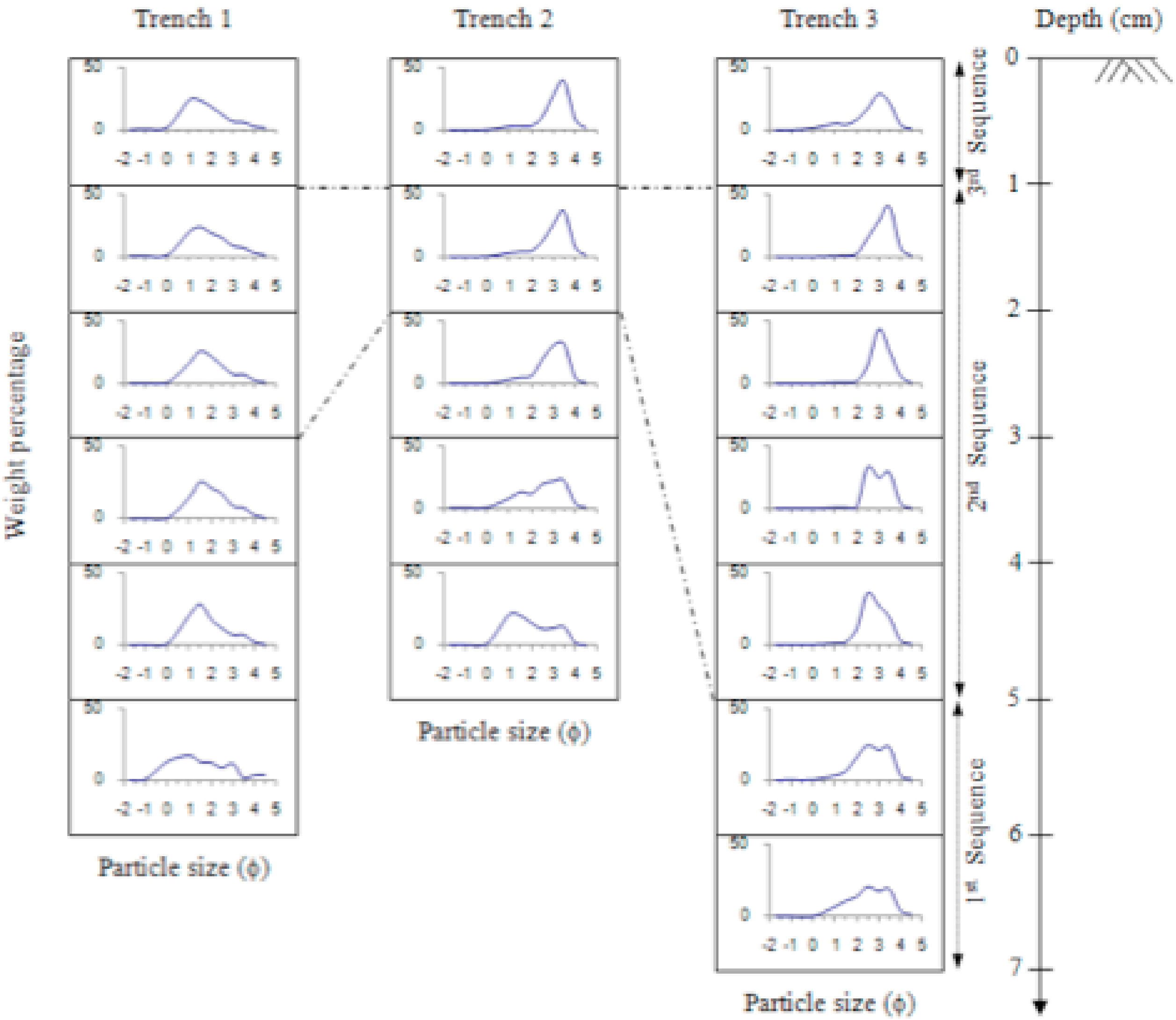

Figure 6. Particle sizes profile for the tsunami deposit at Ao Kheuy beach.

part, with the finer peak increasing in percentage by weight towards the top as the percentage weight of the coarser peak decreases. However, the fining-upwards sequence contains multiple depositional sequences. The depositional sequence boundaries are identified by the increasing of percentage by weight of the coarse particles from the bottom to the top of deposit. It is not easy and not clear to identify the sediment sequences only with grain-size distribution curves as discussed by Smith et al. (2007). Additionally, the plot of standard deviation with depth and grain-size distribution curves for contiguous 1 cm-thick samples are presented to identify major sediment layers in tsunami deposit (Fig. 8). The break points in plot of standard deviation with depth mark a break in turbulence associated with a transition to a lower or higher Reynolds number run-up (Hindson and Andrade, 1999). From figure 8, the break point in plot of standard deviation with depth locates at the depth of

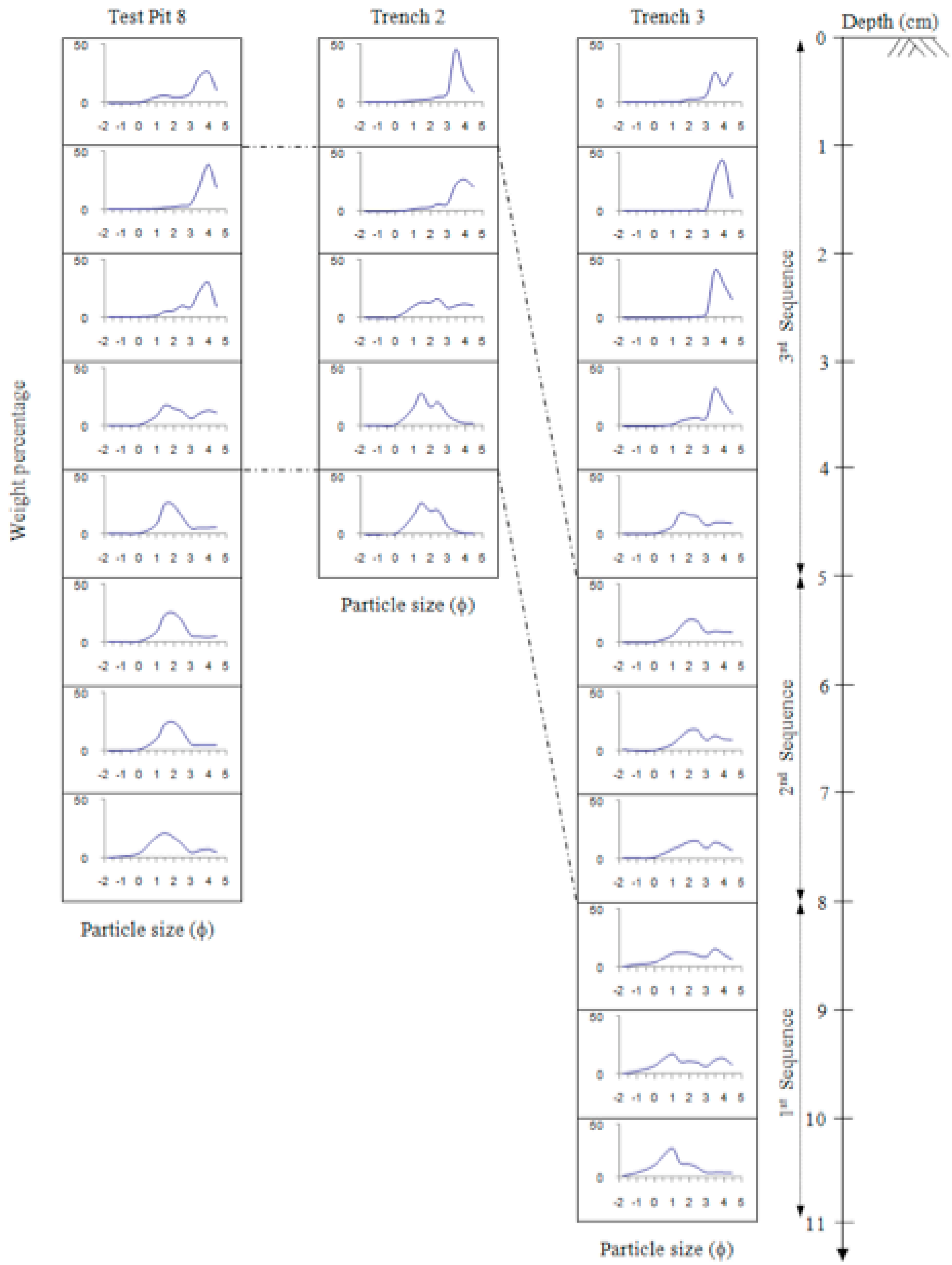

Figure 7. Particle sizes profile for the tsunami deposit at Khuk Khak beach.

increasing of percentage by weight of the coarse particles in the grain-size distribution curve. Thus, that location must be a major sediment boundary. At the study areas, there is a pattern of three depositional sequences in tsunami deposits. There are minor break points in the standard deviation pattern in the 1st depositional sequence in the tsunami deposit at Ao Kheuy beach, and in the 1st and the 2nd depositional sequences in the tsunami deposit at Khuk Khak beach. It could be said that the major sediment layer associates with deposits from two flow characteristics, which might be run-up and backwash (or drawdown). From those depositional sequences, it seems likely that the study areas were reached by three waves, which generated three run-ups.

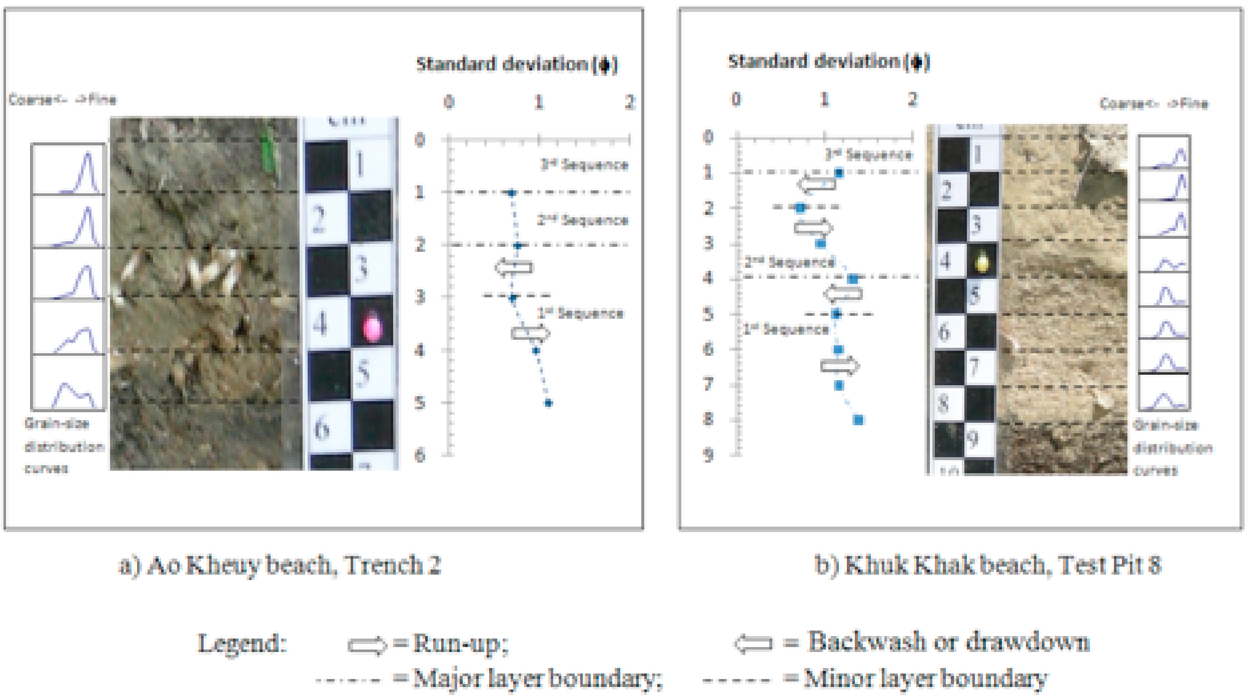

Figure 8. Example plots of standard deviation with depth and grain-size distribution curves for contiguous 1 cm-thick samples at a) Ao Kheuy bech and b) Khuk Khak beach, to show the identification of major sediment layers.

Tsunami sediment transportation analysis

Smith et al (2007) discussed that as each wave of the tsunami flowed onshore, the turbulent water contained a considerable volume of sediment of all sizes. As velocity decreased, turbulence was reduced and the sediment began to settle out. Fining-upwards sequences developed from each wave during the process, with coarser particles settling out first and finer ones later. The direction of run-up flow was almost perpendicular to the coastline, whereas backwash flow directions were controlled by topography (Umitsu et al., 2007). Backwash or drawdown carried sediments, which were not deposited back out to the sea or to the lower level area.

Tsunami sediment transportation pattern is interpreted follow McLaren et al. (2007) for discussion with the considerations articulated by Smith et al. (2007). When the transport direction is unequivocally known, $d_2(s)$ can be related to $d_1(s)$ by a function $X(s)$ as:

$$X(s) = d_2(s)/d_1(s)$$

In this paper, the representative grain-size distribution curve of each depositional sequence (major sediment layer in the tsunami deposit), which is a summary of grain-size distribution curve of contiguous 1 cm-thick in each depositional sequence, is taken sequentially in a known transport direction. For examples:

1) d_1 is the sediment distribution at Trench 1 and d_2 is the sediment distribution at Trench 2;
2) d_1 is the sediment distribution at Trench 2 and d_2 is the sediment distribution at Trench 3; and
3) d_1 is the sediment distribution at Trench 1 and d_2 is the sediment distribution at Trench 3

The resulting patterns of tsunami sediment transportation for Ao Kheuy beach and Khuk Khak beach are shown in figure 9 and figure 10, respectively.

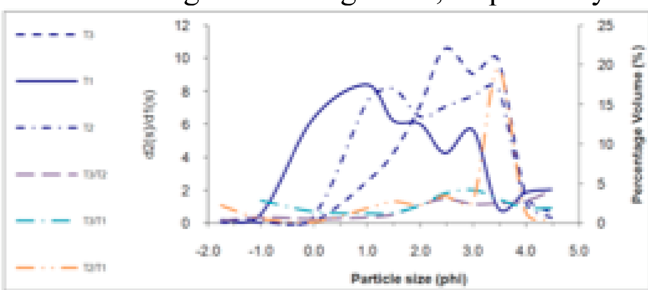

1st depositional sequence

d_1	d_2	Pattern
Trench 1 (T1)	Trench 2 (T2)	Net accretion
Trench 2 (T2)	Trench 3 (T3)	Total deposition 1
Trench 1 (T1)	Trench 3 (T3)	Net accretion

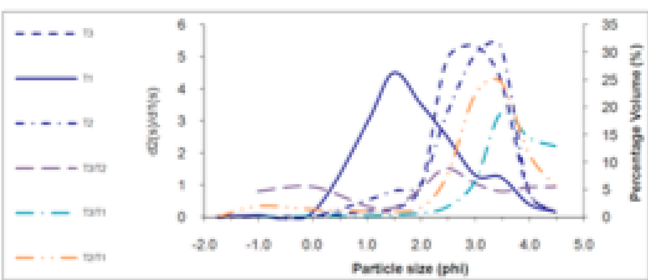

2nd depositional sequence

d_1	d_2	Pattern
Trench 1 (T1)	Trench 2 (T2)	Net accretion
Trench 2 (T2)	Trench 3 (T3)	Dynamic Equilibrium
Trench 1 (T1)	Trench 3 (T3)	Net accretion

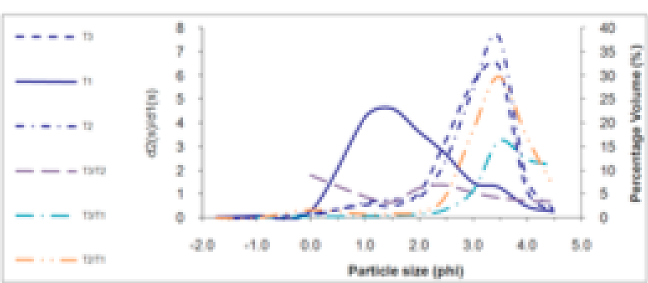

3rd depositional sequence

d_1	d_2	Pattern
Trench 1 (T1)	Trench 2 (T2)	Net accretion
Trench 2 (T2)	Trench 3 (T3)	Total deposition 2
Trench 1 (T1)	Trench 3 (T3)	Net accretion

Figure 9. Sediment trend analysis results for onshore tsunami sediment transportation at Ao Kheuy beach.

The grain-size modes of each depositional sequence at Ao Kheuy beach do not significantly differ, however the deposit fines upward. The major transportation pattern of tsunami sediment during depositional process is net accretion and total deposition, which deposits are fining in the direction of transport, however, more grains are deposited than eroded. The deposit grain-size modes of each depositional sequence at Khuk Khak beach show that the deposit fines upward. The major transportation pattern is total deposition, which sediments must fine in the direction of transport. Once deposited, there is no further transport. Some sediment is usually found far from their sources. In the study areas, there is a net erosion pattern for the transportation pattern, but no erosion evidence on the surface of the lower sequence of sedimentation is observed, and, the net erosion pattern is less compared to other patterns.

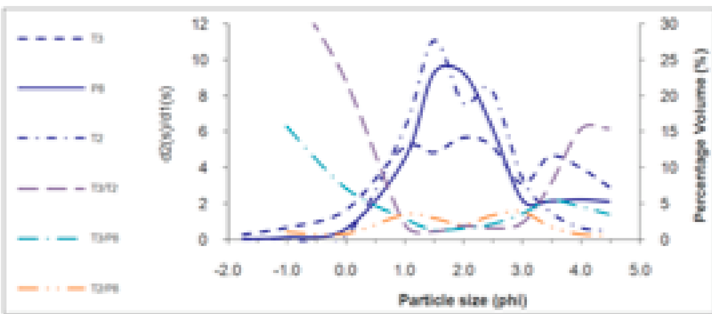

1st depositional sequence

d1	d2	Pattern
Test Pit 8 (P8)	Trench 2 (T2)	Dynamic Equilibrium
Trench 2 (T2)	Trench 3 (T3)	Total deposition 1
Test Pit 8 (P8)	Trench 3 (T3)	Total deposition 1

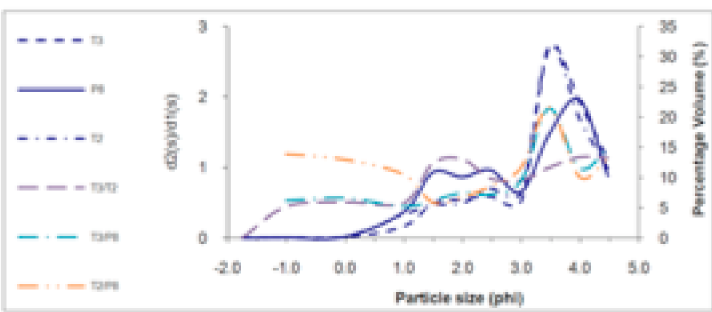

2nd depositional sequence

d1	d2	Pattern
Test Pit 8 (P8)	Trench 2 (T2)	Total deposition 2
Trench 2 (T2)	Trench 3 (T3)	Total deposition 2
Test Pit 8 (P8)	Trench 3 (T3)	Total deposition 2

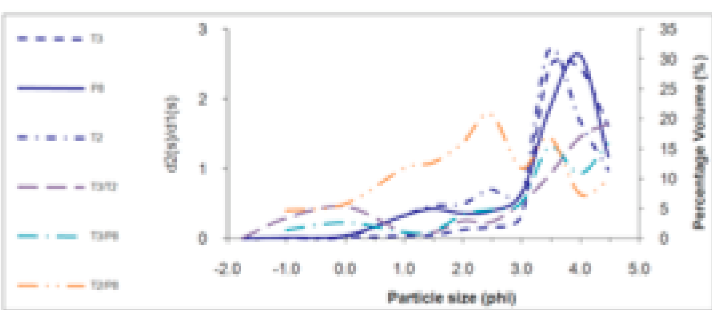

3rd depositional sequence

d1	d2	Pattern
Test Pit 8 (P8)	Trench 2 (T2)	Net erosion
Trench 2 (T2)	Trench 3 (T3)	Total deposition 1
Test Pit 8 (P8)	Trench 3 (T3)	Total deposition 1

Figure 10. Sediment trend analysis results for onshore tsunami sediment transportation at Khuk Khak beach.

DISCUSSION

The tsunami deposits observed at Ao Kheuy beach and Khuk Khak beach share many of the modern tsunami deposit characteristics in locations around the world. For example, Shi et al. (1995) noted the presence of an upward fining sequence in the sediment sheets at Flores. They recognized that the sediment sheet has an erosional contact with the underlying soil (pre-existing soil), and is composed of a wide range of sediment sizes. The particle size profile for the tsunami sediment layer is used to identify major sediment layers in the tsunami deposit, but it is not easy and not as clear as that discussed by Smith et al. (2004, 2006). The identification for major sediment layers gives higher accuracy when the particle size profile from the wet-sieve analysis method and the plot of standard deviation with depth are considered together. The identification for major sediment layers in tsunami deposit gives three depositional sequences, which reflect three tsunami run-ups at Ao Kheuy beach and Khuk Khak beach. The number of run-ups from the identification for major sediment layers in the tsunami deposit corresponds to eyewitness reports. Therefore, the identification method for major sediment layers in the tsunami deposit may be applied to interpret number of tsunami run-ups at tsunami-affected areas where lack of eyewitness reports.

It is recognized that tsunami flow onshore can be complex (e.g. Shi, 1995). Smith et al. (2007) argued that the pattern of fining-upwards sequences across an embayment might show that each sequence was the deposit of an individual wave. Onshore tsunami sediment transportation analysis shows that, deposits fine in the direction of transport. There is a net erosion pattern, which sediment coarsens along the transport path, more gains are eroded than deposited, but there is no evidence of erosion on the surface of the lower sediment sequence. Wang et al. (2006) concluded that in the area where the surface of the lower sediment is non-vegetated (e.g. clean sand deposit), the erosional surface is not apparent. Hindson and Andrade (1999) concluded that multiple wave sets can be detected in tsunami deposits, although it is difficult to distinguish between these and tsunami backwash. In this study, the results show that the sediments in each depositional sequence settled form two flow characteristics, which might be run-up and backwash (or drawdown). The 1st and the 2nd depositional sequences are easy to observe that depositional phenomenon from a particle size profile and a plot of standard deviation with depth (Fig. 8). The thickness of tsunami deposit suggests that the sediments settled from run-up are more significant than the sediment settled from backwash. Tsunamis do not transport significant quantities of material from the offshore zone, with the majority of the erosional activity occurring onshore, and typically involving the removal of sand from the beaches and coastal dunes (Hindson and Andrade, 1999). This conclusion is appropriate for Ao Kheuy beach. However, for Khuk Khak beach, which the slope of shore face is mild, the sediment transportation patterns suggest that the sediments of the 2nd depositional sequence are found far from their source. Therefore, at a mild slope shore face, some sediment is transported far from their sources.

Generally, tsunami is a set of waves, which creates a set of run-ups when it encounters land. Details of tsunami deposit thickness and grain-size from multiple layer identification and transportation pattern analysis for an onshore tsunami deposit can be put in the simple models for reconstructing tsunami run-up (e.g. Jaffe and Gelfenbuam, 2007; Soulsby et al., 2007). The results from reconstructing tsunami run-up with details of tsunami deposit thickness and grain-size from multiple layer identification can be evaluated the individual run-up characteristics.

CONCLUSIONS

The tsunami deposit found at Ao Kheuy beach and Khuk Khak beach is a sand layer overlying pre-existing soil with an erosional base. The sediments fine upward and landward. Apparently, tsunamis are, in general, both erosive and depositional in nature. At Ao Kheuy beach and Khuk Khak beach, Phang-nga province, Thailand, there are three major sediment layers in the tsunami deposit. It suggests that flooding (run-up) took place from three waves and tsunami deposits settled from run-up and backwash (or drawdown). Sediments created by run-up are more significant than sediments created by backwash. The sediment transportation patterns show that tsunami deposits fine landward, more grains being deposited than eroded. There is some evidence of erosion only at the base of the 1st sediment sequence. Sediments are transported far from their origin at a mild slope shore face. The numbers of major sediment layers in the tsunami deposit can be used to interpret the event apart from eyewitness reports (e.g. number of run-ups for ancient tsunamis which the eyewitness reports are not existent, thickness and particle size of sediments which are transported and deposited by individual run-up) for reconstructing individual tsunami run-up by using numerical and/or simple models.

ACKNOWLEDGEMENTS

DAAD (Deutscher Akademischer Austausch Dienst) has provided scholarship (The CCC-/Tsunami programme) to Mr.Chanchai Srisutam for Ph.D. program in Universität Trier, Germany. The authors would like to thank Dr.Watchara Suedee (Irrigation College) for local officer contact; Mr.Suvit Seangjak (Soil Investigation Section, Office of Topographical and Geotechnical Surveys, Royal Irrigation Department, Thailand) for field survey support; Mr. Choosak Sutthi (Lam Roo Yai Dam construction project, Phang-nga) for field survey residential support.

REFERENCES

Dawson, A.G., Foster, I.D.L., Shi, S., Smith, D.E., Long, D., 1991. The identification of tsunami deposits in coastal sediment sequences. Science of tsunami hazards 9, 73-82.

Dawson, A.G., Shi, S., Dawson, S., Takahashi, T., Shuto, N., 1996. Coastal sedimentation associated with the June 2nd and 3rd, 1994 Tsunami in Rajegwesi, Java. Quaternary Science Reviews 15, 901-912.

Dawson, A.G., Shi, S., 2000. Tsunami deposits. Pure Appl. Geophys. 157, 875-897.

Folk, R.L., Ward, W.C., 1957. Barzos river bar. A study in the significance of grain size parameters. Journal of Sediment Petrology 27, 3-26.

Gelfenbaum, G., Jaffe, B., 2003. Erosion and Sedimentation from 17 July, 1998 Papua New Guinea Tsunami. Pure and Applied Geophysics 160, 1969-1999.

Hindson, R.A., Andrade, C., 1999. Sedimentation and hydrodynamic processes associated with the tsunami generated by the 1755 Lisbon earthquake. Quaternary International 56, 27-38.

Jaffe, B. E., Gelfenbuam, G., 2007. A simple model for calculating tsunami flow speed from tsunami deposits. Sedimentary Geology 200, 347-361.

McLaren, P., Hill, S. H., Bowles, D., 2007. Deriving transport pathways in a sediment trend analysis (STA). Sedimentary Geology 202, 469-498.

Minoura, K., Gusiakov, V.G., Kurbatov, A., Takeuti, S., Svendsen, J.I., Bondevik, S., Oda, T., 1996. Tsunami sedimentation associated with the 1923 Kamchatka earthquake. Sedimentary Geology 106, 145-154.

Nelson, A.R., Shennan, I., Lonh, A.J., 1996. Identifying coastal subsidence in tidal wetland stratigraphic sequences at Cascadia subduction zone of western North America. J. Geophys. 101, 6115-6135.

Shi, S, Dawson, A.G., Smith, D.E., 1995. Coastal sedimentation associated with the December 12th, 1992 tsunami in Flores, Indonesia. Pure and Applied Geophysics 144, 525-536.

Singarasubramanian, S.R., Mukesh, M.V., Manoharan, K., Murugan, S., Bakkiaraj, D., John Peter, A., Seralathan, P., 2006. Sediment characteristics of the M-9 tsunami event between Rameswaram and Thoothkudi, gulf of Mannar, southeast coast of India. Science of Tsunami Hazards 25, 160-172.

Smith, D. E., Shi, S., Cullingford, R. A., Dawson, A. G., Dawson, S., Firth, C. R., Foster, I. D. L., Fretwell, P. T., Haggart, B. A., Holloway, L. K., Long, D., 2004. The Holocene Storegga Slide tsunami in the United Kingdom. Quaternary Science Reviews 23, 2291-2321.

Smith, D.E., Fodter, I.D.L., Long, D., Shi, S., 2007. Reconstructing the pattern and depth of flow onshore in a palaeotsunami from associated deposits. Sedimentary geology 200, 362-371.

Soulsby, R. L., Smith, D. E., Ruffman, A., 2007. Reconstructing tsunami run-up from sedimentary characteristics- A simple mathematical model. Sixth International Symposium on Coastal Sediment Process – Coastal Sediments ’07. Coasts, Oceans, Ports and Rivers Institute (COPRI) of the American Society of Civil Engineers, May 13-17, New Orleans, Louisiana. Volume 2, 1075-1088.

Umitsu, M., Tanavud, C., Patanakanog, B., 2007. Effects of landforms on tsunami flow in the plains of Banda Aceh, Indonesia, and Nam Khem, Thailand. Marine Geology 242, 141-153.

Wang, P., Kirby, J.H., Haber, J.D., Horwitz, M.H., Knorr, P.O., Krock, J.R., 2006. Morphological and Sedimentological Impacts of Hurricane Ivan and Immediate Poststorm Beach Recovery along the Northwestern Florida Barrier-Island Coasts. Journal of Coastal Research 22, 1382-1402.

Whelan, F., Kelletat, D., 2003. Analysis of tsunami deposit at Trafalgar, Spain, using GIS and GPS technology. Essener Geographische Arbeiten 35, P.25.

EFFECT OF THE INDIAN OCEAN TSUNAMI ON GROUNDWATER QUALITY IN COASTAL AQUIFERS IN EASTERN SRI LANKA

METHTHIKA VITHANAGE[1,2],
KAREN G. VILLHOLTH[3],
KUSHANI MAHATANTILA[4],
PETER ENGESGAARD[1] AND
KARSTEN H. JENSEN[1]

[1]Department of Geography and Geology, University of Copenhagen, Denmark,
[2]International Water Management Institute, Battaramulla, Sri Lanka,
[3]Geological Survey of Denmark and Greenland, Copenhagen, Denmark
[4]Department of Material Science, Interdisciplinary Faculty of Science and Engineering, Shimane University, Matsue, Japan,

meththikavithanage@gmail.com
Tele: +94 112 833 101

ABSTRACT

Changes in water quality of a sand aquifer on the east coast of Sri Lanka due to the December 26, 2004 tsunami and subsequent disturbance due to well pumping and flushing by precipitation were investigated. Two closely spaced tsunami affected transects, spanning the ocean and an interior lagoon across a 2 km wide land strip were monitored from October, 2005 to September, 2006. Water samples were collected from 15 dug wells and 20 piezometers, from the disturbed and undisturbed sites respectively to evaluate the temporal and spatial trends in water quality.

The EC values observed from the undisturbed area showed a significant decrease (3000 to 1200 µS/cm) with the rain from November 2005 to March 2006, while the values in the disturbed area appeared to have stabilized without further decline through the same period. The concentration range of EC, Ca, K, Na, alkalinity, total hardness and sulphate were higher in the disturbed site than in the undisturbed site. PHREEQC modeling showed that the mixed sea water fraction is higher in the disturbed site than in the undisturbed site, and this is likely due to the movement of the disturbed plume by water extraction through pumping and extensive well cleaning after the tsunami, causing forced diffusion and dispersion. No arsenic contamination was observed as all observed arsenic concentrations were below 10 µg/L. For the sites investigated, there are clear indications of only a slow recovery of the aquifer with time in response to the onset of the monsoon.

Key words: Tsunami, water quality, groundwater, coastal aquifers, geochemical modelling, Sri Lanka

INTRODUCTION

On December 26th 2004, tsunami waves devastated the coastal region of Sri Lanka. Coastal belt of Sri Lanka comprises of shallow coastal sandy aquifers, which provides reliable water resources throughout the year. The severely affected east coast of Sri Lanka consists of regosols overlying directly unconfined sandy aquifers ranging from fine to moderately coarse structure-less sands (Panabokke and Perera, 2004). These shallow groundwater aquifers are very susceptible to contamination. When a dense fluid is situated above the less dense fluid it comprises of an unstable density configuration and is referred to as an unstable-interface problem. Previous studies (Schincariol and Schwartz, 1990; Koch and Zhang, 1992; Oostrom et al., 1992; Simmons et al., 2001) have revealed that when density differences are significant, solute transport is a result not only of forced (hydraulically driven) advection and dispersion or diffusion, but also of free convection (buoyancy driven) resulting in gravitational instabilities. Therefore they have the potential to contaminate larger regions of an aquifer and can mix naturally with the ambient water to a larger degree due to mixed convection (Oostrom et al., 1992). The anthropogenic processes that aggravate mixing (such as water abstraction) could result longer aquifer cleansing time compared to the contamination by natural mixing.

People use shallow open dug wells for their domestic water supply as the surrounding sandy aquifer. However, as a result of the tsunami the coastal belt was completely flooded and the shallow groundwater aquifer was contaminated by saltwater. Open dug wells in the affected areas up to 1.5 km inland were filled with seawater (Villholth et al., 2006a, 2006b). It has been estimated that more than 50,000 water supply wells were affected in Sri Lanka by the tsunami (UNEP, 2005). The diffuse contamination of ground water and the point source contamination of wells along the affected coastal zone were aggravated by the influx of wastes from septic materials, pit latrines, chemical spills, dead bodies and surface debris. The waste and debris directly contaminated the wells or accumulated in the surface depressions and infiltrated into to the aquifer for several days following the event. This study investigates the change in water quality of the highly vulnerable local sand aquifers due to tsunami and its “natural cleaning” response by precipitation over time and the effect of well cleaning and pumping water for domestic uses.

Study area

Location

The present study was carried out in a tsunami affected village located in the Batticaloa District of eastern Sri Lanka (Fig. 1). The east coast is prevalent with elongated, north-south oriented coastal lagoons with land stretches bordered by saline ocean water and brackish lagoon water on both sides. Hydrogeologically, these land stretches act as oceanic islands and local, productive aquifers which are created as freshwater lenses floating on the underlying denser saline water (Underwood et al., 1992). The study area extends as an east west oriented narrow strip of land about two kilometers wide. The ground surface is almost flat and the elevation in the middle part between the sea and the lagoon is about 3 to 4 meters above mean sea level (msl). Freshwater at the site originates entirely from local excess precipitation and the available quantity is thus limited.

Exploitation of the freshwater poses a risk of contamination by sea water due to over extraction and hence the fresh water lens needs to be used in a sustainable manner as there are limited reliable freshwater sources inland to supplement water for the coastal zone.

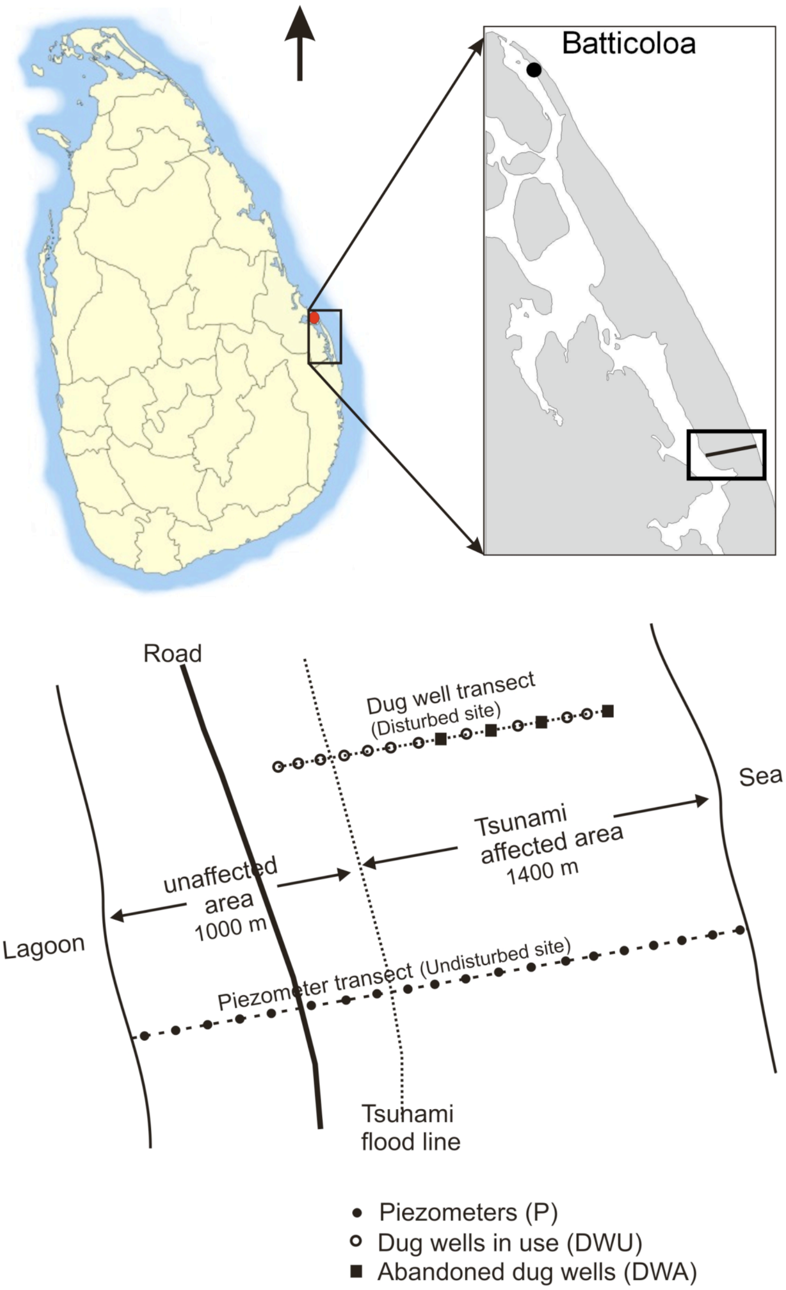

Fig. 1. Location map of the study area. Piezometer transect (undisturbed site) is in 2 km demarcated by the sea (7^0 36' 24" N and 81^0 47' 01") in the east and Lagoon (7^0 35' 59" N and 81^0 45' 50") in the west. The village considered as the disturbed site.

Two transects are located in the Kirankulum village of the Batticaloa District. The two sites have similar characteristics with the major difference being that one of them is only exposed to natural rainfall conditions and no pumping activities present (hereafter referred to as the undisturbed site) while the other site is subject to well pumping (referred to as the disturbed site). The undisturbed site consists of thorny shrubs and cashew plantation, while the adjacent village, which consists of a cluster of small one-story houses and relatively little paved areas with numerous dug wells for water supply, is considered as the disturbed site.

Twenty piezometers were installed along a transect perpendicular to the coast and across the entire land strip in the undisturbed site. Fifteen existing open dug wells from the village along a second transect, covering a smaller section of the land strip, were selected for the detailed study (Fig. 1). The two transects are 0.5 km apart. The disturbed site consists of a total of 57 dug wells within an area of 0.25 km^2 used by 113 families. Fifty wells in this area were affected by the tsunami. Most of these wells are used for household purposes. In both sites, the tsunami run-up was around 1 km from the coast line. In the village transect, only two dug wells were in the tsunami non-affected area, while the undisturbed transect consists of 12 piezometers in the affected area and 8 piezometers in the non-affected area.

Climate

The study area belongs to the dry zone of Sri Lanka with an annual rainfall of 1200 to 1900 mm. Eighty percent of the annual rainfall falls intensively during the north-east monsoon period from November to February and during the inter monsoon period from March to April (Panabokke et al., 2002). As the ambient temperature is high year round (30 – 35 ^{0}C) evaporation is estimated to be high, around 30 – 50 % of the precipitation (Panabokke, 2001).

Geology and hydrogeology of the study area

In Sri Lanka, Miocene limestone are found along the northern and North West coast and throughout the Jaffna Peninsula, while on the southeast, south and southwest coast, rocky headlands are prevalent. The geology around the study area is dominated by Quaternary unconsolidated beach deposits on the top of Precambrian metamorphic rocks Cooray (1985).

The two areas are assumed and expected to be similar in the lithological settings. The lithology of a field site about 15 km north of the study area was reported by Wickremaratne (2004), first, a medium to coarse sand layer of approximately 9 m depth with a small fraction of clay and shell fragments is found.

A clay and silty clay layer of about 5-10 m in thickness is found below the sand layer, which is then followed by a thin coarse sand layer of about 2 m in thickness. The thickness of the sandy formations increases towards sea whereas the thickness of the clayey layers increases towards the lagoon. It was reported that the bed rock is found around 15-25 m deep which is corroborated by transient electromagnetic soundings carried out by Hoareau et al., (2006) in the particular study area.

Pre-tsunami hydrogeochemistry

Few studies have been carried out to investigate the pre-tsunami water quality in the shallow ground water aquifers in eastern Sri Lanka (Mahendran et al., 2000; Vaheesar, 2002; Panabokke et al., 2002; Jeyakumar et al., 2002; Sugirtharan et al., 2004; Wickramaratne, 2004). Some of the recorded EC levels were relatively high in the pre-tsunami studies. According to Panabokke et al., (2002) only in two agro wells out of 25 from the Trincomalee District (located north of the study area) had low EC values (<500 µS/cm) and most were above 1000 µS/cm while some were as high as 2500 µS/cm). However, as agro wells have become larger in size and pumped more heavily to supply water for irrigation, they may not be considered as representative of the domestic wells. As a consequence, agro wells have shown consistently higher salinity levels than domestic dug wells (Vaheesar et al., 2000; Jeyakumar et al., 2002). In the study by Wickramaratne (2004), EC levels below 700 µS/cm were reported for shallow tube wells. Calcium and magnesium concentrations of well water have been recorded between 250 – 1450 mg/L and 30 – 250 mg/L respectively (Mahendran et al., 2000). Nitrate concentration in most areas in the Batticaloa District are above the WHO standard limit (45 mg/L).

Post tsunami water quality

The shallow groundwater aquifers were affected in several ways by the tsunami: direct infiltration from tsunami inundation, infiltration from pooled sea water left behind, permeation from flooded wells, and salinization from flooding of lagoons and river mouths (Villholth et al., 2006a). A few studies have documented the impact on the water quality in wells mainly in terms of electrical conductivity (EC), total dissolved solids (TDS) and salinity (Villholth et al., 2006a; Illangasekare et al., 2006). Water quality measurements carried out by Villholth et al., (2006b) have documented a significant difference between the tsunami affected and non-affected well water. Interestingly, Pilapitiya et al., (2005), have reported on elevated arsenic contamination due to tsunami in Sri Lanka

METERIALS AND METHODS

Twenty piezometers were installed along a 2 km transect with 500 m mutual distance in the undisturbed site. All these piezometers were installed just prior to the onset of the north east monsoon when the water table was the lowest. The depth of piezometers varied along the transect according to the level of the water table and they were installed 1.5 m below the water table to avoid the possibility of being dry. The piezometers were made of standard pvc tubes with an inner diameter of 3.7 cm and equipped with a 15 cm slotted screen at the bottom and with an end cap, which was covered by a 1 mm mesh to protect the piezometer from siltation. They were installed in 8.7 cm diameter boreholes constructed by slug boring method at the proper level and securely sealed. Fifteen existing open dug wells along a transect were selected from the village (disturbed site) for detailed monitoring of water quality (Fig. 1). The wells had an average diameter of 1.3 m and an average depth of 3.2 m. Rainfall at the site was recorded daily at 08:00 using a standard rain gauge provided by the Meteorological Department of Sri Lanka.

Chemical Analysis

EC was measured in the field in both dug wells and piezometers using a Hanna hand held EC meter, during the months of October, 2005, January, March, June and October, 2006. All 57 wells in the village were monitored for EC, however, results given in this paper for the dug wells are all from the 15 wells along the transect.

In January, March and October 2006, duplicate well water samples were collected for chemical analysis. One sample of water was acidified to measure the metal ions and the other was frozen. Nitrates, phosphates and sulphates were measured using a HACH 2400 UV-VIS Spectrophotometer and the inorganic ions, Ca, Mg, Na, K, Fe an Mn were measured using an Atomic Absorption Spectrophotometer (Perking Elmer, 2300).

In-situ arsenic analysis was carried out using the Arsenic measuring field kit (VISUAL ARSENIC DETECTION KIT WAG-WE 10600). In this case only water in open dug wells, which may have been filled with oceanic sediments by the tsunami were analyzed.

Geochemical Modeling

The water quality data sets obtained from all the sites were analyzed using the geochemical model, PHREEQC (Parkhurst and Appelo, 1999), The PHREEQC code simulates chemical reactions and transport processes in water using observed field data. The model has an inverse modeling capability, which attempts to find sets of mineral and gas mole transfers that account for differences in composition between waters while accounting for specified uncertainties (Parkhurst and Appelo, 1999).

Our intention was to use inverse modeling to back calculate and reproduce the data obtained from the water quality analysis, and determine the composition of the water samples. In inverse modeling, one aqueous solution is assumed to be mixed with the other aqueous solutions to react with mineral and gas phases to produce the observed composition of the tertiary solution and all the mixing fractions and mole transfers of the phases are calculated (Parkhurst and Appelo, 1999). Assumed here are three water analyses, sea water (from the PHREEQC data base), fresh water (from none affected dug wells) and water in the affected area (water quality observations) subject to mixing and ending with a certain water composition along the flow path.

The numerical method of inverse modeling of PHREEQC is based on the mole balance equations, which are included for (a) each element, (b) alkalinity, (c) electrons, (d) water and (e) each isotope. Furthermore, it includes inequalities to constrain the uncertainty (Parkhurst and Appelo, 1999).

The uncertainty represents potential analytical error and spatial or temporal variability in concentration of each component in each aqueous solution and in mineral compositions. Uncertainty in the aqueous species in the models was set in between 0.1-0.2 to make the model converge with reasonable results. To consider uncertainties in mineral compositions, three mineral phases (calcite, dolomite and anhydrite) and one gas phase (CO_2) were added to the models.

RESULTS AND DISCUSSION

Precipitation

The precipitation data recorded at the field site is show (Vithanage et al., 2009) that the rainfall due to the onset of the north-east monsoon period in October with the highest rainfall in November. Nearly 90% of total annual rainfall precipitates during the north-east monsoon period from November to February.

Electrical Conductivity (EC)

The tsunami impact on chemical groundwater characteristics was significantly manifested in the salinity levels. Because there were very few records of pre-tsunami EC levels and chemical parameters of shallow ground water (Mahendran et al., 2000; Vaheesar, 2002; Wickaramaratne, 2004) the data from the present study of the areas not flooded by the tsunami, basically the 8 and 2 most inland wells for the undisturbed and disturbed site, respectively (Fig. 2), were considered representative of the original water quality of the local aquifer system. The original EC levels of the Kirankulum study area, except for the well closest to the lagoon, which could have been affected by the tsunami by the seawater flooding directly into the lagoon mouths (Villholth et al., 2006b), were relatively lower than the data from previous reports, generally < 300 μS/cm.

It is noted that the EC levels showed more spatial variability across the transect in the disturbed site than in the undisturbed site (Fig. 2).

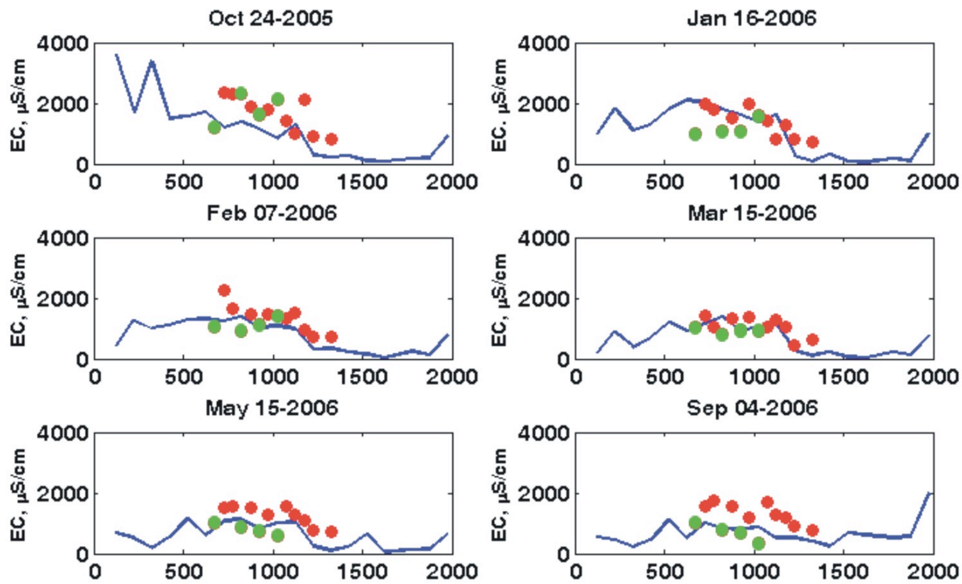

Fig. 2. Change in EC levels both in undisturbed (solid line) and disturbed sites (circles) in October, 2005, January, February, March, May and September, 2006. Red circles represent dug wells that are pumped for cleaning purposes and green circles represent abandoned dug wells.

This could indicate that different patterns of use of individual wells after the tsunami had meant a different degree of residual tsunami imprint. This pattern of larger small-scale variability within the disturbed transect than the undisturbed one was also evident in most of the other chemical variables, supporting the hypothesis that the degree of reminiscence of the tsunami impact locally is a function of the aquifer disturbance in terms of well pumping and cleaning going on in the wells since the tsunami. Intensive and frequent well cleaning through emptying of wells and chlorination had been carried out since shortly after the tsunami. Furthermore, the most prevalent cleaning procedure was simple and entailed discharging the well water next to the well and hence basically recycling the contaminated water into the system and increasing the overall mixing and retarding the downward and lateral movement of the tsunami pulse. Hence, well cleaning, abstraction of water and degradation of debris may have delayed the natural recession of the tsunami effect at the disturbed site. In the undisturbed site, natural flow process had taken place, encompassing rapid sinking of the denser saltwater immediately after the tsunami (Illangasekare et al., 2006) and hence, the tsunami effect, after about one and half years, was less and more uniform across the transect compared to the disturbed site. Further supporting this hypothesis is the fact that well no. 1, 4, and 11 in the disturbed site were abandoned since the tsunami and these wells showed lower values of the chemical parameters.

Water Quality Analysis

The values obtained from the water quality analysis were normalized according to the sea water and plotted against time. The results of water quality analysis in January, 2006 showed that Ca concentrations in dug wells are slightly higher than in the piezometers (Fig. 3).

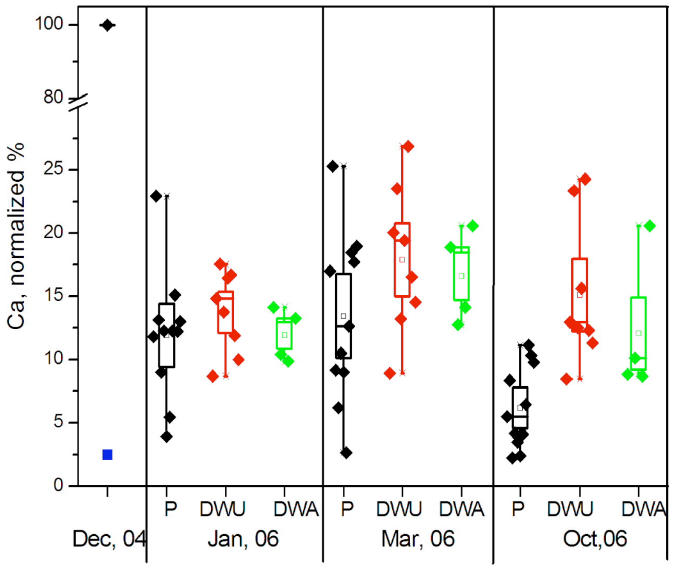

Fig. 3. Normalized calcium concentrations in the undisturbed site (P), dug wells in use (DWU) and abandoned dug wells (DWA) for January, March and October, 2006

Sodium concentrations for undisturbed site were almost same (>100 mg/L) as for the disturbed site in January. In March the concentrations decreased for both sites, most notably for the undisturbed site (Fig. 4). The original Na concentration in the aquifer was below 10 mg/L, and still most of the dug wells had much higher Na concentrations in March, 2006 (several above 100 mg/L) which is a clear imprint of the tsunami.

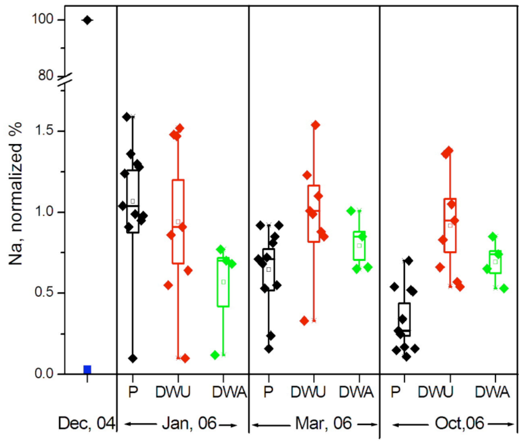

Fig. 4. Normalized sodium concentrations in the undisturbed site (P), dug wells in use (DWU) and abandoned dug wells (DWA) for January, March and October, 2006

The behavior of potassium concentrations was similar to Na (Fig. 5). The original K levels were less than 4 mg/L, and as shown by the figure many of the dug wells were higher in concentrations. Similar to sodium the concentrations are generally higher than for the piezometer measurements except for the two piezometers adjacent to the sea and lagoon respectively.

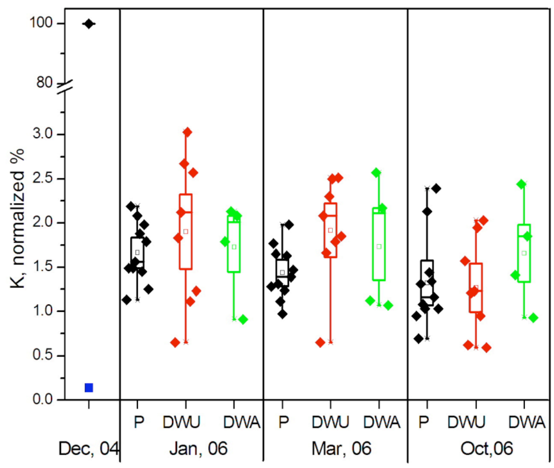

Fig. 5. Normalized potassium concentrations in the undisturbed site (P), dug wells in use (DWU) and abandoned dug wells (DWA) for January, March and October, 2006

The measured concentrations for alkalinity corroborate the findings for the other chemical parameters that the concentration levels for the disturbed site are marginally higher than for the undisturbed site (Fig. 6). Manganese also shown a similar behavior, and conversely, iron concentrations were high in undisturbed environment. Manganese from the sea sediments, which has deposited in the dug wells may have played a major role here causing the difference in between affected and non-affected area of the village transect. Though Pilapitiya et al., (2005) has measured elevated arsenic contaminations in groundwater due to tsunami there were no sign of arsenic in the water samples tested onsite. All the samples showed concentrations below 10 µg/L (WHO recommended guidelines).

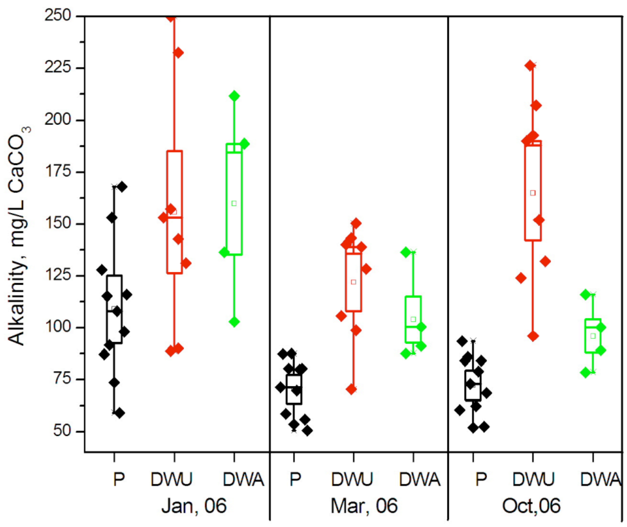

Fig. 6. Alkalinity concentrations in the undisturbed site (P), dug wells in use (DWU) and abandoned dug wells (DWA) for January, March and October, 2006

Hydrogeochemical Modeling of data

PHREEQC was used to model the chemical datasets from both undisturbed and disturbed sites to validate the analytical work and obtain the mixed sea water and fresh water fractions. Different mineral and gas phases were added according to the inequalities obtained in the output. Some samples showed that they are strongly undersaturated with solid sulphates and iron, and saturated with respect to calcite and dolomite. Therefore, possible precipitation of calcite or dolomite and dissolution of anhydrite were set as model constraints. For those solutions, it was necessary to add redox phases such as goethite or pyrite. A possible sink for CH_2O and a CO_2 source were set for equilibrate the reactions with organic matter. Since the upper most layer of the aquifer is geologically characterized as coarse to fine sand and no clay minerals are present, cation exchange was not considered. Sea water composition was obtained from the PHREEQC data base. The observed values of pH, alkalinity, C, Cl, Mg, Na, S and Ca were used as input to include mole balance equations for elements not contained in any of the phases.

Most solutions had 1-3 possible simulated models. Dissolution of anhydrite was encountered in all models, while most of the models were characterized by small amount of precipitating carbonates as calcite and dolomite. PHREEQC was able to simulate the observed chemical data well as shown by the scatter plots of simulated versus observed results for various parameters collected during the month of October 2006 (Fig. 7 and Fig. 8). The correlation coefficients of each parameter was very high (0.82 – 1.0) indicating an excellent fit by the model.

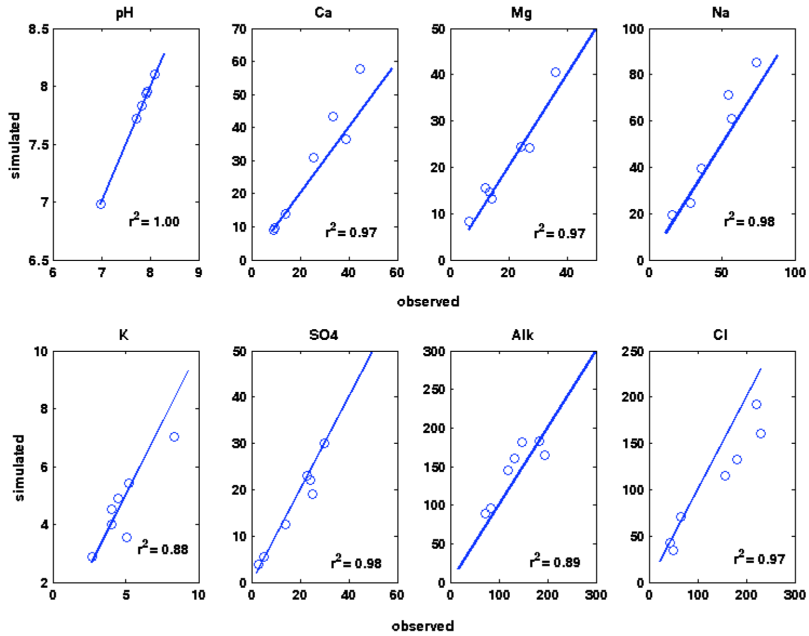

Fig. 7. Fitted results for the October, 2006 in the undisturbed site with correlation coefficients obtained from hydrogeochemical modeling using PHREEQC.

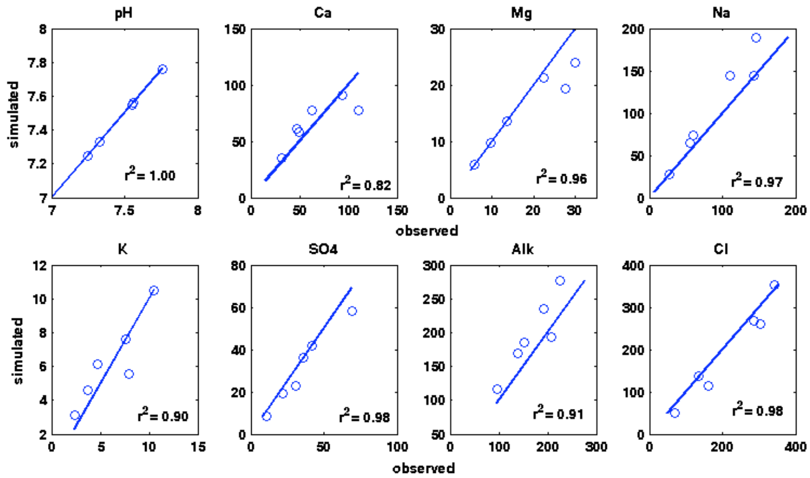

Fig. 8. Fitted results for the October, 2006 in the disturbed site with correlation coefficients obtained from hydrogeochemical modeling using PHREEQC.

Mixing of solution fractions

Mixing of solution fractions (sea water and fresh water) were obtained from the PHREEQC simulations. All the solution fractions from the month October, 2006 are plotted as a box and whisker plot (Fig. 9). The box plot of the undisturbed site has a median of 5.5×10^{-3} of sea water fraction and the range of data lies below 1×10^{-2}. The sea water fraction, is more uniform over the undisturbed site. However, the median value of the sea water fraction of the disturbed site with dug wells is 9×10^{-3}, which is about twice as that for the undisturbed site. Furthermore, the variance of data in the disturbed site is greater than the undisturbed site. Hence, it can be postulated that the mixing is higher in the disturbed site compared to the undisturbed site. The higher fraction of mixing can be due to the difference of usage of these dug wells, in terms of pumping, and the well cleaning in the area. As the sea water is denser than fresh water, the salt water will move downward into an undisturbed aquifer with lesser diffusion and dispersion. This phenomenon may be the cause of lesser variance observed for the undisturbed site. Conversely, the wells in the disturbed site were subjected to frequent cleaning and thereafter water extraction by pumping activities which may have disturbed the natural downward movement of dense salt water plume accelerating the contamination of wells with a possible permanent damage to the aquifer. This was also evident from the water quality analyses.

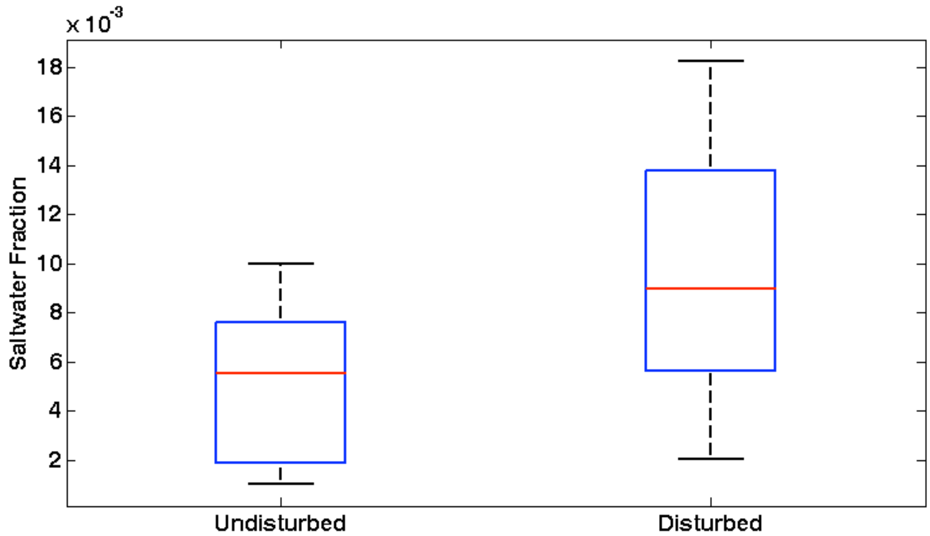

Fig. 9. Salt water fractions obtained by PHREEQC simulations for both disturbed and undisturbed sites data.

CONCLUSION

Observed values of electrical conductivity, alkalinity, total hardness and concentrations of calcium, sodium, potassium, manganese, and sulphate in the disturbed site were slightly higher than that in the undisturbed site during the months of January, March, and October 2006. Furthermore, water quality parameter values in dug wells were generally higher than in abandoned wells within the disturbed site. This was also evident from the geochemical inverse modelling with PHREEQC. The geochemical modelling showed excellent fits of observed data and it showed that the mixing fraction of sea water fraction in the disturbed site was twice as high compared to the undisturbed area. These findings support the hypothesis that well cleaning and abstraction of water for general purposes disturb the natural downward movement and the recession of the tsunami impacts and therefore, the imprint of the tsunami may have been prolonged in the disturbed site compared to the undisturbed site. Even after a more than one and half years since the tsunami tragedy, the detrimental effect of it on water quality still appear to persists in both sites and the aquifer has not recovered to its original status.

Acknowledgements

Authors acknowledge Dr. David Parkhurst, Dr. Jayantha Obeysekera and Dr. Rohana Chandrajith for their valuable assistance. *Action contre la Faim* (AcF), for the travel arrangements and assistance given. Lawrence in Tharmapuram village, Predeeban and Amalraj at the Eastern University are also acknowledged for their support given throughout the study.

REFERENCES

Cooray P.G. (1985). *Geology of Sri Lanka*. National Museum of Sri Lanka.

Hoareau J. Guérin R. Vouillamoz J. M. & Vithanage M. (2006). The use of Transient Electro-Magnetism to localize saline water intrusion in Sri Lanka. 32nd WEDC International Conference. Sustainable Development of Water Resources, Water Supply and Environmental Sanitation. Colombo, Sri Lanka, Nov. 13-17, 2006

Illangasekare T., Tyler S.W., Clement T.P., Villholth K.G., Perera A.P.G.R.L., Obeysekera J., Gunatilaka A., Panabokke C.R., Hyndman D.W., Cunningham K.J., Kaluarachchi J.J., Yeh W.W-G., Van Genuchten M.R. & Jensen K.H. (2006). Impacts of the 2004 Tsunami on Groundwater Resources in Sri Lanka. *Water Resources Research*, 42, W05201.

Jeyakumar P., Premanatharajah P. & Mahendran S. (2002). Water quality of agro-wells in the coastal area of the Batticaloa District. *Symposium proceedings on the Use of Groundwater for Agriculture in Sri Lanka*, 99-107

Koch, M. & Zhang G. (1992). Numerical simulation of the effects of variable density in a contaminant plume, *Groundwater* 30(5): 731–742.

Mahendran S., Jeyakumar P., Premanatharajah P. & Thiruchelvam T. (2000). Study on groundwater quality of some selected wells during dry season in the municipal council area of Batticaloa. *Proceedings of first annual research sessions*- Eastern University of Sri Lanka. 53-61

Oostrom M., Hayworth J. S., Dane J. H. & Güven O. (1992). Behavior of dense aqueous phase leachate plumes in homogeneous porous media, *Water Resources. Research* 28(8): 2123– 2134.

Panabokke C.R. & Perera A.P.G.R.L. (2004). *Groundwater resources of Sri Lanka*. World water Assessment Program, Sri Lanka.

Panabokke C.R. (2001). Groundwater studies of the coastal sand aquifers of Sri Lanka, Consultancy Report, International Water Management Institute, Sri Lanka

Panabokke C.R., Pathirana S.R.K. & Wijekoon D. (2002). Water quality of agro-wells in the coastal sand aquifer in Trincomalee District. *Symposium proceedings on the Use of Groundwater for Agriculture in Sri Lanka*, 85-98

Parkhurst D.L. & Appelo C.A.J. (1999). User's guide to PHREEQC (version 2) – A computer program for speciation, batch reaction, one dimensional transport and inverse geochemical calculations. *USGS Water Resources Investigation Report*. 99-4259. Denver.

Pilapitiya S., Vidanaarachchi C. and Yuen S. (2006). Effect of tsunami on waste management in Sri Lanka. *Waste Management*. 26, 107-109

Schincariol R.A. & Schwartz F. W. (1990). An experimental investigation of variable density flow and mixing in homogeneous and heterogeneous media, *Water Resources. Research* 26(10): 2317– 2329.

Simmons C.T., Fenstemaker T. R. & Sharp Jr. J. M. (2001). Variable-density groundwater flow and solute transport in heterogeneous porous media: approaches and challenges. *Journal of Contaminant. Hydrology* 52(1-4): 245- 275.

Sugirtharan M., Sutharsan S. & Thiruchelvam T. (2004). Quality assessment of well water at Thuraneelawanai area of Batticaloa District. *Annual Research Sessions*- Eastern University of Sri Lanka

Underwood M.R., Peterson F.L. & Voss, C.I. (1992). Groundwater lens dynamics of atoll islands, *Water Resources Research*, 28(11): 2889-2902

UNEP (2005). After the Tsunami: Rapid Environmental Assessment (available at http://www.unep.org/tsunami/reports/TSUNAMI_report_complete.pdf)

Vaheesar K., Mahendran T. & Priyantha N. (2000). Analytical studies on irrigation water at Kaluthaweli in the Batticaloa District. *Journal of Science*-Eastern University of Sri Lanka. 1(1), 10-15

Villholth K.G., Amerasinghe P.H. & Jeyakumar P. (2006a). Tsunami Impacts on Shallow Groundwater and Associated Water Supply on the East Coast of Sri Lanka, International Ground Water Conference, Feb., India

Villholth K.G., Manamperi A.S.P. & Buergi N. (2006b). Chemical Characteristics of Tsunami-Affected Groundwater and Lagoon on the East Coast of Sri Lanka. Paper submitted to the 32nd WEDC International Conference. Sustainable Development of Water Resources, Water Supply and Environmental Sanitation. Colombo, Sri Lanka, Nov. 13-17, 2006

Vithanage M., Engesgaard P., Villholth, K. & Jensen, K. (2009). Effect of December 2004 tsunami on groundwater in a coastal aquifer on the East coast of Sri Lanka: Field observations and numerical modeling (Under review, *Journal of Contaminant Hydrology*).

Wicremaratne H.U. (2004). Use of groundwater for coastal water supply schemes, minimizing the salinity problem; A case study at Kattankudy in Batticaloa District, Sri Lanka. MSc Thesis. Post Graduate Institute of Science, University of Peradeniya, Peradeniya, Sri Lanka.

Tsunami Society
1741 Ala Moana Blvd. #70
Honolulu, HI 96815, USA

WWW.TSUNAMISOCIETY.ORG